THE SINGLE-GAP CYLINDRICAL LOOP IN NON-CONDUCTING AND CONDUCTING MEDIA

ABSTRACT

The frequency response characteristics of the cylindrical loop are calculated for both non-conducting and conducting media for two types of cylindrical loop design. In the case of conducting media, the frequency response characteristics are considerably improved by adding insulating regions both inside and outside the loop.

FOREWORD

Due to the length of this note and the large number of figures, the figures are grouped together after the text. The overall division of this note is therefore the text followed by the figures and then an appendix. This appendix was written by Mr. D. E. Brannon of the Dikewood Corporation and A2C F. Brewster, Jr., of the Air Force Weapons Laboratory. It contains a discussion of the numerical techniques used to calculate the various quantities concerning the cylindrical loop response from the expressions developed in the text.

We would particularly like to thank Ann Brewster for preparing all the figures.

THE SINGLE-GAP CYLINDRICAL LOOP IN NON-CONDUCTING AND CONDUCTING MEDIA

ABSTRACT

The frequency response characteristics of the cylindrical loop are calculated for both non-conducting and conducting media for two types of cylindrical loop design. In the case of conducting media, the frequency response characteristics are considerably improved by adding insulating regions both inside and outside the loop.

FOREWORD

Due to the length of this note and the large number of figures, the figures are grouped together after the text. The overall division of this note is therefore the text followed by the figures and then an appendix. This appendix was written by Mr. D. E. Brannon of the Dikewood Corporation and A2C F. Brewster, Jr., of the Air Force Weapons Laboratory. It contains a discussion of the numerical techniques used to calculate the various quantities concerning the cylindrical loop response from the expressions developed in the text.

We would particularly like to thank Ann Brewster for preparing all the figures.

Contents

Section

List of Illustrations

I. Introduction

Two previous notes have discussed the response of the cylindrical $\dot{B}$ loop using rough approximations for the loop characteristics.[1,2] The first of these notes considered the case of negligible air conductivity and pointed out that for the proper amount of loading (from the associated signal cable) the frequency response is limited by the radian wavelength, λ, being of the order of, or greater than the loop radius. In the second note this was generalized to include the case of the nonlinear, time varying air conductivity in which the conduction currents dominate the displacement currents ($\sigma >> \omega\varepsilon$). In this latter case the frequency response is limited in that the skin depth, δ, must be of the order of, or greater than the loop radius. If a skin depth is defined by taking the maximum air conductivity (for times of interest) in the vicinity of the loop and the maximum frequency of interest, then for lower frequencies the loop response is approximately independent of the air conductivity even though this conductivity is nonlinear and time varying. Thus, an analysis of the response of a $\dot{B}$ loop which assumes a linear, time independent air conductivity, even though it does not accurately describe this response, is still useful in determining the upper frequency response and in comparing the performance of different loop designs. The purpose of this note is to perform just such an analysis on the cylindrical $\dot{B}$ loop. This analysis starts with the case of negligible air conductivity and then goes to the case of $\sigma >> \omega\varepsilon$. In the latter case, modifications in the design consisting of the addition of insulation inside and outside the loop structure are considered, showing the resulting improvement in the upper frequency response for a given loop sensitivity.

In this note we consider two general kinds of cylindrical loops as illustrated in figures 1 and 2. To distinguish the two cases, the first (in figure 1) is referred to as a cylindrical loop below a ground plane and the second (in figure 2) is referred to as an exposed cylindrical loop. These two cases are treated together in this note because of the similarities in the mathematical forms of their response characteristics. For the cylindrical loop below a ground plane the ground plane (as well as the loop structure) is assumed perfectly conducting for simplicity. It is also assumed that $\ell >> a$ and that the ends of the cylindrical structure are smoothly transitioned through the ground plane as indicated in figure 1A. These restrictions are necessary if the magnetic field in the direction of the loop axis is to have the same value inside the loop (over the whole cross section area, πa^2) as outside the loop (above the conducting ground plane).

Consider a case in which the external or incident magnetic field is in the z direction and independent of z (the coordinate in the direction of the loop axis). Then, from previous analysis, this component of the magnetic field should be approximately uniform inside and outside the loop structure when the radian wavelength, λ, or skin depth, δ, (as appropriate) is significantly larger than the loop radius and when the signal cable impedance loading the loop gap is sufficiently large. If the magnetic field

1. Lt Carl E. Baum, Sensor and Simulation Note VIII, Maximizing Frequency Response of a $\dot{B}$ Loop, Dec. 1964.
2. Lt Carl E. Baum, Sensor and Simulation Note XXIX, The Influence of Radiation and Conductivity on $\dot{B}$ Loop Design, Oct. 1966.

is not in the z direction and the field arrives at different positions along the length of the loop at different times, then λ or δ will have to be even larger for the measurement of a component of this magnetic field parallel to the loop axis. As indicated in figure 1B, two coordinate systems are used for this case. One of these, the (r,ϕ,z) or (x,y,z) system is used to analyze the loop interior. The other, the (r',ϕ',z') or (x',y',z') system with the z' axis in the middle of the loop gap is used to analyze the loop exterior above the conducting ground plane. In this note, as the various parameters, response characteristics, etc., are considered, we first consider the cylindrical loop below a ground plane because, in some cases, the mathematics are a little simpler. We sometimes identify certain parameters which pertain to the response of the loop below the ground plane, but not the exposed loop, by the addition of a prime to the symbol.

The exposed cylindrical loop is also assumed to have $\ell >> a$ so that end effects can be ignored. In a typical application, as in figure 2A, this type of loop might be at some height, h, above a conducting or not-so-conducting (e.g., soil or water) ground plane with the loop gap on top and a signal cable extending from the loop (vertically) to beneath the ground plane. In this configuration the fields scatter from the vertical cable and interact with the loop, and the field scattering from the loop interacts, because of the ground plane, back on the loop. In some cases, these problems can be minimized by symmetrically placing the loop structure with respect to the cable structure and by having the loop relatively far from the ground plane. This may not be sufficient in all cases, however,particularly for a nonlinear air conductivity at frequencies for which h is greater than an approximate skin depth, δ. In any event such problems are not considered in this note. The loop is considered as if there were no connecting signal cable to interact with the fields, and the ground plane is considered to be far away compared to the loop radius. The same comments regarding the magnetic field direction, the arrival time along the loop length, and λ or δ apply to the exposed cylindrical loop as to the loop below the ground plane. As indicated in figure 2B only one coordinate system is used in this structure, the (r,ϕ,z) or (x,y,z) system with the z axis taken as the loop axis. This coordinate system is used to analyze both the loop interior and exterior. For convenience in both these types of loop structures the $\phi = 0$ and $\phi' = 0$ directions are defined by the directions of the y and y' axes (which are themselves in the same direction).

The general scheme of solution of this problem involves the basic assumption that $\ell >> a$ so that the solution may be approximated as one involving two instead of three spatial dimensions. The resistive loading at the loop gap is considered to be approximately uniform with z so that all the electromagnetic parameters are z independent for a distance (ℓ) which is large compared to the loop radius. Practically, this resistive loading at the loop gap may be at several discrete points which are ideally uniformly spaced along the loop gap. The separations between adjacent load points should be small compared to the loop radius to approximate a continuous load distribution. We next assume all electromagnetic parameters such as ε, μ, σ, etc., to be constants, specifically not functions of the fields or time. The parameters of the various media are taken as scalar constants

which are independent of position within any defined region. The parameters ε, μ, and σ have a subscript, ℓ, applying to inside the loop and no subscript for the external medium as indicated in figures 1B and 2B. When a third medium (e.g., an insulator) is added to the loop exterior, these parameters are designated by a subscript, 1. Then a magnetic field is assumed in the various media which has only a z or z' component and which is a function of only r and ϕ, or r' and ϕ' as appropriate. This magnetic field distribution, and the associated electric field distribution, is then expanded in the appropriate cylindrical coordinate system in the appropriate functions which solve the vector wave equation.[3]

The form of the field expansions for this problem, with only a z component of the magnetic field which is also z independent, is[4]

$$H_z = H_{z_o} \sum_{n=0}^{\infty} a_n C_n^{(\ell)}(kr) \begin{Bmatrix} \cos(n\phi) \\ \sin(n\phi) \end{Bmatrix} \tag{1}$$

$$E_r = -jZH_{z_o} \sum_{n=0}^{\infty} a_n \frac{C_n^{(\ell)}(kr)}{kr} n \begin{Bmatrix} -\sin(n\phi) \\ \cos(n\phi) \end{Bmatrix} \tag{2}$$

and

$$E_\phi = jZH_{z_o} \sum_{n=0}^{\infty} a_n C_n^{(\ell)'}(kr) \begin{Bmatrix} \cos(n\phi) \\ \sin(n\phi) \end{Bmatrix} \tag{3}$$

where a time dependence of the form $e^{j\omega t}$ is assumed but is suppressed from all the expressions. The positive direction for the field components is defined by the standard convention of the direction of increasing the various coordinates. The use of the braces with the trigonometric functions inside indicates that a linear combination (the same combination for the three field components) of the two functions is used. Integer n is used so that the trigonometric functions are periodic over 2π. The function $C_n^{(\ell)}(kr)$ denotes one of the Bessel functions $J_n(kr)$, $Y_n(kr)$, $H_n^{(1)}(kr)$, and $H_n^{(2)}(kr)$ for an ℓ of 1, 2, 3, or 4 in that order. A prime over a Bessel function denotes the derivative with respect to the argument. By using the constant, H_{z_o}, with dimensions amperes/meter the expansion coefficients, a_n, are dimensionless convenient numbers.[5] The propagation constant has the general form

$$k = \sqrt{-j\omega\mu(\sigma + j\omega\varepsilon)} \tag{4}$$

where for $\sigma << \omega\varepsilon$ this reduces to

$$k = \omega\sqrt{\mu\varepsilon} = \frac{1}{\lambda} \tag{5}$$

3. Notation for the various functions and formulas for their manipulation can be found in AMS 55, Handbook of Mathematical Functions, National Bureau of Standards, 1964.

4. For these expansions see, for example, J.A. Stratton, Electromagnetic Theory (Chap. VI), 1941.

5. Units are rationalized MKSA unless otherwise specified. Results are generally expressed in dimensionless form.

and for $\sigma >> \omega\varepsilon$ this reduces to

$$k = \sqrt{-j\omega\mu\sigma} = \frac{1-j}{\delta} \tag{6}$$

The wave impedance has the general form

$$Z = \sqrt{\frac{j\omega\mu}{\sigma+j\omega\varepsilon}} \tag{7}$$

These two parameters can also be subscripted to apply to the various media. Expanding the fields in the various media as in equations (1) through (3), we apply the boundary conditions that tangential E and H be continuous across boundaries. Due to the convenient boundary of a circular cylinder (constant r), H_z and E_ϕ become of chief concern, and E_r is not, therefore, listed with the field expansions. However, using equations (1) through (3) the expansions for the remaining two of the three field components can be constructed if the expansion for any one of the field components is given (except possibly for n=0).

The mathematical procedure for determining the loop response characteristics involves the independent consideration of the parameters of a Norton equivalent circuit. Since the loop structures have $\ell >> a$, with the mathematics based on an infinite length, the parameters are defined per unit length. First, we consider a short circuit surface current density due to an incident plane wave. Shorting the loop gaps makes the geometry very convenient (planes and circular cylinders) for this calculation. This model is not entirely appropriate for the case of $\sigma >> \omega\varepsilon$ (in the external medium), and with the use of external dielectrics another model is introduced based on the average of the incident magnetic field over the dielectric surface. The surface current density is normalized to the magnetic field giving a transfer function which goes to unity for large λ or δ as appropriate. Only one orientation of the electric field (oriented in the y or y' direction) is considered for the incident plane wave. This note considers the frequency response characteristics of these cylindrical loops for $\sigma << \omega\varepsilon$ and $\sigma >> \omega\varepsilon$, including some variations in the structures for the latter case. The loop sensitivity to the direction of wave incidence (or sometimes called electric field sensitivity) is not treated here, but may be in some future note.

After the short circuit current density the admittances per unit length at the loop gap are considered. There are three such admittances considered, one associated with the loop interior, a second with the loop exterior, and a third with the signal cables (a conductance per unit length). The first two of these require field expansions on the inside and outside of the loop structure, respectively, to relate voltage across the loop gap to surface current density. The boundary condition at the loop gap for the electric field is obtained from a quasi-static approximation of the electric field distribution at the loop gap. The approximation only applies for cases in which the loop gap width, 2b, is much less than the loop radius and much less than radian wavelengths or skin depths of interest in media adjacent to the loop gap. In cases for which λ or δ, as appropriate, is of the order of the loop radius or larger (for flat frequency response), b is

automatically much less than λ or δ if $b<<a$. Conveniently the three admittances per unit length can be separately considered. These admittances per unit length are normalized by dividing by the low frequency form of the admittance per unit length of the loop structure, a simple inductance. The sum of the normalized admittances then goes to one for sufficiently large λ or δ, as appropriate. Combining these normalized admittances with the short circuit current transfer function then gives the response characteristics of the particular loop configuration.

In this note we first consider the case of only two distinct media of interest (inside and outside the loop structure). After calculating the short circuit current transfer function and the normalized admittances, they are combined for the case of $\sigma<<\omega\varepsilon$ with identical μ's and ε's in both media to give the response characteristics versus the various parameters. Then the same case is considered for $\sigma>>\omega\varepsilon$ with identical μ's and σ's in both media. Next, the conductivity inside the loop structure is assumed negligible compared to the external conductivity for $\sigma>>\omega\varepsilon$, showing some improvement in the response. A second case, with three distinct media, is then considered. The third medium is added to isolate the loop structure from the external medium. The short circuit current transfer function and the normalized admittance associated with the loop exterior are recalculated. For $\sigma>>\omega\varepsilon$ but negligible σ's inside the loop and in the medium just outside the loop and for identical μ's in all three media the response functions are again calculated showing a considerable further improvement in the response.

For the reader's benefit, if he wishes to gain some additional insight into other types of electromagnetic interaction (scattering, radiation, etc.) with cylindrical structures similar to those employed here a few references are included.[6,7]

II. Short Circuit Currents with no External Insulating Dielectrics

Consider the loop gaps, as in figures 1 and 2, shorted. The assumed incident plane wave produces a surface current density which is divided by the magnetic field in the incident wave to obtain a short circuit current transfer function.

A. Cylindrical Loop below Ground Plane

Considering the cylindrical loop below a ground plane as in figure 1B, if we short the loop gap the ground plane is made continuous and flat and is described by $y' = 0$. For this type of loop the boundary at the loop gap is considered as $r = a$ or as $y' = 0$, whichever is more convenient for a particular calculation. As long as the gap width is much less than the loop radius these two expressions give essentially the same boundary.

The incident plane wave is of the form (for the magnetic field)

6. R.W.P. King and T.T. Wu, The Scattering and Diffraction of Waves, 1959.
7. J. R. Wait, Electromagnetic Radiation from Cylindrical Structures, 1959.

$$H_{z'_{inc}}(r',\phi') = H_{z_o} e^{-jkx'} = H_{z_o} e^{jkr'\sin(\phi')} \tag{8}$$

With the loop gap shorted this plane wave has the electric field perpendicular to the infinite conducting plane and thus no additional waves are necessary to combine with the incident wave to match the boundary conditions. Note that this plane wave is conveniently defined such that

$$H_{z'_{inc}}(r',0) = H_{z_o} \tag{9}$$

With the boundary condition that the surface current density (units of amps/meter) on the conducting plane equal the adjacent tangential magnetic field (H), the short circuit surface current density at the loop gap is just

$$J_{s_o} = H_{z_o} \tag{10}$$

where J_{s_o} is taken in the + x' direction. Defining a short circuit current transfer function, T', as the ratio of J_{s_o} to the magnetic field in the incident wave (at x' = 0) then gives

$$T' = 1 \tag{11}$$

for the cylindrical loop below a ground plane.

B. Exposed Cylindrical Loop

Consider now the exposed cylindrical loop as in figure 2B. If the loop gap is shorted the circular cylinder is made continuous and is described by r = a. For this case the boundary at the loop gap is considered as r = a for calculations relating to both inside and outside the loop. Again the gap width is considered much less than the loop radius.

Again the incident plane wave is of the form

$$H_{z_{inc}}(r,\phi) = H_{z_o} e^{-jkx} = H_{z_o} e^{jkr\sin(\phi)} \tag{12}$$

Unlike the cylindrical loop below a ground plane, we need to add a reflected wave to match the boundary conditions, making a somewhat more complicated short circuit current transfer function. So first expand equation (12) in cylindrical coordinates, using the appropriate functions for the wave equation solution, as [8,9]

8. See reference 3 for the expansion of $\cos[kr\sin(\phi)]$ and $\sin[kr\sin(\phi)]$.

9. In the notation used for the summations, $\sum_{n=n_1}^{n_2,n_3}$, n_1 is the lower limit (as normal), n_2 is the upper limit (∞ in this case), and n_3 is the increment in n (starting at the lower limit) for the successive terms. In equation (13), for example, the two summations are then for even and odd n, in that order. For the case of $n_3 = 1$, n_3 can be dropped from the summation, leaving the standard form.

$$H_{z_{inc}}(r,\phi) = H_{z_o}\left[J_o(kr)+2\sum_{n=2}^{\infty,2} J_n(kr)\cos(n\phi)+j2\sum_{n=1}^{\infty,2} J_n(kr)\sin(n\phi)\right] \quad (13)$$

Referring to equations (1) through (3) we have an associated azimuthal electric field of

$$E_{\phi_{inc}}(r,\phi) = jZH_{z_o}\left[J_o'(kr)+2\sum_{n=2}^{\infty,2} J_n'(kr)\cos(n\phi)+j2\sum_{n=1}^{\infty,2} J_n'(kr)\sin(n\phi)\right] \quad (14)$$

To this incident wave add a reflected wave which has the general form

$$H_{z_{refl}}(r,\phi) = H_{z_o}\left[a_o H_o^{(2)}(kr)+2\sum_{n=2}^{\infty,2} a_n H_n^{(2)}(kr)\cos(n\phi)+j2\sum_{n=1}^{\infty,2} a_n H_n^{(2)}(kr)\sin(n\phi)\right] \quad (15)$$

and

$$E_{\phi_{refl}}(r,\phi) = jZH_{z_o}\left[a_o H_o^{(2)'}(kr)+2\sum_{n=2}^{\infty,2} a_n H_n^{(2)'}(kr)\cos(n\phi)+j2\sum_{n=1}^{\infty,2} a_n H_n^{(2)'}(kr)\sin(n\phi)\right] \quad (16)$$

Applying the boundary condition that the tangential electrical field is zero on the cylindrical surface, the relationships for the coefficients of the reflected wave, from equations (14) and (16) are given by

$$J_n'(ka) + a_n H_n^{(2)'}(ka) = 0 \quad (17)$$

or

$$a_n = -\frac{J_n'(ka)}{H_n^{(2)'}(ka)} \quad (18)$$

The surface current density (in the $+\phi$ direction) is given by

$$J_s(\phi) = -[H_{z_{inc}}(a,\phi) + H_{z_{refl}}(a,\phi)] \quad (19)$$

In this expression, as the individual terms are combined, an expression appears which is defined as

$$T_n = J_n(ka) - \frac{J_n'(ka)}{H_n^{(2)'}(ka)} H_n^{(2)}(ka) \quad (20)$$

or

$$T_n = \frac{J_n(ka)H_n^{(2)'}(ka) - J_n'(ka)H_n^{(2)}(ka)}{H_n^{(2)'}(ka)} \quad (21)$$

The numerator reduces by expanding the Hankel functions, cancelling terms, and applying a Wronskian relationship to give

$$T_n = \left[j \frac{\pi ka}{2} H_n^{(2)'}(ka) \right]^{-1} \tag{22}$$

Then

$$\frac{J_s(\phi)}{H_{z_o}} = - \left[T_o + 2 \sum_{n=2}^{\infty,2} T_n \cos(n\phi) + j2 \sum_{n=1}^{\infty,2} T_n \sin(n\phi) \right] \tag{23}$$

The short circuit surface current density is then

$$J_{s_o} = J_s(0) \tag{24}$$

where, for this calculation, the variation of $J_s(\phi)$ over $-\phi_o \leq \phi \leq \phi_o$ is ignored. Define the short circuit current transfer function as

$$T = - \frac{J_{s_o}}{H_{z_o}} = T_o + 2 \sum_{n=2}^{\infty,2} T_n \tag{25}$$

The minus sign is placed in the definition so that $T \to +1$ for small $|ka|$.

As mentioned before only one wave orientation for this transfer function is considered, or equivalently one position on the cylinder for the loop gap. For $\sigma << \omega\varepsilon$ equation (5) is used to express k in terms of λ and to plot T versus λ/a in figure 3. Similarly for the case of $\sigma >> \omega\varepsilon$ T versus δ/a is plotted in figure 4. Note that in these cases T is essentially one for $\lambda/a > 10$, and that for $1 < \lambda/a < 10$, T is rather well behaved. This latter region is significant for the upper frequency response. Note also for $\sigma >> \omega\varepsilon$ that for small δ/a the incident magnetic field (as in equation (12)) has an exponentially decreasing amplitude for increasing x. Thus, for negative x the surface current density on the cylinder can be much larger than at the gap. This points out a limitation in the use of such a plane wave to represent the incident magnetic field in the conducting source region. Since we are only considering the one wave direction for these calculations, this causes no problems and is used. In a later section, when external insulators are considered, however, this is a significant problem, and a more appropriate definition for that case is used.

III. Admittances With no External Insulating Dielectrics

Removing the incident waves consider the loop gaps to be unshorted or open. Drive the gap uniformly along its length with a voltage, V_{gap}, and calculate the surface current densities produced. These current densities give the three admittances per unit length for the loops attributable to the loop interior, loop exterior, and the signal cable load. First, however, consider the boundary conditions at the loop gap.

A. Boundary Conditions at Loop Gap

Assume that the electric field has a quasi-static distribution in the vicinity of the loop gap. By having a quasi-static distribution, we restrict the width, 2b, of the loop gap to be much less than λ or δ, as appropriate. Also assuming that b<<a, then the loop structure near the gap is approximately flat. Consider, then, the loop gap and immediate vicinity as in figure 5. The electric field distribution across the loop gap is approximated by calculating this distribution across a gap in an infinite conducting plane in the low frequency limit.[10] An appropriate conformal transformation for this problem is

$$\frac{z''}{b} = \sin(w) \tag{26}$$

where

$$z'' = x''+jy'' \tag{27}$$

and

$$w = u+jv \tag{28}$$

The coordinates for the two-dimensional gap structure are x'' and y''. The equipotentials are given by lines of constant u and the electric field lines by lines of constant v.

Along $y'' = 0$ (in the loop gap) we have $v = 0$ giving

$$u = \arcsin\left(\frac{x''}{b}\right) \tag{29}$$

The potential distribution is then

$$V(x'') = -\frac{V_{gap}}{\pi} \arcsin\left(\frac{x''}{b}\right) \tag{30}$$

and the electric field distribution is

$$E(x'') = -\frac{\partial V}{\partial x''} = \frac{V_{gap}}{\pi b}\left[1 - \left(\frac{x''}{b}\right)^2\right]^{-1/2} \tag{31}$$

Define a distribution function

$$f(\xi) = \frac{1}{\pi}\left[1-\xi^2\right]^{-1/2} \tag{32}$$

Then for cylindrical coordinates since

$$b = a\phi_o \tag{33}$$

for small ϕ_o, the electric field distribution at r = a for $|\phi| \leq \phi_o$ is taken as

$$E_\phi(a,\phi) = -\frac{V_{gap}}{a\phi_o} f\left(\frac{\phi}{\phi_o}\right) \tag{34}$$

10. This same approximation is used in connection with a gap in a cylinder in P. M. Morse and H. Feshback, Methods of Theoretical Physics, Vol. II, pp. 1387-1398, 1953.

There is a limitation in the use of this electric field distribution in that the loop gap has objects in it, such as signal cable connections, which distort the field. Equations (32) and (34) strictly apply only to the case in which no such perturbing objects exist, such as for no signal cable load. In ignoring z variations of the structure these perturbations associated with the signal cable inputs are also ignored. However, within the limitations of the assumption of z independent geometry this is a reasonable electric field distribution to use.

B. Internal Admittance of Cylindrical Loop

Turning to the admittances per unit length, consider first the internal admittance per unit length which is the same for both types of loops (which have the same internal geometries as in figures 1B and 2B). Expand the fields inside the loop as

$$H_z(r,\phi) = H_{z_o}\left[a_o J_o(k_\ell r) + 2\sum_{n=1}^{\infty} a_n J_n(k_\ell r)\cos(n\phi)\right] \tag{35}$$

and

$$E_\phi(r,\phi) = jZ_\ell H_{z_o}\left[a_o J_o'(k_\ell r) + 2\sum_{n=1}^{\infty} a_n J_n'(k_\ell r)\cos(n\phi)\right] \tag{36}$$

The first kind of Bessel function makes the field finite at the origin and the use of $\cos(n\phi)$ makes E_ϕ even in ϕ as required by the boundary conditions. The associated surface current density at the open loop gap (in the $+\phi$ direction) is

$$J_{s_\ell} = H_z(a,\pm\phi_o) \tag{37}$$

This is driven by the gap voltage, V_{gap}, giving an admittance per unit length

$$y_\ell = \frac{J_{s_\ell}}{V_{gap}} \tag{38}$$

For sufficiently low frequencies this is just $1/(j\omega\mu_\ell \pi a^2)$ and is the dominant loop admittance. Thus, normalize this admittance per unit length (and others to follow) and define

$$Y_\ell = j\omega\mu_\ell \pi a^2 y_\ell \tag{39}$$

which we call the normalized internal admittance of the cylindrical loop. In this form we can observe the deviation of the admittances from the ideal low-frequency form and thus the deviation of the loop response from the ideal case for a B loop. Note that $Y_\ell \to 1$ for small $|ka|$.

The boundary condition to be satisfied is that $E_\phi(a,\phi)$ is given by equation (34) in the loop gap and is zero elsewhere. Equating the expressions for $E_\phi(a,\phi)$ from equations (34) and (36), multiply each side by $\cos(n\phi)$ and integrate over ϕ between 0 and 2π. Only the nth term in the summation contributes giving for each n

$$-\frac{V_{gap}}{a\phi_o}\int_{-\phi_o}^{\phi_o} f\left(\frac{\phi}{\phi_o}\right)\cos(n\phi)d\phi = j2\pi Z_\ell H_{z_o} a_n J_n'(k_\ell a) \tag{40}$$

Solving for the coefficients gives

$$a_n = \frac{jV_{gap}}{2\pi a Z_\ell H_{z_o} J_n'(k_\ell a)} \frac{1}{\phi_o}\int_{-\phi_o}^{\phi_o} f\left(\frac{\phi}{\phi_o}\right)\cos(n\phi)d\phi \tag{41}$$

Letting $\phi/\phi_o = \xi$ we have[11]

$$\frac{1}{\phi_o}\int_{-\phi_o}^{\phi_o} f\left(\frac{\phi}{\phi_o}\right)\cos(n\phi)d\phi = \int_{-1}^{1} f(\xi)\cos(n\phi_o\xi)d\xi$$

$$= \frac{1}{\pi}\int_{-1}^{1}\frac{\cos(n\phi_o\xi)}{\sqrt{1-\xi^2}}\,d\xi$$

$$= J_o(n\phi_o) \tag{42}$$

Then

$$a_n = \frac{jV_{gap}\,J_o(n\phi_o)}{2\pi a Z_\ell H_{z_o} J_n'(k_\ell a)} \tag{43}$$

For convenience define

$$Y_{\ell_n} = -\frac{J_n(k_\ell a)}{J_n'(k_\ell a)} \tag{44}$$

Combining these equations the admittance per unit length is

$$y_\ell = -\frac{j}{2\pi a Z_\ell}\left[Y_{\ell_o} + 2\sum_{n=1}^{\infty} Y_{\ell_n} J_o(n\phi_o)\cos(n\phi_o)\right] \tag{45}$$

11. H. B. Dwight, Tables of Integrals and Other Mathematical Data, 1965, equation 859.042.

In normalized form (from equation (39)), combining the terms using equations (4) and (7),

$$Y_\ell = \frac{K_\ell a}{2} \left[Y_{\ell_o} + 2 \sum_{n=1}^{\infty} Y_{\ell_n} J_o(n\phi_o)\cos(n\phi_o) \right] \tag{46}$$

Figure 6 has Y_ℓ plotted against λ/a for the case of $\sigma << \omega\varepsilon$. Note that in this instance Y_ℓ has no imaginary component, i.e., it is a real number. Figure 6A shows the first few resonances for small λ/a. In figure 6B the vertical scale is expanded to show the departure of Y_ℓ from one as λ/a is decreased. In figure 7 Y_ℓ is plotted against δ/a for the case of $\sigma >> \omega\varepsilon$. In this instance the normalized admittance is a complex number and there are no resonances. Note that Y_ℓ also goes to one for large δ/a. The general expression for Y_ℓ (equation (46)) allows for arbitrary ε_ℓ, μ_ℓ, and σ_ℓ. For the graphs in this note these parameters, where significant, are taken the same as the external parameters: ε, μ, and σ. In particular μ_ℓ and μ_1 are always taken as μ for the plots. The conductivity, σ_ℓ, is taken as equal to σ or as having negligible influence, and the same applies to ε_ℓ.

C. External Admittance of Cylindrical Loop Below Ground Plane

Consider now the admittance per unit length attributable to fields outside the cylindrical loop below a ground plane. Referring to figure 1B, the loop radius does not enter into this admittance due to the presence of the ground plane. Thus, the case in which $|kb| << 1$ is considered. This still allows $|ka|$ to be of order one since $b << a$. For this admittance we then consider the first term in a field expansion plus a correction term for the capacitance and/or conductance near the loop gap. An approximate field distribution outside the loop is of the form

$$H_{z'}(r',\phi') \approx H_{z_o} a_o H_o^{(2)}(kr') \tag{47}$$

and

$$E_{\phi'}(r',\phi') \approx jZH_{z_o} a_o H_o^{(2)}(kr') \tag{48}$$

The Hankel functions of the second kind represent an outward travelling wave. For $|kb| << 1$ we have

$$b \int_o^{\pi} E_{\phi'}(b,\phi')d\phi' = - V_{gap} \tag{49}$$

Since the path of integration is not along $y' = 0$ but along $r' = b$ there is a small error associated with the time rate of change of the magnetic flux through the semicircular area enclosed by these two paths of integration. This is ignored for present purposes but is reintroduced, for convenience, when we consider the use of external insulators. Solving equations (48) and (49) we have

$$a_o = \frac{jV_{gap}}{\pi bZH_{z_o} H_o^{(2)'}(kb)} \tag{50}$$

Higher order terms in the electric field expansion (involving $\cos(n\phi')$) do not contribute to the integral in equation (49), thus not affecting the result for a_o.

The surface current density (in the $-x'$ direction) is

$$J_{s_{ext}} = - H_{z'}(b, \pm \frac{\pi}{2}) \tag{51}$$

This gives an approximate admittance per unit length as

$$y'_{ext} = \frac{J_{s_{ext}}}{V_{gap}} \approx - \frac{j}{\pi b Z} \frac{H_o^{(2)}(kb)}{H_o^{(2)'}(kb)} \tag{52}$$

For $|kb| \ll 1$ this is basically a capacitance and/or conductance per unit length.

Let us correct this admittance for the electric field distortion near the loop gap. Consider again the conformal transformation used in section III A. Expanding equation (26) using the (x',y') coordinates gives

$$\frac{x'}{b} + j\frac{y'}{b} = \sin(u)\cosh(v) + j\cos(u)\sinh(v) \tag{53}$$

Along the right half of the ground plane ($y'=0$, $x' \geq b$) we have

$$u = \frac{\pi}{2} \tag{54}$$

and

$$v = \operatorname{arccosh}\left(\frac{x'}{b}\right) \tag{55}$$

If we consider all the electric field out to a distance, x', we have an admittance

$$y_1 = \frac{\sigma + j\omega\varepsilon}{\pi} \operatorname{arccosh}\left(\frac{x'}{b}\right) \tag{56}$$

If we consider the circular electric field distribution of equation (48) in the limit of small $|kr'|$ we have an admittance

$$y_2 = \frac{\sigma + j\omega\varepsilon}{\pi} \ln\left(\frac{x'}{b}\right) \tag{57}$$

For $r' \gg b$ the two field distributions are nearly the same. The increase in y_1 over y_2 is then mostly due to the electric field distribution near the loop gap. As a correction to the admittance consider the difference, $y_1 - y_2$, in the limit of large x'. Define

$$\Delta y = \lim_{\frac{x'}{b} \to \infty} (y_1 - y_2)$$

$$= \lim_{\frac{x'}{b} \to \infty} \frac{\sigma+j\omega\varepsilon}{\pi} \left\{ \ln \left[\frac{x'}{b} + \left(\left(\frac{x'}{b} \right)^2 - 1 \right)^{1/2} \right] - \ln \left(\frac{x'}{b} \right) \right\}$$

$$= \lim_{\frac{x'}{b} \to \infty} \frac{\sigma+j\omega\varepsilon}{\pi} \ln \left[1 + \left(1 - \left(\frac{b}{x'} \right)^2 \right)^{1/2} \right] \tag{58}$$

Thus

$$\Delta y = \frac{\sigma+j\omega\varepsilon}{\pi} \ln(2) \tag{59}$$

which is a rather simple correction term. Correcting equation (52) then gives

$$y'_{ext} = -\frac{j}{\pi b Z} \frac{H_o^{(2)}(kb)}{H_o^{(2)'}(kb)} + \frac{\sigma+j\omega\varepsilon}{\pi} \ln(2) \tag{60}$$

or

$$y'_{ext} = \frac{j}{\pi b Z} \left\{ \frac{H_o^{(2)}(kb)}{H_1^{(2)}(kb)} + kb \ln(2) \right\} \tag{61}$$

Normalizing this to the ideal loop admittance per unit length gives

$$Y'_{ext} = j\omega\mu_\ell \pi a^2 y'_{ext} \tag{62}$$

or

$$Y'_{ext} = -\left(\frac{a}{b} \right)^2 \frac{\mu_\ell}{\mu} kb \left\{ \frac{H_o^{(2)}(kb)}{H_1^{(2)}(kb)} + kb \ln(2) \right\} \tag{63}$$

This is called the normalized external admittance of the cylindrical loop below a ground plane. The preceding equation can be rearranged as

$$\frac{\mu}{\mu_\ell} \left(\frac{b}{a} \right)^2 Y'_{ext} = -kb \left\{ \frac{H_o^{(2)}(kb)}{H_1^{(2)}(kb)} + kb \ln(2) \right\} \tag{64}$$

such that the right side is only a function of kb.

Considering the case of $\mu_\ell = \mu$, this normalized admittance is plotted in figures 8 and 9 in the form of equation (64). The case of $\sigma << \omega\varepsilon$ is shown in figure 8 with λ/b as the independent variable. The case of $\sigma >> \omega\varepsilon$ is shown in figure 9 with δ/b as the independent variable. In both cases the normalized admittance is a complex number and is negligible compared to Y_ℓ in the limit of small $|kb|$.

D. External Admittance of Exposed Cylindrical Loop

For the external admittance per unit length of the exposed cylindrical loop we have the geometry of figure 2B. The solution is very similar to that in section IIIB. Expand the fields outside the loop as

$$H_z(r,\phi) = H_{z_o}\left[a_o H_o^{(2)}(kr) + 2\sum_{n=1}^{\infty} a_n H_n^{(2)}(kr)\cos(n\phi)\right] \tag{65}$$

and

$$E_\phi(r,\phi) = jZH_{z_o}\left[a_o H_o^{(2)'}(kr) + 2\sum_{n=1}^{\infty} a_n H_n^{(2)'}(kr)\cos(n\phi)\right] \tag{66}$$

The Hankel functions of the second kind are used to give an outward propagating wave. The $\cos(n\phi)$ terms make E_ϕ even in ϕ as required by the boundary conditions which are symmetrical in ϕ. The associated surface current density at the loop gap (in the $+\phi$ direction) is

$$J_{s_{ext}} = - H_z(a,\pm\phi_o) \tag{67}$$

The admittance per unit length due to the loop exterior is

$$y_{ext} = \frac{J_{s_{ext}}}{V_{gap}} \tag{68}$$

As before this is normalized by defining

$$Y_{ext} = j\omega\mu_\ell \pi a^2 y_{ext} \tag{69}$$

which is called the normalized external admittance of the exposed cylindrical loop.

Equating the expressions for $E_\phi(a,\phi)$ from equations (34) and (66), multiply each side by $\cos(n\phi)$ and integrate over ϕ between zero and 2π giving for each n

$$-\frac{V_{gap}}{a\phi_o}\int_{-\phi_o}^{\phi_o} f\left(\frac{\phi}{\phi_o}\right)\cos(n\phi)d\phi = j2\pi ZH_{z_o} a_n H_n^{(2)'}(ka) \tag{70}$$

Or, using the results of equation (42)

$$a_n = \frac{jV_{gap}J_o(n\phi_o)}{2\pi aZH_{z_o}H_n^{(2)'}(ka)} \tag{71}$$

Define

$$Y_{ext_n} = \frac{H_n^{(2)}(ka)}{H_n^{(2)'}(ka)} \tag{72}$$

Combining these equations the admittance per unit length is

$$y_{ext} = -\frac{j}{2\pi aZ}\left[Y_{ext_o} + 2\sum_{n=1}^{\infty} Y_{ext_n} J_o(n\phi_o)\cos(n\phi_o)\right] \tag{73}$$

In normalized form

$$Y_{ext} = \frac{\mu_\ell}{\mu}\frac{ka}{2}\left[Y_{ext_o} + 2\sum_{n=1}^{\infty} Y_{ext_n} J_o(n\phi_o)\cos(n\phi_o)\right] \tag{74}$$

Again letting $\mu_\ell = \mu$ this normalized admittance is plotted in figures 10 and 11 for the cases of $\sigma << \omega\varepsilon$ and $\sigma >> \omega\varepsilon$, respectively. For small $|ka|$ this is again negligible compared to Y_ℓ.

E. Cable Admittance

The final admittance per unit length is that due to the signal cable loading which we define as g_c. Actually this loading is at discrete points along the loop gap. Ideally the spacing between these points is much less than the loop circumference.[12] In any event, g_c is calculated from

$$g_c = \frac{1}{Z_c \ell} \tag{75}$$

where Z_c is the cable impedance driven at the loop gap. In normalized form define

$$G_c = j\omega\mu_\ell \pi a^2 g_c \tag{76}$$

which is called the normalized cable conductance.

For the case of $\sigma << \omega\varepsilon$ it is convenient to rewrite equation (76) in the form

$$G_c = j\frac{\mu_\ell}{\mu}\pi ka\left(\frac{g_c a}{Y}\right) \tag{77}$$

12. See reference 1 for a discussion of this point based on transit times.

where

$$Y = \frac{1}{Z} \tag{78}$$

and is the wave admittance. For the special case of negligible conductivity,

$$Y_o = \frac{1}{Z_o} = \sqrt{\frac{\epsilon_o}{\mu_o}} = 2.654 \times 10^{-3} \text{ mho} \tag{79}$$

Also assuming that $\mu_\ell = \mu = \mu_o$ we have the special case

$$G_c = j\pi \left(\frac{\lambda}{a}\right)^{-1} \left(\frac{g_c a}{Y_o}\right) \tag{80}$$

which is used for the plots with $g_c a/Y_o$ as a convenient dimensionless parameter.

If $\sigma >> \omega\epsilon$, then for the case of $\mu_\ell = \mu = \mu_o$

$$G_c = -\pi(ka)^2 \left(\frac{g_c}{\sigma}\right) \tag{81}$$

or

$$G_c = j2\pi \left(\frac{\delta}{a}\right)^{-2} \left(\frac{g_c}{\sigma}\right) \tag{82}$$

This is also used for the appropriate graphs with g_c/σ as a convenient dimensionless parameter.

IV. Frequency Response Characteristics With no External Insulating Dielectrics.

For the cylindrical loop we define a response function based on the normalized admittances. For the cylindrical loop below a ground plane define

$$R'_y = \left[Y_\ell + Y'_{ext} + G_c\right]^{-1} \tag{83}$$

and for the exposed cylindrical loop define

$$R_y = \left[Y_\ell + Y_{ext} + G_c\right]^{-1} \tag{84}$$

Including the short circuit current transfer functions, for the cylindrical loop below a ground plane define

$$R' = T'R'_y \tag{85}$$

and for the exposed cylindrical loop define

$$R = TR_y \tag{86}$$

These functions relate, in normalized form, the response of the types of cylindrical loop considered to the time derivative of the magnetic field, $\dot{B}$, in the incident wave. In the limit of small $|ka|$ (for nonzero gap width and finite cable conductance per unit length), all four of these functions go to unity. The effects of the admittances are given by R'_y and R_y and the effects of the short circuit current are included in R' and R to give the overall response functions. For the cylindrical loop below a ground plane R'_y and R' are the same for the cases considered so far. With the later addition of another external medium these two response functions differ.

Using these response functions the frequency response characteristics of these loops may be calculated. The gap width and cable conductance are varied in order to observe their effects on the loop response. For the case of $\sigma >> \omega\varepsilon$ the conductivity inside the loop is also made negligible so as to improve the loop response. The minimum λ/a or δ/a as appropriate (or the upper frequency response) is defined as the maximum value of λ/a or δ/a for which

$$|R'| = \frac{1}{\sqrt{2}} \tag{87}$$

or

$$|R| = \frac{1}{\sqrt{2}} \tag{88}$$

whichever is appropriate. For the case of $\sigma << \omega\varepsilon$ resonances occur and the upper frequency response, as above, is inadequate to characterize the frequency response. Thus, the damping of the first resonance to flatten the frequency response curve is also considered.

A. No Conductivity and Same Parameters Both Inside and Outside Loop

First consider the case of $\sigma << \omega\varepsilon$ in which the permittivity and permeability are the same both inside and outside the loop. Given the loop radius and gap width we would like to be able to choose a best value of g_c for optimum frequency response characteristics of the loop. The length of the cylinder can then be chosen together with the cable impedance to obtain this optimum g_c.

The response functions versus λ/a for a given b/a with $g_c a/Y_o$ as a parameter may be plotted, and on the basis of this a best value of $g_c a/Y_o$ may be chosen. However, the definition of "best" is somewhat arbitrary. Defining the upper frequency response by equations (87) and (88) the associated λ/a is minimized by setting g_c to zero. With negligible conductivity, however, the loop is a resonant structure, seriously perturbing the frequency response curve, significantly raising the normalized frequency response (above the low frequency limiting value) for frequencies lower than this upper frequency response. Thus, this definition of upper frequency response may not be appropriate. A larger g_c may flatten out the resonance in the frequency response curve so that equations (87) and (88) provide a more adequate description of the upper frequency response.

Define the first resonance as the lowest frequency (or largest λ/a) for which the real part of the total normalized admittance is zero. Calling this λ as λ_r gives

$$\mathrm{Re}\left[Y_\ell + Y_{ext}\right]\Big|_{\frac{\lambda}{a} = \frac{\lambda_r}{a}} = 0 \tag{89}$$

This equation does not include G_c because it is a purely imaginary number (equation (80)). (For the loop below a ground plane substitute Y'_{ext} for Y_{ext} and similarly throughout this section.) This normalized resonant wavelength, λ_r/a, is a function of b/a.

Consider now an approximate model for the loop response near this resonance by considering the sum of the loop admittances to be a parallel combination of an inductance, L, a capacitance, C, and a conductance, G. Resonance occurs at that frequency at which the admittances of the inductance and capacitance cancel each other. If L, C, and G are assumed to be frequency independent, then we may consider a few choices of G based on circuit theory calculations. Dividing by the admittance of the inductor, $1/j\omega L$, (similar to the case with the loop admittance), the normalized admittance of these three elements is

$$Y_t = 1 - \omega^2 LC + j\omega LG \tag{90}$$

This gives a response function

$$R_y = \left[1 - \omega^2 LC + j\omega LG\right]^{-1} \tag{91}$$

The short circuit current transfer function is assumed constant for this approximate analysis.

Assuming that L, C, and G are frequency independent, the response is critically damped if

$$G\sqrt{\frac{L}{C}} = 2 \tag{92}$$

A critically damped response has the property that the response to a step function (of $\dot{B}$ in this case) has no overshoot and that G as in equation (92) is the minimum value with this characteristic. There is also the case of maximum flat frequency response given by

$$G\sqrt{\frac{L}{C}} = \sqrt{2} \tag{93}$$

This has the property that G is the minimum value for which the magnitude of the frequency response curve of equation (91) is less than or equal to one for all frequencies. However, since the loops considered here are distributed systems these definitions of critical damping and maximum flatness are only approximate. This can be seen in some of the figures where the magnitude of the response function goes a little above one for the maximum flatness case.

Apply these results to the loops to get a rough idea of the optimum choices for g_c. Define the parameters in equation (91) such that at the first resonance R_y has the same value as in equation (83) or (84) whichever is appropriate. At this resonance the real part of the admittance is zero, or

$$\omega^2 LC \Big|_{\frac{\lambda}{a} = \frac{\lambda_r}{a}} = 1 \tag{94}$$

Then, at this resonance, the imaginary part of the admittance is

$$j\omega LG \Big|_{\frac{\lambda}{a} = \frac{\lambda_r}{a}} = jG\sqrt{\frac{L}{C}} \tag{95}$$

From equations (92) and (93) we can assign the two values to the imaginary part of the loop admittance. Since Y_ℓ is a purely real number, then for critical damping set

$$\text{Im}\left[Y_{ext} + G_c\right]\Big|_{\frac{\lambda}{a} = \frac{\lambda_r}{a}} = 2 \tag{96}$$

and for maximum flat frequency response set

$$\text{Im}\left[Y_{ext} + G_c\right]\Big|_{\frac{\lambda}{a} = \frac{\lambda_r}{a}} = \sqrt{2} \tag{97}$$

Substituting for G_c from equation (77) gives for critical damping

$$\frac{g_c a}{Y_o} = \frac{\mu}{\mu_\ell}\frac{1}{\pi}\frac{\lambda_r}{a}\left\{2 - \text{Im}\left[Y_{ext}\right]\right\}\Big|_{\frac{\lambda}{a} = \frac{\lambda_r}{a}} \tag{98}$$

and for maximum flatness

$$\frac{g_c a}{Y_o} = \frac{\mu}{\mu_\ell}\frac{1}{\pi}\frac{\lambda_r}{a}\left\{\sqrt{2} - \text{Im}\left[Y_{ext}\right]\right\}\Big|_{\frac{\lambda}{a} = \frac{\lambda_r}{a}} \tag{99}$$

where again for the plots $\mu_\ell = \mu$.

The case of $\sigma << \omega\varepsilon$ with $\mu_\ell = \mu$ and $\varepsilon_\ell = \varepsilon$ is treated in figures 12 through 15 for the loop below a ground plane and in figures 16 through 21 for the exposed loop. In each of the groups of figures there is first λ_r/a plotted against b/a. This is followed by $g_c a/Y_o$, for the two cases of critical damping and maximum flatness, plotted against b/a. Next, the response functions are plotted for two values of b/a(.01 and .1) versus λ/a with $g_c a/Y_o$ (including the two special cases) as a parameter. Since R'_y and R' are the same only R' is considered for the loop below a ground

plane. Then the frequency responses as contained in the characteristic λ/a from equations (87) and (88) are plotted versus $g_c a/Y_o$ with b/a as a parameter. These plots are only taken down to a minimum $g_c a/Y_o$ given by the approximate maximum flat frequency response, lower values losing some significance. Finally, in figure 22, ℓ/a is plotted against $g_c a/Y_o$ for a few values of the cable impedance so that the reader can easily relate the loop length to the loop radius, the cable impedance, and the desired value of $g_c a/Y_o$. Considering the maximum flatness criterion, the upper frequency response (for b/a = .1) occurs at a λ/a of about 2.9 for the loop below a ground plane and of about 2.8 for the exposed cylindrical loop.

B. High Conductivity and Same Parameters Both Inside and Outside Loop

Consider the case of $\sigma >> \omega\varepsilon$ in which the permeability and conductivity are the same both inside and outside the loop. The permittivities are unimportant as long as both are much less than σ/ω. In this case the response functions versus δ/a are plotted for a given b/a with g_c/σ as a parameter. The cylindrical loop below a ground plane is treated in figures 23 through 25. The exposed cylindrical loop is treated in figures 26 through 30. In each case, the final figure has the frequency response (from equations (87) and (88)), in the form of a characteristic δ/a, plotted versus g_c/σ with b/a as a parameter and versus b/a with g_c/σ as a parameter.

There are no resonances of concern here for $\sigma >> \omega\varepsilon$ and so the maximum frequency response occurs at $g_c/\sigma = 0$. However, practically we need a nonzero g_c so the optimum situation is to have $g_c/\sigma << 1$. For b/a = .1, the upper frequency response for negligible g_c/σ occurs at a δ/a of about 3.8 for the loop below a ground plane and of about 3.6 for the exposed loop.

C. High Conductivity Only Outside Loop

For $\sigma >> \omega\varepsilon$, as a first attempt at improving the frequency response, constrain $\sigma_\ell << \sigma$ while $\mu_\ell = \mu$. This can be accomplished by using some insulator such as a typical plastic (polyethylene, teflon, an insulating epoxy, etc.) to fill the loop. The restriction on the relative conductivities applies during the intense radiation pulse which makes the air conducting and hopefully makes this other material conducting to a much lesser extent. Also assume that $\sigma >> \omega\varepsilon_\ell$. Then for frequencies such that δ/a is of order one, the skin depth or radian wavelength (as appropriate) inside the loop is much larger than the loop radius. Thus, for frequencies of interest Y_ℓ is one and for this case the response functions are of the form

$$R' = R'_y = \left[1 + Y'_{ext} + G_c\right]^{-1} \tag{100}$$

and

$$R = TR_y = T\left[1 + Y_{ext} + G_c\right]^{-1} \tag{101}$$

Again $g_c/\sigma<<1$ is necessary for optimum frequency response. The cylindrical loop below a ground plane is covered in figures 31 through 33. The exposed cylindrical loop is covered in figures 34 through 38. For $b/a = .1$ the upper frequency response for negligible g_c/σ occurs at a δ/a of about 2.8 for the loop below a ground plane and of about 2.6 for the exposed cylindrical loop. These figures represent about a 30% decrease in the characteristic δ/a or about double the upper frequency response. Thus, reducing the conductive load on the loop gap by making the conductivity inside the loop insignificant does improve the loop response characteristics.

V. Short Circuit Currents with External Insulating Dielectrics

Now consider a possible improvement of the cylindrical loop for $\sigma>>\omega\varepsilon$. This improvement consists of placing an insulator, of mathematically convenient geometry, on the outside of the loop structure so as to avoid, to some extent, the shorting effect of the conducting air across the loop gap. The insulator inside the loop is of course retained. As illustrated in figure 39A, the cylindrical loop below a ground plane has an insulating hemicylinder (of radius, d) above the ground plane, symmetrically located over the loop gap. The exposed cylindrical loop, as in figure 39B, has an insulating cylindrical shell of inner radius, a, and outer radius, d, completely around the loop and centered on the loop axis. The same notation is used for the short circuit currents, admittances, etc. A subscript one is used for the parameters of the added external medium. For the plots we only consider the case of $\mu_\ell = \mu_1 = \mu$ (or practically, μ_o), $\sigma_\ell<<\sigma$, and $\sigma_1<<\sigma$. All three permittivities are assumed to be small compared to σ/ω.

We would expect the upper frequency response to be determined by the larger of $|ka|$ and $|kd|$ which are of order one. The new dimension, d, can enter into this limitation in that the amplitude and phase of the incident wave can very over the extent of the external dielectric. Then for frequencies of interest (on the order of the upper frequency response or less), the restrictions on the parameters of two of the media make $|k_\ell a|<<1$ and $|k_1 a|<<1$, simplifying the form of the results somewhat. The additional external medium requires a recalculation of the short circuit current transfer functions and the normalized external admittances. We first consider the short circuit current transfer functions.

A. Cylindrical Loop Below Ground Plane

Consider the loop gap shorted for the cylindrical loop below a ground plane in figure 39A. The incident plane wave is of the form

$$H_{z_{inc}}(r',\phi') = H_{z_o} e^{-jkx'} = H_{z_o} e^{jkr'\sin(\phi')} \tag{102}$$

which, as in equations (13) and (14), gives two of the field components in cylindrical coordinates as

$$H_{z_{inc}}(r',\phi') = H_{z_o}\left[J_o(kr')+2\sum_{n=2}^{\infty,2} J_n(kr')\cos(n\phi')+j2\sum_{n=1}^{\infty,2} J_n(kr')\sin(n\phi')\right] \tag{103}$$

and

$$E_{\phi'_{inc}}(r';\phi') = jZH_{z_o}\left[J'_o(kr')+2\sum_{n=2}^{\infty,2} J'_n(kr')\cos(n\phi')+j2\sum_{n=1}^{\infty,2} J'_n(kr')\sin(n\phi')\right] \tag{104}$$

Due to the presence of the additional external medium we must add additional waves to match the boundary conditions. Inside the external insulating region there is a wave with two of the components as

$$H_{z'_1}(r';\phi') = H_{z_o}\left[a_oJ_o(k_1r')+2\sum_{n=2}^{\infty,2} a_nJ_n(k_1r')\cos(n\phi')+j2\sum_{n=1}^{\infty,2} a_nJ_n(k_1r')\sin(n\phi')\right] \tag{105}$$

and

$$E_{\phi'_1}(r';\phi') = jZ_1H_{z_o}\left[a_oJ'_o(k_1r')+2\sum_{n=2}^{\infty,2} a_nJ'_n(k_1r')\cos(n\phi')+j2\sum_{n=1}^{\infty,2} a_nJ'_n(k_1r')\sin(n\phi')\right] \tag{106}$$

The Bessel functions of the first kind are used so that the fields are finite at the origin. There is also a wave outside the dielectric, reflected from the structure, with two of the components as

$$H_{z'_{refl}}(r';\phi') = H_{z_o}\left[b_oH_o^{(2)}(kr')+2\sum_{n=2}^{\infty,2} b_nH_n^{(2)}(kr')\cos(n\phi')+j2\sum_{n=1}^{\infty,2} b_nH_n^{(2)}(kr')\sin(n\phi')\right] \tag{107}$$

and

$$E_{\phi'_{refl}}(r';\phi') = jZH_{z_o}\left[b_oH_o^{(2)'}(kr')+2\sum_{n=2}^{\infty,2} b_nH_n^{(2)'}(kr')\cos(n\phi')+j2\sum_{n=1}^{\infty,2} b_nH_n^{(2)'}(kr')\sin(n\phi')\right] \tag{108}$$

For this reflected wave the Hankel functions of the second kind are used to give an outward propagating wave.

The boundary conditions to be satisfied are that $H_{z'}$ and $E_{\phi'}$ are continuous at $r' = d$, giving from the magnetic field (equations (103), (105), and (107))

$$J_n(kd) + b_nH_n^{(2)}(kd) = a_nJ_n(k_1d) \tag{109}$$

and from the electric field (equations (104), (106), and (108))

$$ZJ_n'(kd)+b_nZH_n^{(2)'}(kd) = a_nZ_1J_n'(k_1d) \tag{110}$$

Solving these last two equations for a_n gives

$$a_n = \frac{J_n(kd)H_n^{(2)'}(kd)-J_n'(kd)H_n^{(2)}(kd)}{J_n(k_1d)H_n^{(2)'}(kd)-\frac{Z_1}{Z}J_n'(k_1d)H_n^{(2)}(kd)} \tag{111}$$

The wave impedances are replaced by

$$\frac{Z_1}{Z} = \frac{\mu_1}{\mu}\frac{k}{k_1} \tag{112}$$

Then in equation (111) expand the Hankel functions in the numerator, cancel terms, and apply a Wronskian relationship to give

$$a_n = \left\{ j\frac{\pi kd}{2}\left[J_n(k_1d)H_n^{(2)'}(kd)-\frac{\mu_1}{\mu}\frac{k}{k_1}J_n'(k_1d)H_n^{(2)}(kd)\right]\right\}^{-1} \tag{113}$$

Now (and for later use) we expand the Bessel functions and their derivatives for small arguments as

$$\begin{aligned}
&n = 0 \\
&\quad J_o(z) \simeq 1 && J_o'(z) = -J_1(z) \simeq -\frac{z}{2} \\
&\quad Y_o(z) \simeq \frac{2}{\pi}\ln(z) && Y_o'(z) = -Y_1(z) \simeq \frac{2}{\pi z} \\
&n \geq 1 \\
&\quad J_n(z) \simeq \frac{1}{n!}\left(\frac{z}{2}\right)^n && J_n'(z) \simeq \frac{1}{2(n-1)!}\left(\frac{z}{2}\right)^{n-1} \\
&\quad Y_n(z) \simeq -\frac{(n-1)!}{\pi}\left(\frac{z}{2}\right)^{-n} && Y_n'(z) \simeq \frac{n!}{2\pi}\left(\frac{z}{2}\right)^{-n-1}
\end{aligned} \tag{114}$$

Limiting the results now to the case of $\sigma >> \omega\varepsilon$, as discussed above, we constrain that $|k_1d| << 1$. The coefficients then considerably simplify. Consider then the individual terms for the magnetic field in the external insulator from equation (105) with the coefficients from equation (113). For n = 0,

$$a_o J_o(k_1 r') = \left\{ j\frac{\pi kd}{2} \left[H_o^{(2)'}(kd) + \frac{\mu_1}{\mu} \frac{kd}{2} H_o^{(2)}(kd) \right] \right\}^{-1} \tag{115}$$

which is independent of $k_1 d$. For $n \geq 1$ we have

$$a_n J_n(k_1 r') = \left(\frac{r}{d}\right)^n \left\{ j\frac{\pi kd}{2} \left[H_n^{(2)'}(kd) - \frac{\mu_1}{\mu} \frac{nkd}{(k_1 d)^2} H_n^{(2)}(kd) \right] \right\}^{-1} \tag{116}$$

which for small $|k_1 d|$ is proportional to $(k_1 d)^2$. Then in the limit of small $|k_1 d|$ only the n=0 term is important. This is significant in that for the case of interest the magnetic field in the external insulator is uniform, in spite of the fact that the magnetic field in the incident wave for $|kd|$ or order one can vary considerably over the extent, 2d, of the outer surface of this external insulator.

The short circuit surface current density at the loop gap is given by

$$J_{s_o} = H_{z_1'}(0,\phi') \tag{117}$$

(using previously established conventions). Since r'=0 for this calculation only the first term in equation (105) is nonzero. Also for the case being considered ($|k_1 d| \ll 1$), the first term is dominant for the magnetic field throughout the external insulator. The short circuit current transfer function (as before) is then (from equations (105) and (115))

$$T' = \frac{J_{s_o}}{H_{z_o}} = \left\{ j\frac{\pi kd}{2} \left[H_o^{(2)'}(kd) + \frac{\mu_1}{\mu} \frac{kd}{2} H_o^{(2)}(kd) \right] \right\}^{-1} \tag{118}$$

Or, for $\mu_1 = \mu$, this simplifies to

$$T' = \left\{ -j\frac{\pi}{4}(kd)^2 H_2^{(2)}(kd) \right\}^{-1} \tag{119}$$

This is plotted versus δ/d in figure 40A. However, notice the behavior of $|T'|$. For small δ/d it rapidly diverges. This is a physically unreasonable result because it indicates that instead of the loop response rolling off for high frequencies it increases very rapidly with frequency.

The problem lies in the manner of defining the loop response. We have considered the response to a plane wave by dividing the short circuit surface current density by the magnetic field in the incident wave extrapolated to the x'=0 plane. However, because $\sigma \gg \omega\varepsilon$ this plane wave is attenuating with the distance, x'. Thus, the magnetic field in the incident wave at the leading edge of the external insulator, x'=-d, can be much greater than the magnetic field in this wave at x'=0. It is the magnetic field at the leading edge of the insulator which is propagating into the insulator and

determining the short circuit surface current density. This would indicate that we need to redefine the short circuit current transfer function. Since the external insulator extends into the medium with the incident wave, perhaps it is not meaningful to consider the field that would be at r'=0 if the external insulator were not there, particularly for the case of $\sigma >> \omega\varepsilon$. Also, in the real case (measuring the close-in nuclear EMP), such a plane wave does not characterize the incident fields because the sensor is in a source region.

There may be various ways to define this short circuit current transfer function. The one we choose is that obtained by relating the short circuit surface current density to the average value of the magnetic field in the incident wave at the surface of the insulator. This is a reasonable definition in that the magnetic field inside the external insulator is uniform, irrespective of the direction of wave incidence (in the (r',ϕ') plane); only the first term (which has no ϕ' dependence) in the field expansion determines the field in this region. Inherent in this definition is the recognition that this kind of sensor cannot spatially resolve the incident wave to distances smaller than the appropriate sensor dimensions, without knowledge of some pertinent parameters of the incident wave, such as, whether or not it is a plane wave and, if so, what its direction of propagation is.

Conveniently, the average value (over ϕ' at constant r') in the incident wave is just given by the first term (n=0) in the expansion as in equation (103). Thus, a new short circuit current transfer function based on the average value of the incident magnetic field at r'=d is defined as

$$T'_{avg} = \frac{J_{s_o}}{H_{z_o} J_o(kd)} = \frac{T'}{J_o(kd)} = \left\{ j\frac{\pi kd}{2} J_o(kd) \left[H_o^{(2)'}(kd) + \frac{\mu_1}{\mu} \frac{kd}{2} H_o^{(2)}(kd) \right] \right\}^{-1} \tag{120}$$

As before for $\mu_1 = \mu$, this reduces to

$$T'_{avg} = \left\{ -j\frac{\pi}{4}(kd)^2 J_o(kd) H_2^{(2)}(kd) \right\}^{-1} \tag{121}$$

This is plotted versus δ/d in figure 40B. Note that T'_{avg} falls off for small δ/d, a reasonable behavior for such a frequency response curve. It is down to $1/\sqrt{2}$ at a δ/d of about .35, indicating a good upper frequency response for the short circuit surface current density.

Of course, this definition of the short circuit current transfer function is somewhat artificial, but it may be a reasonable one. At least it gives some quantitative limitation on the frequency response. There are perhaps other possible definitions of this transfer function, such as one relating the surface current density to the total magnetic field at r'=d (not just the incident field). However, for our limitation of $|k_1 d| << 1$, the transfer function would be unity for all frequencies of interest, providing no limitation on the frequency response which is expected because of the perturbations in the field due to the loop structure. This latter

definition would then be less reasonable. The definition leading to equation (121) still has limitations, however, in that the δ/d for upper frequency response is small enough that the incident wave has an extent of several skin depths across the structure, indicating that for such frequencies we cannot consider this as a measurement at one point in space. This is, however, still a small number of skin depths and we thus use this definition of the short circuit current transfer function in this note.

B. Exposed Cylindrical Loop

Short the loop gap for the exposed cylindrical loop in figure 39B. Again the incident plane wave is of the form

$$H_{z_{inc}}(r,\phi) = H_{z_o} e^{-jkx} = H_{z_o} e^{jkr\sin(\phi)} \tag{122}$$

which gives two of the field components in cylindrical coordinates as

$$H_{z_{inc}}(r,\phi) = H_{z_o}\left[J_o(kr)+2\sum_{n=2}^{\infty,2} J_n(kr)\cos(n\phi)+j2\sum_{n=1}^{\infty,2} J_n(kr)\sin(n\phi)\right] \tag{123}$$

and

$$E_{\phi_{inc}}(r,\phi) = jZH_{z_o}\left[J_o'(kr)+2\sum_{n=2}^{\infty,2} J_n'(kr)\cos(n\phi)+j2\sum_{n=1}^{\infty,2} J_n'(kr)\sin(n\phi)\right] \tag{124}$$

Inside the external insulating region ($a \leq r \leq d$) two components of the wave are

$$H_{z_1}(r,\phi) = H_{z_o}\left\{\left[a_oJ_o(k_1r)+b_oY_o(k_1r)\right]+2\sum_{n=2}^{\infty,2}\left[a_nJ_n(k_1r)+b_nY_n(k_1r)\right]\cos(n\phi)\right.$$
$$\left.+j2\sum_{n=1}^{\infty,2}\left[a_nJ_n(k_1r)+b_nY_n(k_1r)\right]\sin(n\phi)\right\} \tag{125}$$

and

$$E_{\phi_1}(r,\phi)=jZ_1H_{z_o}\left\{\left[a_oJ_o'(k_1r)+b_oY_o'(k_1r)\right]+2\sum_{n=2}^{\infty,2}\left[a_nJ_n'(k_1r)+b_nY_n'(k_1r)\right]\cos(n\phi)\right.$$
$$\left.+j2\sum_{n=1}^{\infty,2}\left[a_nJ_n'(k_1r)+b_nY_n'(k_1r)\right]\sin(n\phi)\right\} \tag{126}$$

The wave reflected from the structure has two components as

$$H_{z_{refl}}(r,\phi) = H_{z_o}\left[c_oH_o^{(2)}(kr)+2\sum_{n=2}^{\infty,2} c_nH_n^{(2)}(kr)\cos(n\phi)+j2\sum_{n=1}^{\infty,2} c_nH_n^{(2)}(kr)\sin(n\phi)\right] \tag{127}$$

and

$$E_{\phi_{refl}}(r,\phi) = jZH_{z_o}\left[c_o H_o^{(2)'}(kr)+2\sum_{n=2}^{\infty,2} c_n H_n^{(2)'}(kr)\cos(n\phi)+j2\sum_{n=1}^{\infty,2} c_n H_n^{(2)'}(kr)\sin(n\phi)\right] \tag{128}$$

The first boundary condition to be satisfied is that E_ϕ is zero at r=a giving from equation (126)

$$a_n J_n'(k_1 a) + b_n Y_n'(k_1 a) = 0 \tag{129}$$

or

$$\frac{b_n}{a_n} = -\frac{J_n'(k_1 a)}{Y_n'(k_1 a)} \tag{130}$$

At r=d the boundary conditions are that H_z and E_ϕ are continuous giving from the magnetic field (equations (123), (125), and (127))

$$J_n(kd)+c_n H_n^{(2)}(kd) = a_n J_n(k_1 d)+b_n Y_n(k_1 d) \tag{131}$$

and from the electric field (equations (124), (126), and (128))

$$ZJ_n'(kd)+c_n ZH_n^{(2)'}(kd) = a_n Z_1 J_n'(k_1 d)+b_n Z_1 Y_n'(k_1 d) \tag{132}$$

Combining these last two equations to remove c_n, substituting for b_n from equation (130), and solving for a_n gives

$$a_n = \frac{J_n(kd)H_n^{(2)'}(kd)-J_n'(kd)H_n^{(2)}(kd)}{\left\{J_n(k_1 d)-\frac{J_n'(k_1 a)}{Y_n'(k_1 a)}Y_n(k_1 d)\right\}H_n^{(2)'}(kd)-\frac{Z_1}{Z}\left\{J_n'(k_1 d)-\frac{J_n'(k_1 a)}{Y_n'(k_1 a)}Y_n'(k_1 d)\right\}H_n^{(2)}(kd)} \tag{133}$$

Simplifying the numerator and substituting for the wave impedances gives

$$a_n = \left\{j\frac{\pi kd}{2}\left[\left\{J_n(k_1 d)-\frac{J_n'(k_1 a)}{Y_n'(k_1 a)}Y_n(k_1 d)\right\}H_n^{(2)'}(kd) - \frac{\mu_1}{\mu}\frac{k}{k_1}\left\{J_n'(k_1 d)-\frac{J_n'(k_1 a)}{Y_n'(k_1 a)}Y'_n(k_1 d)\right\}H_n^{(2)}(kd)\right]\right\}^{-1} \tag{134}$$

We also have b_n from this last equation and equation (130).

Limiting the results now to the case of $\sigma >> \omega\varepsilon$, also let $|k_1 d| << 1$. The terms in the magnetic field expansion (equation (125)) in the external insulator simplify. Considering first the a_n terms we have for n=0

$$a_o J_o(k_1 r) = \left\{ j\frac{\pi kd}{2} \left[\left\{ 1 + \frac{(k_1 a)^2}{2} \ln(k_1 d) \right\} H_o^{(2)'}(kd) + \frac{\mu_1}{\mu} \frac{kd}{2} \left\{ 1 - \left|\frac{a}{d}\right|^2 \right\} H_o^{(2)}(kd) \right] \right\}^{-1} \tag{135}$$

and for $n \geq 1$

$$a_n J_n(k_1 r) = \left(\frac{r}{d}\right)^n \left\{ j\frac{\pi kd}{2} \left[\left\{ 1 + \left|\frac{a}{d}\right|^{2n} \right\} H_o^{(2)'}(kd) - \frac{\mu_1}{\mu} \frac{nkd}{(k_1 d)^2} \left\{ 1 - \left|\frac{a}{d}\right|^{2n} \right\} H_n^{(2)}(kd) \right] \right\}^{-1} \tag{136}$$

In the limit of small $|k_1 d|$, the n=0 term is independent of $k_1 d$ while the higher order terms are proportional to $(k_1 d)^2$. Thus, only the a_o term is important. Relating the b_n terms to the a_n terms from equations (125) and (130) for n=0,

$$\frac{b_o Y_o(k_1 r)}{a_o J_o(k_1 r)} = \frac{(k_1 a)^2}{2} \ln(k_1 r) \tag{137}$$

which goes to zero so that the b_o term can be neglected compared to the a_o term, and for $n \geq 1$

$$\frac{b_n Y_n(k_1 r)}{a_n J_n(k_1 r)} = \left(\frac{a}{r}\right)^{2n} \tag{138}$$

so that the b_n terms are of the same order as the a_n terms for $n \geq 1$. But since these a_n terms can be neglected compared to the a_o term, the b_n terms can likewise be neglected. Then in the limit of small $|k_1 d|$ only the a_o term is important, meaning that the magnetic field in the external insulator is uniform. This is the same as the result for the cylindrical loop below a ground plane.

The short circuit surface current density at the loop gap is given by

$$J_{s_o} = - H_{z_1}(a,0) \tag{139}$$

(using previously established conventions). Actually since the magnetic field is uniform throughout the external insulator the surface current density is independent of ϕ. The short circuit current transfer function (using the first definition) is then (from equations (125) and (135))

$$T = -\frac{J_{s_o}}{H_{z_o}} = \left\{ j\frac{\pi kd}{2} \left[-H_1^{(2)}(kd) + \frac{\mu_1}{\mu} \frac{kd}{2} \left\{ 1 - \left|\frac{a}{d}\right|^2 \right\} H_o^{(2)}(kd) \right] \right\}^{-1} \tag{140}$$

For $\mu_1 = \mu$, this is plotted versus δ/a with d/a as a parameter in figure 41. Again $|T|$ diverges rapidly for small δ/a, indicating the same problems as T'.

Note the use of d/a=1 in the curves. This is a limiting case of d/a. Remember that we first took the limiting case of $k_1 d = 0$. In doing this we have constrained the displacement and conduction currents in the external insulator to have negligible influence compared to those in the conducting air. However, this requires that there be such an insulating region in the first place. Without this additional region the short circuit current transfer function is as in equation (25) and plotted in figure 4. In equations (135) and (136) we can see that, for small but finite $|k_1 d|$, if d/a is set equal to one then the terms for $n \geq 1$ are no longer proportional to $(k_1 d)^2$ and are of the same order as the a_o term. Likewise the b_n terms for $n \geq 1$ also contribute to the sum for the magnetic field. Thus, the use of d/a = 1 is only meant in the sense of a limiting case. The limit is taken after the limit of $k_1 d = 0$ is taken. Actually d/a must be greater than one, how much greater depending on how small $|k_1 d|$ is for frequencies of interest.

As for the case of the cylindrical loop below a ground plane define a new short circuit current transfer function based on the average value of the incident magnetic field at r = d. This average value is just the first term in equation (123) giving

$$T_{avg} = -\frac{J_{s_o}}{H_{z_o} J_o(kd)} = \frac{T}{J_o(kd)} = \left\{ j\frac{\pi kd}{2} J_o(kd) \left[-H_1^{(2)}(kd) + \frac{\mu_1}{\mu} \frac{kd}{2} \left\{ 1 - \left(\frac{a}{d}\right)^2 \right\} H_o^{(2)}(kd) \right] \right\}^{-1} \tag{141}$$

For $\mu_1 = \mu$, this is plotted in figure 42, again giving a more reasonable short circuit current transfer function.

Since only the first term in the magnetic field expansion (which has no ϕ dependence) gives the short circuit current transfer function, the loop response is independent of the azimuthal (ϕ) direction of wave incidence. From another viewpoint the magnetic field in the external insulating region is independent of ϕ, as is the surface current density, so that it makes no difference at which ϕ the loop gap is placed. The external insulator somewhat isolates the loop conductors from the conducting air. The loop radius is ideally only a very small fraction of the radian wavelength or skin depth, as appropriate, in the external insulator. There is also assumed to be a sufficient thickness, d-a, of this insulator to maintain the isolation from the currents in the conducting air.

VI. External Admittances with External Insulating Dielectrics

Now reconsider the loop admittances. The normalized cable conductance remains the same. Likewise the normalized internal admittance is unchanged by the addition of external insulators and for the cases of interest in the remaining sections is just one for all frequencies of interest. However, the presence of the external insulators significantly changes the normalized external admittances which need to be recalculated for the new geometries.

A. Cylindrical Loop Below Ground Plane

Consider first the external admittance per unit length of the cylindrical loop below a ground plane using the geometry of figure 39A. As in the case without the external insulator take the first term in the field expansion with a correction for the field distribution near the loop gap. Since we are interested in the case in which $\sigma >> \omega\varepsilon$ but $|k_1 d| << 1$ the currents (conduction plus displacement) in the external insulator are insignificant compared to those in the conducting air. Thus, we do not correct for the capacitance and conductance, but rather for the inductance in the vicinity of the loop gap.

Inside the external insulating region there is then a wave with two of the components as

$$H_{z_1'}(r';\phi') \approx H_{z_o}\left[a_o J_o(k_1 r') + b_o Y_o(k_1 r')\right] \tag{142}$$

and

$$E_{\phi_1'}(r';\phi') \approx jZ_1 H_{z_o}\left[a_o J_o'(k_1 r') + b_o Y_o'(k_1 r')\right] \tag{143}$$

Outside the insulator there is a wave with two of the components as

$$H_{z'}(r';\phi') \approx H_{z_o} c_o H_o^{(2)}(kr') \tag{144}$$

and

$$E_{\phi'}(r';\phi') \approx jZH_{z_o} c_o H_o^{(2)'}(kr') \tag{145}$$

The boundary conditions to be satisfied are that $H_{z'}$ and $E_{\phi'}$ are continuous at $r' = d$ giving from the magnetic field

$$a_o J_o(k_1 d) + b_o Y_o(k_1 d) = c_o H_o^{(2)}(kd) \tag{146}$$

and from the electric field

$$a_o Z_1 J_o'(k_1 d) + b_o Z_1 Y_o'(k_1 d) = c_o Z H_o^{(2)'}(kd) \tag{147}$$

Removing c_o from these last two equations gives

$$\frac{b_o}{a_o} = -\frac{H_o^{(2)'}(kd) Z J_o(k_1 d) - H_o^{(2)}(kd) Z_1 J_o'(k_1 d)}{H_o^{(2)'}(kd) Z Y_o(k_1 d) - H_o^{(2)}(kd) Z_1 Y_o'(k_1 d)} \tag{148}$$

Setting $r' = b$ we have

$$\pi b E_{\phi_1'}(b,\phi') \approx -V_{gap} \tag{149}$$

giving from equation (143)

$$a_o \simeq \frac{jV_{gap}}{\pi b Z_1 H_{z_o}} \left[J_o'(k_1 b) + \frac{b_o}{a_o} Y_o'(k_1 b) \right]^{-1} \tag{150}$$

The surface current density is

$$J_{s_{ext}} = -H_{z_1}'(b, \pm \frac{\pi}{2}) \simeq -H_{z_o} a_o \left[J_o(k_1 b) + \frac{b_o}{a_o} Y_o(k_1 b) \right] \tag{151}$$

The admittance per unit length is then

$$y'_{ext} = \frac{J_{s_{ext}}}{V_{gap}} \simeq -\frac{j}{\pi b Z_1} \frac{J_o(k_1 b) + \frac{b_o}{a_o} Y_o(k_1 b)}{J_o'(k_1 b) + \frac{b_o}{a_o} Y_o'(k_1 b)} \tag{152}$$

Substituting from equation (148) for b_o/a_o and rearranging terms, then

$$y'_{ext} \simeq -\frac{j}{\pi b Z_1} \frac{\left\{ \begin{array}{l} J_o(k_1 b)[H_o^{(2)'}(kd) Z Y_o(k_1 d) - H_o^{(2)}(kd) Z_1 Y_o'(k_1 d)] \\ \quad - Y_o(k_1 b)[H_o^{(2)'}(kd) Z J_o(k_1 d) - H_o^{(2)}(kd) Z_1 J_o'(k_1 d)] \end{array} \right\}}{\left\{ \begin{array}{l} J_o'(k_1 b)[H_o^{(2)'}(kd) Z Y_o(k_1 d) - H_o^{(2)}(kd) Z_1 Y_o'(k_1 d)] \\ \quad - Y_o'(k_1 b)[H_o^{(2)'}(kd) Z J_o(k_1 d) - H_o^{(2)}(kd) Z_1 J_o'(k_1 d)] \end{array} \right\}}$$

$$= -\frac{j}{\pi b Z_1} \frac{\left\{ \begin{array}{l} H_o^{(2)'}(kd) Z [J_o(k_1 b) Y_o(k_1 d) - J_o(k_1 d) Y_o(k_1 b)] \\ \quad - H_o^{(2)}(kd) Z_1 [J_o(k_1 b) Y_o'(k_1 d) - J_o'(k_1 d) Y_o(k_1 b)] \end{array} \right\}}{\left\{ \begin{array}{l} H_o^{(2)'}(kd) Z [J_o'(k_1 b) Y_o(k_1 d) - J_o(k_1 d) Y_o'(k_1 b)] \\ \quad - H_o^{(2)}(kd) Z_1 [J_o'(k_1 b) Y_o'(k_1 d) - J_o'(k_1 d) Y_o'(k_1 b)] \end{array} \right\}}$$

$$- \frac{H_o^{(2)'}(kd)Z}{H_o^{(2)}(kd)Z_1} \frac{J_o(k_1b)Y_o(k_1d)-J_o(k_1d)\,Y_o(k_1b)}{J_o(k_1b)Y_o'(k_1d)-J_o'(k_1d)Y_o(k_1b)} + 1$$

$$= -\frac{j}{\pi b Z_1} \left\{ - \frac{H_o^{(2)'}(kd)Z}{H_o^{(2)}(kd)Z_1} \frac{J_o'(k_1b)Y_o(k_1d)-J_o(k_1d)Y_o'(k_1b)}{J_o(k_1b)Y_o'(k_1d)-J_o'(k_1d)Y_o(k_1b)} + \frac{J_o'(k_1b)Y_o'(k_1d)-J_o'(k_1d)Y_o'(k_1b)}{J_o(k_1b)Y_o'(k_1d)-J_o'(k_1d)Y_o(k_1b)} \right\} \tag{153}$$

Substituting for the wave impedances from equation (112) and letting $|k_1 d| << 1$, expand the appropriate Bessel functions for small arguments giving

$$y'_{ext} \approx -\frac{j}{\pi b Z_1} \frac{- \frac{H_o^{(2)'}(kd)}{H_o^{(2)}(kd)} \frac{\mu}{\mu_1} \frac{(k_1 d)^2}{kd} \ln\left(\frac{d}{b}\right) + 1}{\frac{H_o^{(2)'}(kd)}{H_o^{(2)}(kd)} \frac{\mu}{\mu_1} \frac{k_1 d}{kd} \frac{d}{b} + \frac{k_1}{2b}[d^2-b^2]} \tag{154}$$

Neglecting the first term in the numerator because it is proportional to $(k_1 d)^2$ and using

$$k_1 Z_1 = \omega \mu_1 \tag{155}$$

then

$$y'_{ext} \approx \left\{ j \frac{\omega \mu \pi d}{k} \frac{H_o^{(2)'}(kd)}{H_o^{(2)}(kd)} + j \frac{\omega \mu_1 \pi}{2} [d^2-b^2] \right\}^{-1} \tag{156}$$

Considering small $|k_1 d|$ then leads to a considerable simplification in the form of the result. Looking at this last equation note that the external admittance per unit length is the series combination of an inductance attributable to the external insulator (the last term in the braces) and the impedance of the external medium (the first term in the braces).

Note the factor $\pi[d^2-b^2]/2$ in the term for the inductance of the external insulator. This is just the cross section area of the external insulator except for a small area $\pi b^2/2$. This is accounted for by noting that the electric field is related to V_{gap} in equation (149) by an integral

along a path constrained by r'=b instead of directly across the loop gap. The area enclosed by these two paths is precisely $\pi b^2/2$. Thus, correct y'_{ext} to give

$$y'_{ext} = \left\{ -j\frac{\omega\mu\pi d}{k} \frac{H_1^{(2)}(kd)}{H_o^{(2)}(kd)} + j\frac{\omega\mu_1\pi d^2}{2} \right\}^{-1} \tag{157}$$

which is no longer a function of the loop gap width,2b. Multiplying by $j\omega\mu_\ell\pi a^2$ we have in normalized form

$$Y'_{ext} = \frac{\mu_\ell}{\mu_1} 2 \left(\frac{a}{d}\right)^2 \left\{ 1 - \frac{\mu}{\mu_1} \frac{2}{kd} \frac{H_1^{(2)}(kd)}{H_o^{(2)}(kd)} \right\}^{-1} \tag{158}$$

Rearranging this gives

$$\frac{\mu_1}{\mu_\ell}\left(\frac{d}{a}\right)^2 Y'_{ext} = 2 \left\{ 1 - \frac{\mu}{\mu_1} \frac{2}{kd} \frac{H_1^{(2)}(kd)}{H_o^{(2)}(kd)} \right\}^{-1} \tag{159}$$

such that the right side is independent of a. Considering the case of $\mu_\ell = \mu_1 = \mu$ and $\sigma >> \omega\varepsilon$, this normalized admittance is plotted versus δ/d in figure 43. Note that in the limit of small $|kd|$ the normalized admittance is arbitrarily small.

B. Exposed Cylindrical Loop

Turning to the external admittance per unit length of the exposed cylindrical loop we have the geometry of figure 39B. Inside the external insulator there is a wave with two of the components as

$$H_{z_1}(r,\phi) = H_{z_o} \left\{ \left[a_o J_o(k_1 r) + b_o Y_o(k_1 r) \right] + 2\sum_{n=1}^{\infty} \left[a_n J_n(k_1 r) + b_n Y_n(k_1 r) \right] \cos(n\phi) \right\} \tag{160}$$

and

$$E_{\phi_1}(r,\phi) = jZ_1 H_{z_o} \left\{ \left[a_o J'_o(k_1 r) + b_o Y'_o(k_1 r) \right] + 2\sum_{n=1}^{\infty} \left[a_n J'_n(k_1 r) + b_n Y'_n(k_1 r) \right] \cos(n\phi) \right\} \tag{161}$$

Outside the insulator the two components are

$$H_z(r,\phi) = H_{z_o} \left[c_o H_o^{(2)}(kr) + 2\sum_{n=1}^{\infty} c_n H_n^{(2)}(kr) \cos(n\phi) \right] \tag{162}$$

and

$$E_\phi(r,\phi) = jZH_{z_o}\left[c_o H_o^{(2)'}(kr)+2\sum_{n=1}^{\infty} c_n H_n^{(2)'}(kr)\cos(n\phi)\right] \tag{163}$$

Since H_z and E_ϕ are continuous at r=d, then from the magnetic field

$$a_n J_n(k_1 d)+b_n Y_n(k_1 d) = c_n H_n^{(2)}(kd) \tag{164}$$

and from the electric field

$$a_n Z_1 J_n'(k_1 d)+b_n Z_1 Y_n'(k_1 d) = c_n Z H_n^{(2)'}(kd) \tag{165}$$

Removing c_n gives

$$\frac{b_n}{a_n} = -\frac{H_n^{(2)'}(kd)ZJ_n(k_1 d) - H_n^{(2)}(kd)Z_1 J_n'(k_1 d)}{H_n^{(2)'}(kd)ZY_n(k_1 d) - H_n^{(2)}(kd)Z_1 Y_n'(k_1 d)} \tag{166}$$

At r = a, E_ϕ is zero except in the loop gap where it is given by equation (34). Equating this distribution for $E(a,\phi)$ with that from equation (161), multiplying each by $\cos(n\phi)$, and integrating over ϕ from 0 to 2π gives

$$-\frac{V_{gap}}{a\phi_o}\int_{-\phi_o}^{\phi_o} f\left(\frac{\phi}{\phi_o}\right)\cos(n\phi)d\phi = j2\pi Z_1 H_{z_o} a_n\left[J_n'(k_1 a)+\frac{b_n}{a_n}Y_n'(k_1 a)\right] \tag{167}$$

Or, using the results of equation (42)

$$a_n = \frac{jV_{gap}J_o(n\phi_o)}{2\pi a Z_1 H_{z_o}}\left[J_n'(k_1 a)+\frac{b_n}{a_n}Y_n'(k_1 a)\right]^{-1} \tag{168}$$

The surface current density is

$$J_{s_{ext}} = -H_{z_1}(a,\pm\phi_o) \tag{169}$$

The external admittance per unit length is then

$$y_{ext} = \frac{J_{s_{ext}}}{V_{gap}} = -\frac{j}{2\pi a Z_1}\left[\frac{J_o(k_1 a)+\frac{b_o}{a_o}Y_o(k_1 a)}{J_o'(k_1 a)+\frac{b_o}{a_o}Y_o'(k_1 a)} + 2\sum_{n=1}^{\infty}\frac{J_n(k_1 a)+\frac{b_n}{a_n}Y_n(k_1 a)}{J_n'(k_1 a)+\frac{b_n}{a_n}Y_n'(k_1 a)}J_o(n\phi_o)\cos(n\phi_c\right. \tag{170}$$

Considering the nth term and substituting for b_n/a_n, then

$$\frac{J_n(k_1a)+\frac{b_n}{a_n}Y_n(k_1a)}{J_n'(k_1a)+\frac{b_n}{a_n}Y_n'(k_1a)}$$

$$= \frac{\left\{\begin{array}{l} J_n(k_1a)[H_n^{(2)'}(kd)ZY_n(k_1d)-H_n^{(2)}(kd)Z_1Y_n'(k_1d)] \\ \qquad -Y_n(k_1a)[H_n^{(2)'}(kd)ZJ_n(k_1d)-H_n^{(2)}(kd)Z_1J_n'(k_1d)] \end{array}\right\}}{\left\{\begin{array}{l} J_n'(k_1a)[H_n^{(2)'}(kd)ZY_n(k_1d)-H_n^{(2)}(kd)Z_1Y_n'(k_1d)] \\ \qquad -Y_n'(k_1a)[H_n^{(2)'}(kd)ZJ_n(k_1d)-H_n^{(2)}(kd)Z_1J_n'(k_1d)] \end{array}\right\}}$$

$$= \frac{\left\{\begin{array}{l} H_n^{(2)'}(kd)Z[J_n(k_1a)Y_n(k_1d)-J_n(k_1d)Y_n(k_1a)] \\ \qquad -H_n^{(2)}(kd)Z_1[J_n(k_1a)Y_n'(k_1d)-J_n'(k_1d)Y_n(k_1a)] \end{array}\right\}}{\left\{\begin{array}{l} H_n^{(2)'}(kd)Z[J_n'(k_1a)Y_n(k_1d)-J_n(k_1d)Y_n'(k_1a)] \\ \qquad -H_n^{(2)}(kd)Z_1[J_n'(k_1a)Y_n'(k_1d)-J_n'(k_1d)Y_n'(k_1a)] \end{array}\right\}}$$

$$- \frac{H_n^{(2)'}(kd)Z}{H_n^{(2)}(kd)Z_1}\frac{J_n(k_1a)Y_n(k_1d)-J_n(k_1d)Y_n(k_1a)}{J_n(k_1a)Y_n'(k_1d)-J_n'(k_1d)Y_n(k_1a)} + 1$$

$$= \frac{}{- \frac{H_n^{(2)'}(kd)Z}{H_n^{(2)}(kd)Z_1}\frac{J_n'(k_1a)Y_n(k_1d)-J_n(k_1d)Y_n'(k_1a)}{J_n(k_1a)Y_n'(k_1d)-J_n'(k_1d)Y_n(k_1a)} + \frac{J_n'(k_1a)Y_n'(k_1d)-J_n'(k_1d)Y_n'(k_1a)}{J_n(k_1a)Y_n'(k_1d)-J_n'(k_1d)Y_n(k_1a)}}$$

(171)

Substituting for the wave impedances from equation (112) and letting $|k_1 d| \ll 1$, expand the appropriate Bessel functions for small arguments. For n=0 this gives

$$\frac{J_o(k_1 a)+\frac{b_o}{a_o}Y_o(k_1 a)}{J_o'(k_1 a)+\frac{b_o}{a_o}Y_o'(k_1 a)} = \frac{-\frac{H_o^{(2)'}(kd)}{H_o^{(2)}(kd)}\frac{\mu}{\mu_1}\frac{(k_1 d)^2}{kd}\ln\left(\frac{d}{a}\right)+1}{\frac{H_o^{(2)'}(kd)}{H_o^{(2)}(kd)}\frac{\mu}{\mu_1}\frac{k_1 d}{kd}\frac{d}{a}+\frac{k_1}{2a}[d^2-a^2]} \tag{172}$$

Neglecting the first term in the numerator because it is proportional to $(k_1 d)^2$, this n=0 term is then proportional to $(k_1 d)^{-1}$. For $n \geq 1$ we have

$$\frac{J_n(k_1 a)+\frac{b_n}{a_n}Y_n(k_1 a)}{J_n'(k_1 a)+\frac{b_n}{a_n}Y_n'(k_1 a)} = \frac{-\frac{H_o^{(2)'}(kd)}{H_n^{(2)}(kd)}\frac{\mu}{\mu_1}\frac{(k_1 d)^2}{kd}\frac{1-\left(\frac{a}{d}\right)^{2n}}{1+\left(\frac{a}{d}\right)^{2n}}+1}{\frac{H_n^{(2)'}(kd)}{H_n^{(2)}(kd)}\frac{\mu}{\mu_1}\frac{k_1 d}{kd}\frac{d}{a}-\frac{n}{k_1 d}\frac{d}{a}\frac{1-\left(\frac{a}{d}\right)^{2n}}{1+\left(\frac{a}{d}\right)^{2n}}} \tag{173}$$

For a/d < 1 and for small $|k_1 d|$ this general term is proportional to $k_1 d$ and is thus negligible compared to the n=0 term. Then keeping only the n=0 term and combining Z_1 with k_1 as in equation (155)

$$y_{ext} = \left\{ -j\frac{\omega\mu 2\pi d}{k}\frac{H_1^{(2)}(kd)}{H_o^{(2)}(kd)} + j\omega\mu_1\pi[d^2-a^2] \right\}^{-1} \tag{174}$$

Again consideration of small $|k_1 d|$ has lead to a significant simplification in the form of the result. Looking at the form of this last equation, note that, as with the cylindrical loop below a ground plane, the external admittance per unit length is the series combination of an inductance associated with the external insulator and the impedance of the external medium (driven at the surface of the external insulator).

In normalized form then

$$Y_{ext} = \frac{\mu_\ell}{\mu_1}\left(\frac{a}{d}\right)^2\left\{1-\left(\frac{a}{d}\right)^2-\frac{\mu}{\mu_1}\frac{2}{kd}\frac{H_1^{(2)}(kd)}{H_o^{(2)}(kd)}\right\}^{-1} \tag{175}$$

For $\mu_\ell = \mu_1 = \mu$ and $\sigma \gg \omega\varepsilon$ this normalized admittance is plotted versus δ/a with d/a as a parameter in figure 44. As with the short circuit current transfer function, the case of d/a=1 is a limiting case. The limit of $k_1 d=0$ is taken first, and d/a must actually be at least a little larger than one.

VII. Frequency Response Characteristics with External Insulating Dielectrics

For this case in which the insulators are used both inside and outside the loop, we are only interested in the limits of $\sigma >> \omega\varepsilon$ and $|k_1 d| << 1$. Also constrain that $\mu_\ell = \mu_1 = \mu$. Conveniently Y_ℓ is then just one. Using the short circuit current transfer functions and normalized external admittances from the previous two sections, we can then calculate the response functions and compare the results to those obtained without the external dielectric.

A. Cylindrical Loop Below Ground Plane

The cylindrical loop below a ground plane now has response functions of the form

$$R'_y = [1 + Y'_{ext} + G_c]^{-1} \tag{176}$$

and

$$R'_{avg} = T'_{avg}\, R'_y \tag{177}$$

where we have defined a new response function, R'_{avg}, to be used with the short circuit current transfer function, T'_{avg}. Considering the effects of the normalized admittances,

$$R'_y = \left\{ 1+2\left(\frac{a}{d}\right)^2 \left[1 - \frac{2}{kd} \frac{H_1^{(2)}(kd)}{H_o^{(2)}(kd)} \right]^{-1} - \pi(ka)^2 \frac{g_c}{\sigma} \right\}^{-1} \tag{178}$$

This is plotted in figure 45 versus δ/a with d/a as a parameter and with $g_c/\sigma = 0$. Note that for large d/a this response function falls off very little for small δ/a.

Using T'_{avg} from equation (121), R'_{avg} is then calculated. It is plotted in figure 46 versus δ/a with d/a as a parameter and with $g_c/\sigma = 0$. In figure 47 it is replotted but with g_c/σ as the parameter for a specific d/a of 2. As summarized in figure 48 optimum upper frequency response is obtained with negligible g_c/σ and for d/a somewhere between $1/\sqrt{2}$ and 2. This optimum upper frequency response corresponds to a δ/a of about 1.1. Comparing these results to the case of no external insulator, but insulator inside the loop, the addition of the external insulator has decreased the characteristic δ/a by about 60% or has raised the upper frequency response by a factor of about 6.5. Compared to the case of no insulators, external or internal, these results represent a decrease in the characteristic δ/a of about 70%, or an increase in the upper frequency response of a factor of about 12, better than an order of magnitude. The use of an external insulator (together with the internal insulator) then represents a considerable improvement in the response characteristics of the cylindrical loop below a ground plane.

B. Exposed Cylindrical Loop

The exposed cylindrical loop now has response functions of the form

$$R_y = [1+Y_{ext}+G_c]^{-1} \tag{179}$$

and

$$R_{avg} = T_{avg} R_y \tag{180}$$

where again we have defined a new response function, R_{avg}, to be used with the short circuit current transfer function, T_{avg}. From the normalized admittances,

$$R_y = \left\{ 1 + \left(\frac{a}{d}\right)^2 \left[1 - \left(\frac{a}{d}\right)^2 - \frac{2}{kd} \frac{H_1^{(2)}(kd)}{H_o^{(2)}(kd)} \right]^{-1} - \pi(ka)^2 \frac{g_c}{\sigma} \right\}^{-1} \tag{181}$$

which is plotted in figure 49 versus δ/a with d/a as a parameter and with $g_c/\sigma = 0$. Again for large d/a the response function falls off very little for small δ/a.

Using T_{avg} from equation (141) we also have R_{avg}. Conveniently there is a special case of R_{avg} given by $g_c/\sigma = 0$ in which the form of the result simplifies to

$$R_{avg}\Big|_{\frac{g_c}{\sigma}=0} = \left\{ -j\frac{\pi}{4}(kd)^2 J_o(kd) H_2^{(2)}(kd) \right\}^{-1} \tag{182}$$

which is independent of a. This is plotted versus δ/d in figure 50. Note that this is of the same form as T'_{avg} in equation (121) showing that for this case of $g_c/\sigma = 0$, R_{avg} is just the response function for the penetration of magnetic field (parallel to the loop axis) into an insultaing cylinder of radius, d, immersed in a conducting medium. Figure 51 has R_{avg} plotted against δ/a with g_c/σ as a parameter for the limiting case of $d/a = 1$. Figure 52 summarizes the results for the upper frequency response. As expected, optimum upper frequency response requires negligible g_c/σ (say small compared to .1). Note that optimum upper frequency response occurs for the limiting case of $d/a = 1$ for which the characteristic δ/a is about .35. As discussed before, d/a must actually be somewhat larger than one if the short circuit current transfer function and normalized external admittance are to have the forms developed in sections V B and VI B, respectively. Comparing these results to those for no external insulator, but insulator inside the loop, the characteristic δ/a has been decreased by about 87% and the upper frequency response has been increased by a factor of about 55. Compared to the case of no insulators, external or internal, these results give a decrease in the characteristic δ/a of about 90%, or an increase in the upper frequency response of a factor of about 110, better than two orders of magnitude. Of course, the requirement of making d/a a little larger than one lowers this frequency response improvement somewhat. Also, such

a small characteristic δ/a brings us back to the problem of the definition of the short circuit current transfer function because the incident magnetic field is several skin depths in extent across the loop structure at the upper frequency response limit. In any case, however, the use of an external insulator (together with the internal insulator) represents a large improvement in the response characteristics of the exposed cylindrical loop.

VIII. Summary

Considering two types of cylindrical loop, the cylindrical loop below a ground plane and the exposed cylindrical loop, these loops are both assumed to have axial lengths much greater than their radii. Also, the resistive signal cable loading at the loop gap is assumed to be uniformly distributed along the length of the loop. Calculating the response of such a loop to an incident plane wave with the magnetic field parallel to the loop axis, the solution is then only a two dimensional problem. Only one orientation (an optimum one) of the loop gap with respect to the direction of wave propagation is considered. This is because the purpose of this note is to compare the frequency responses of this type of loop in different kinds of media and in some different configurations (to improve the frequency response).

The case of negligible air conductivity is considered first. The upper frequency response is given from the result that the radian wavelength is of the order of the loop radius. An optimum (non zero) cable conductance per unit length is required to dampen the first resonance and thus optimize the frequency response characteristics.

Then the case of $\sigma >> \omega\varepsilon$ is considered. For this solution the air conductivity is assumed independent of both time and the electric field. For this high air conducitivity three variations on the design of the cylindrical loop are considered for their frequency response characteristics. First, no insulators are used so that a high air conductivity is present both inside and outside the loop. Next, the inside of the loop is filled with an insulator to exclude the high air conductivity from the inside, and then an insulator is used both inside and outside the loop structure to exclude the high air conductivity from the immediate vicinity of the loop. For each of these variations the upper frequency response is given by a skin depth in the air which is of the order of the loop radius. Note that there is a significant improvement with each addition of a local insulating medium. This is most pronounced for the exposed cylindrical loop in that progressing from no insulators to both internal and external insulators results in about an order of magnitude relative decrease in the characteristic δ/a for upper frequency response. Or, this produces about two orders of magnitude relative increase in the upper frequency response. For optimum frequency responses it is also necessary for the cable conductance per unit length to be sufficiently small compared to the air conductivity.

However, there are other problems associated with the high air conductivity case. Since in measurements of the close-in nuclear EMP the sensor is in a source region, a plane wave without local sources does not accurately describe the field distribution. Thus, the short circuit current transfer functions are somewhat artificial. Also the air conductivity in this source region is nonlinear and time varying. This makes the analysis somewhat approximate for such a situation.

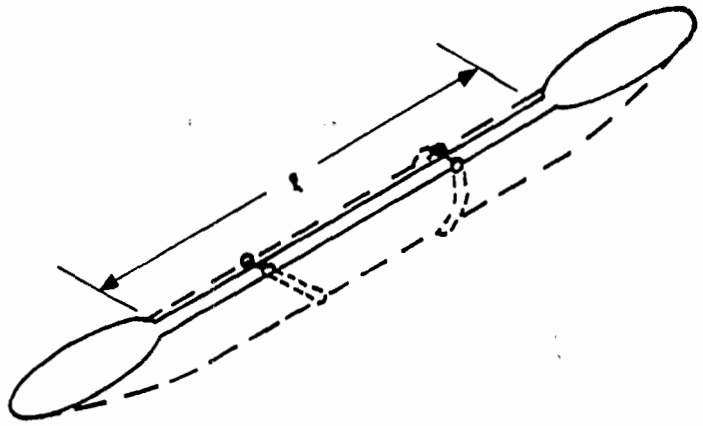

A. ANGULAR VIEW

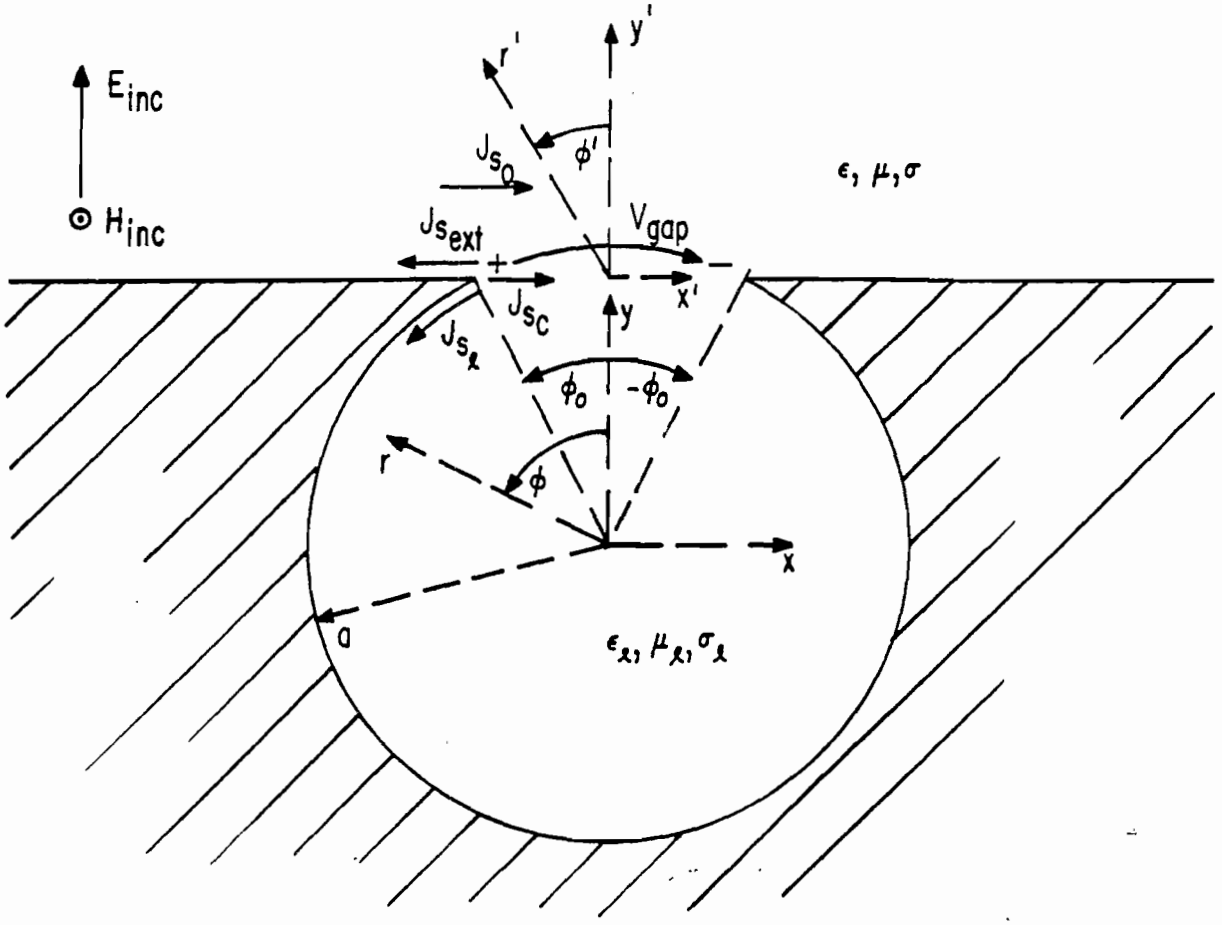

B. CROSS SECTION

FIGURE 1. CYLINDRICAL LOOP BELOW GROUND PLANE

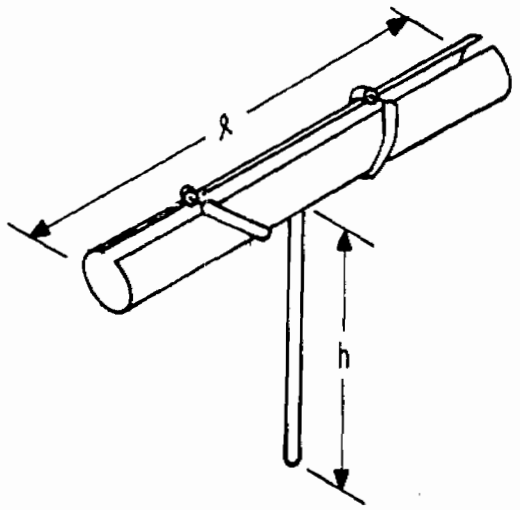

A. ANGULAR VIEW

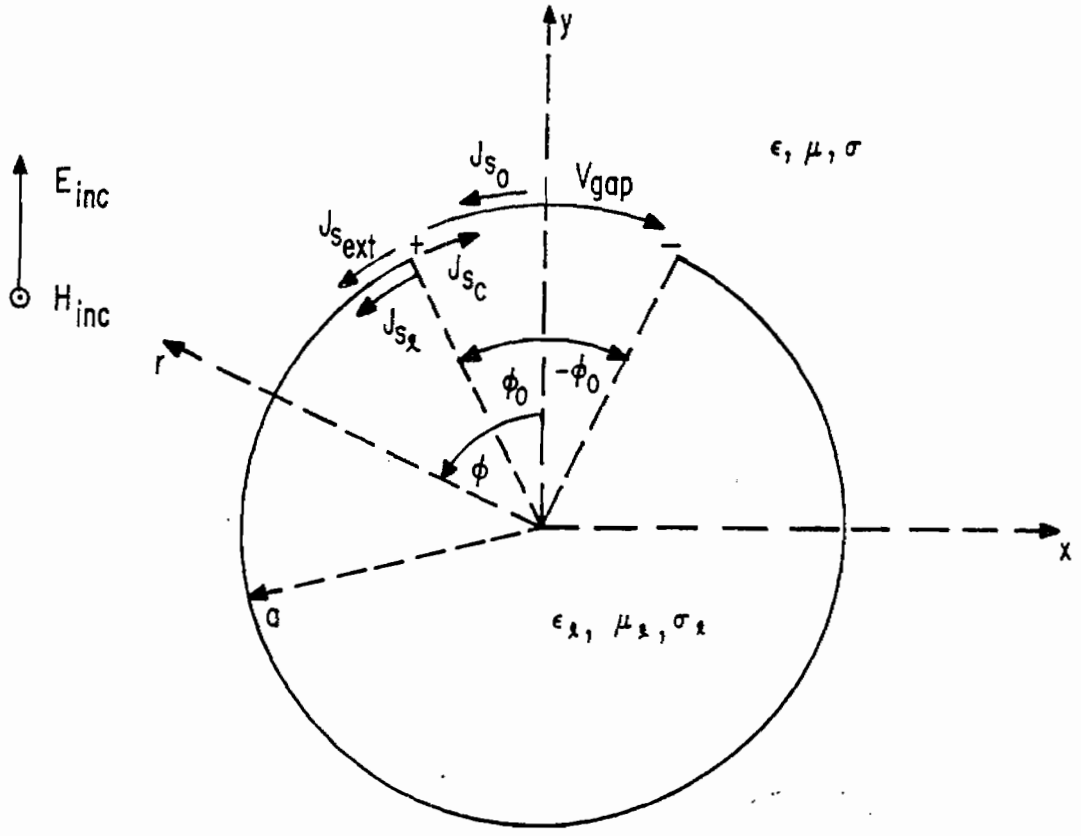

B. CROSS SECTION

FIGURE 2. EXPOSED CYLINDRICAL LOOP

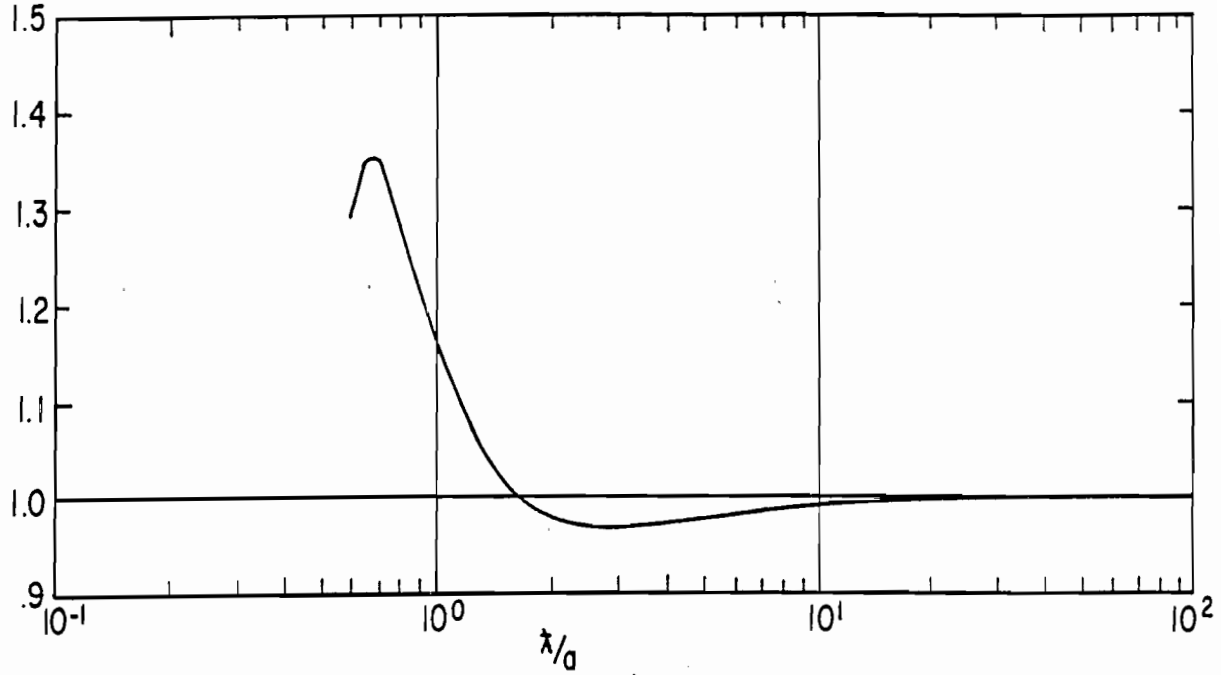

A. MAGNITUDE OF T vs. λ/a

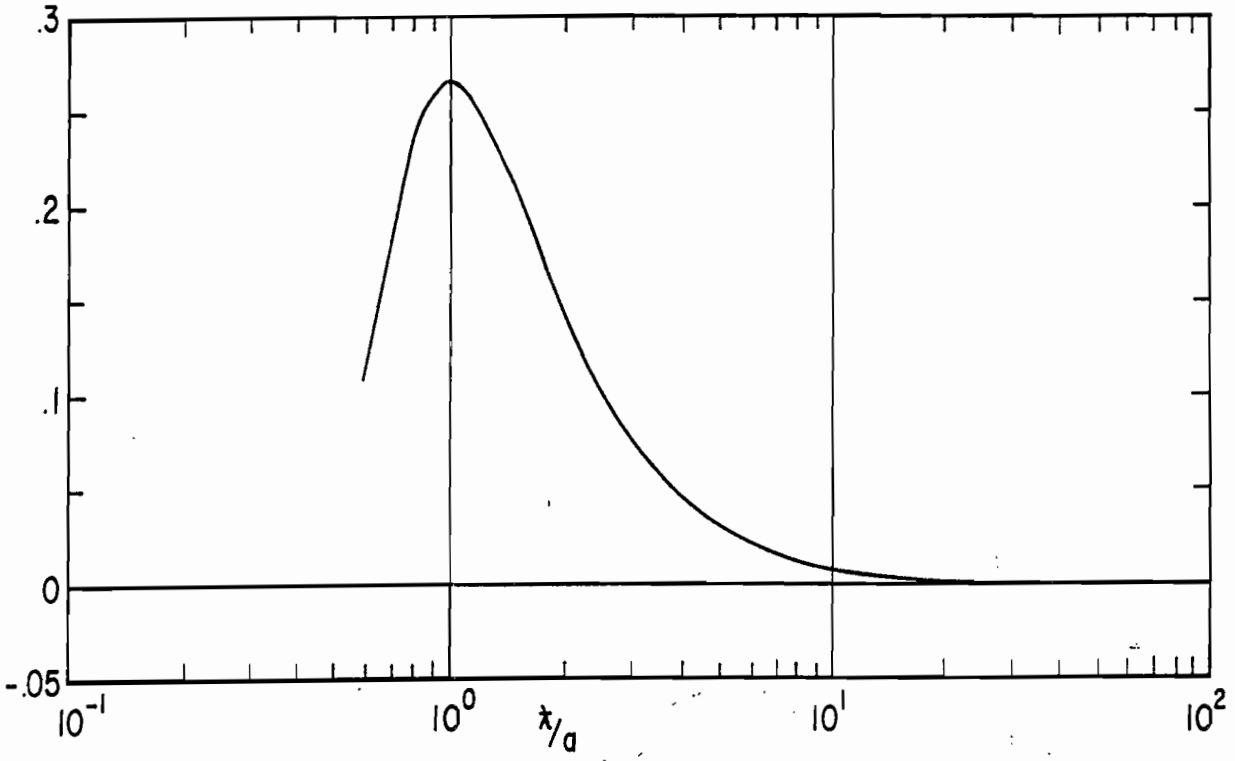

B. PHASE OF T vs. λ/a

FIGURE 3. SHORT CIRCUIT CURRENT TRANSFER FUNCTION FOR EXPOSED CYLINDRICAL LOOP WITH NO CONDUCTIVITY

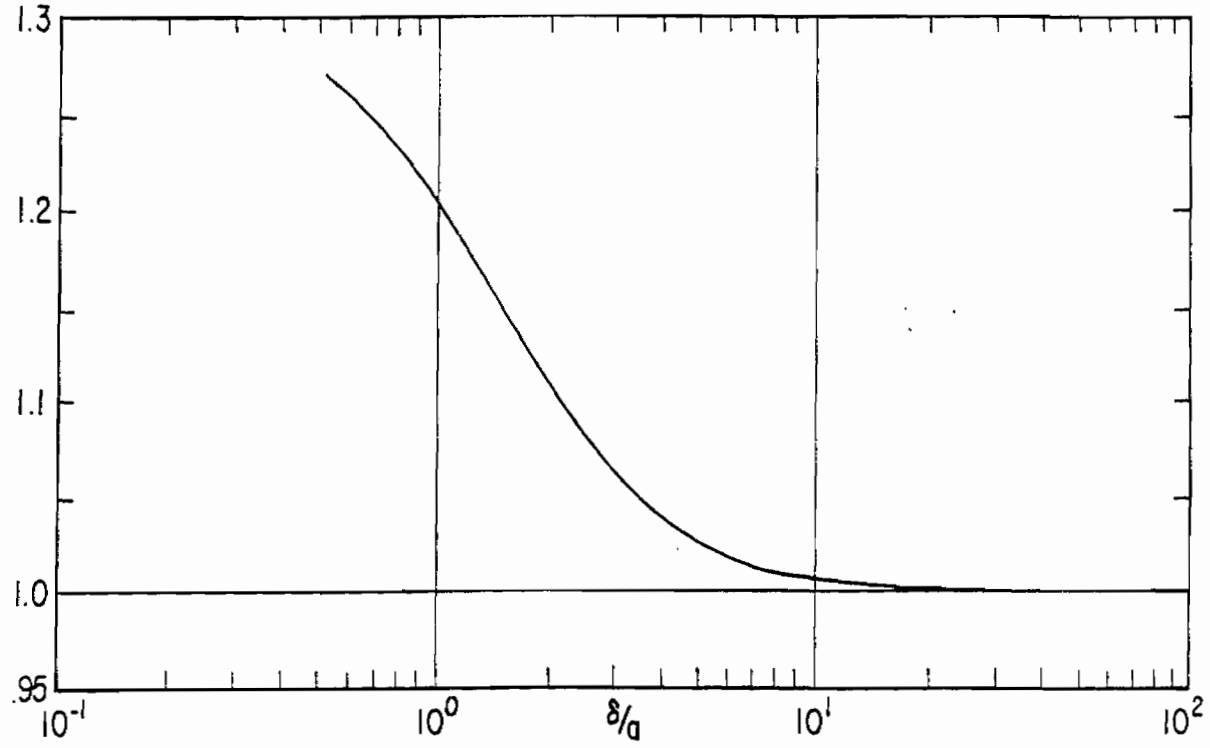

A. MAGNITUDE OF T vs. δ/a

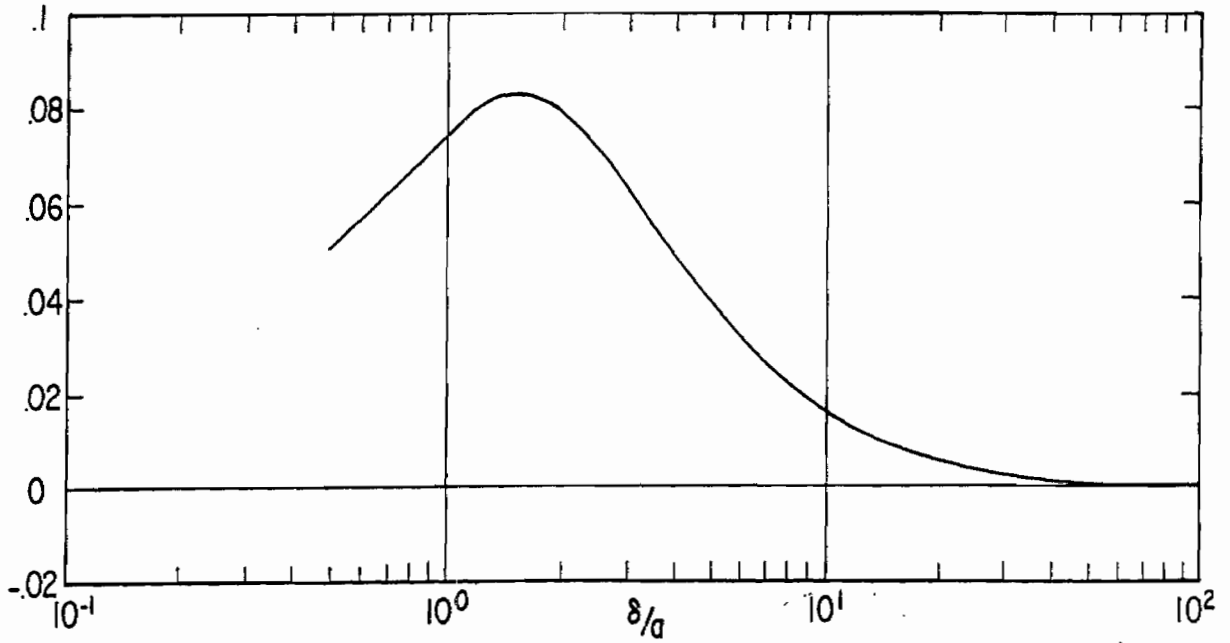

B. PHASE OF T vs. δ/a

FIGURE 4. SHORT CIRCUIT CURRENT TRANSFER FUNCTION FOR EXPOSED CYLINDRICAL LOOP WITH HIGH CONDUCTIVITY

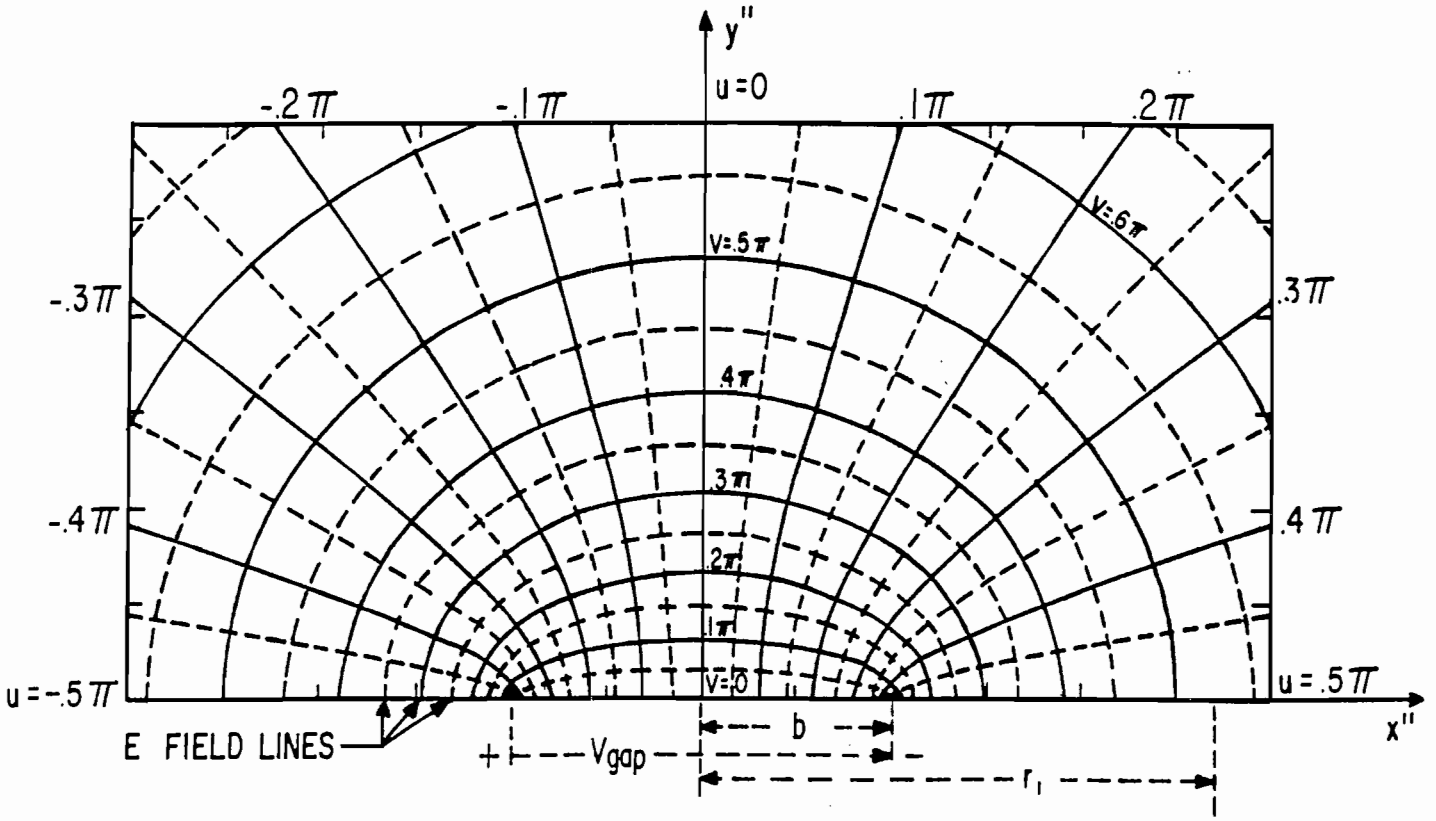

A. IDEALIZATION OF LOOP GAP

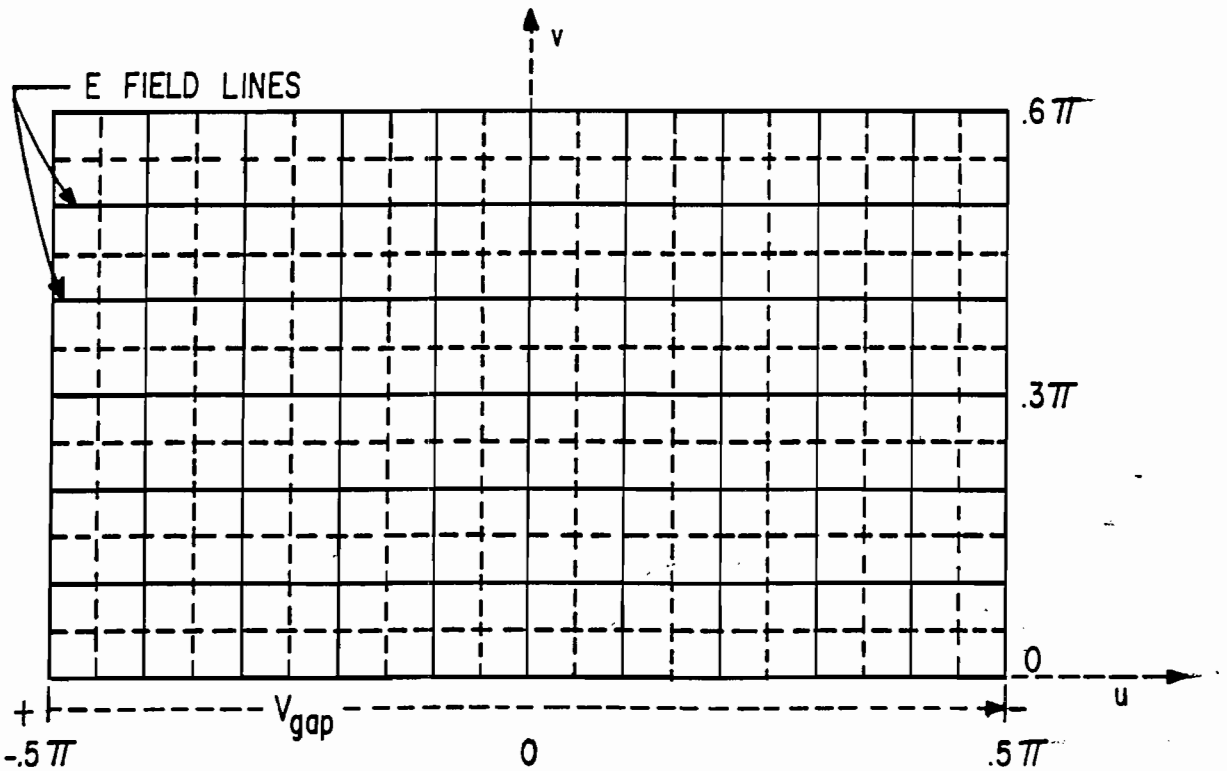

B. CONFORMAL TRANSFORMATION OF LOOP GAP

FIGURE 5. ELECTRIC FIELD DISTRIBUTION NEAR CYLINDRICAL LOOP GAP

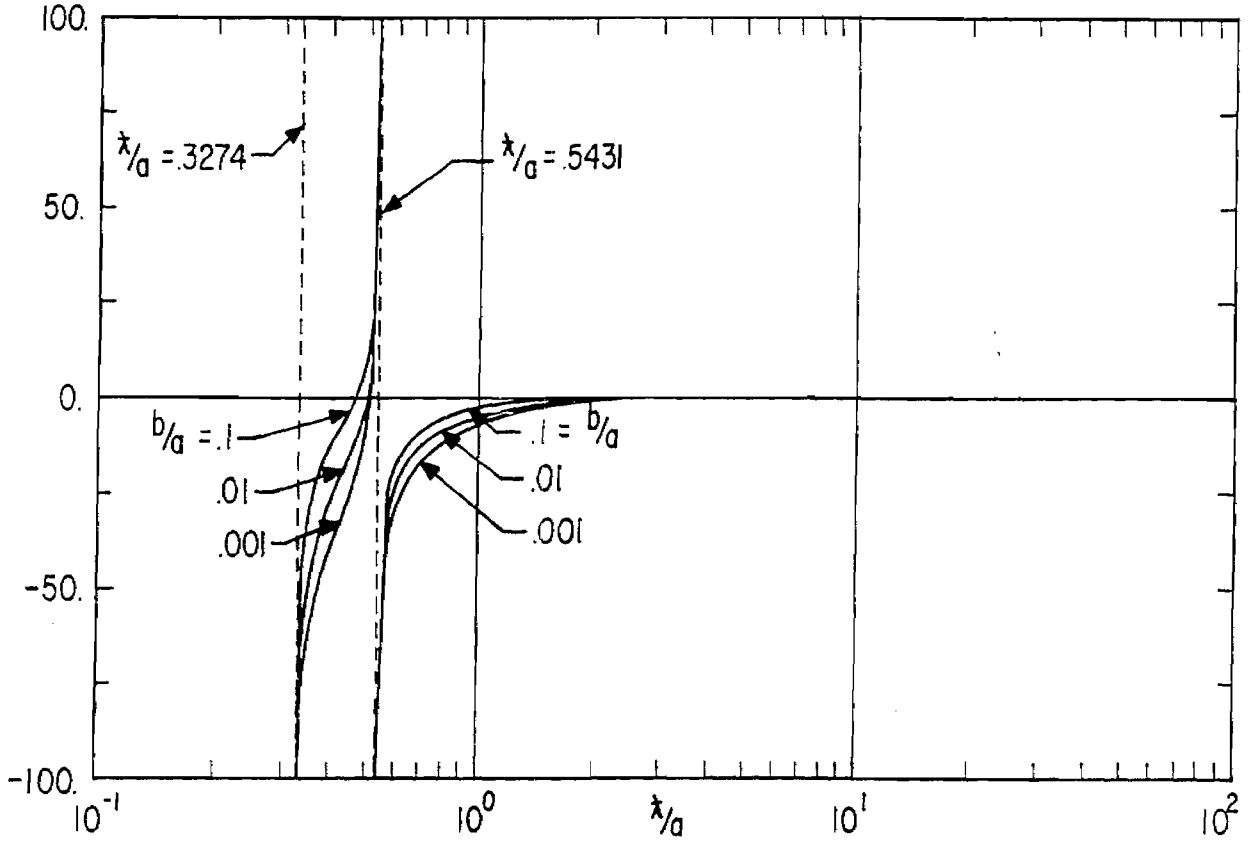

A. Y_ℓ vs. λ/a WITH b/a AS A PARAMETER

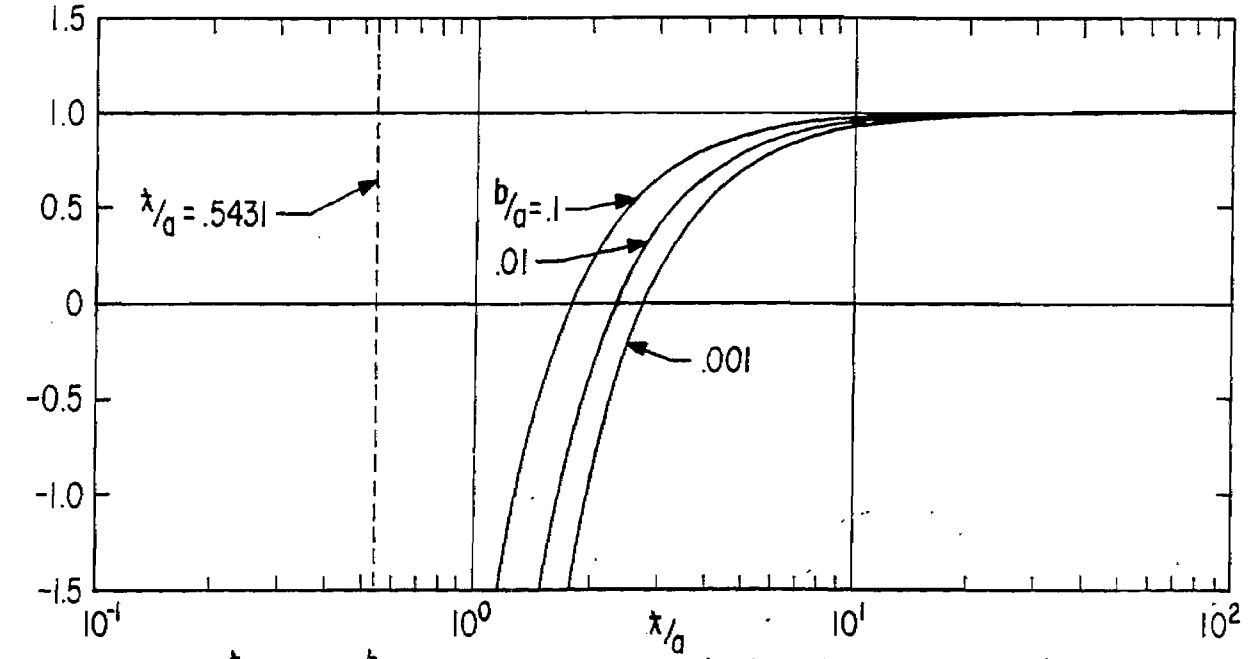

B. Y_ℓ vs. λ/a WITH b/a AS A PARAMETER (SCALE OF A EXPANDED)

FIGURE 6. NORMALIZED INTERNAL ADMITTANCE OF CYLINDRICAL LOOP WITH NO CONDUCTIVITY

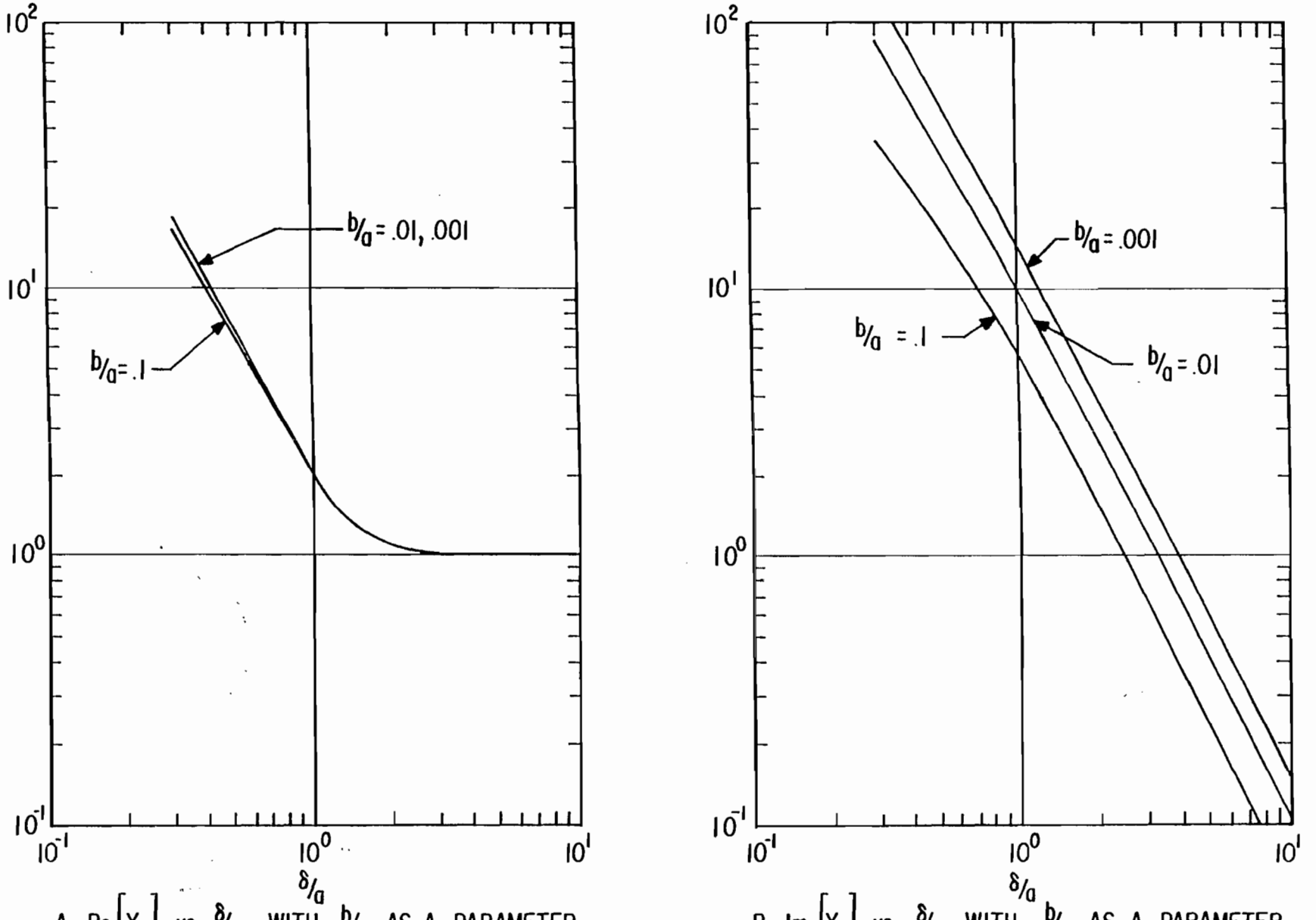

A. Re $[Y_s]$ vs. δ/a WITH b/a AS A PARAMETER

B. Im $[Y_s]$ vs. δ/a WITH b/a AS A PARAMETER

FIGURE 7. NORMALIZED INTERNAL ADMITTANCE OF CYLINDRICAL LOOP WITH HIGH CONDUCTIVITY

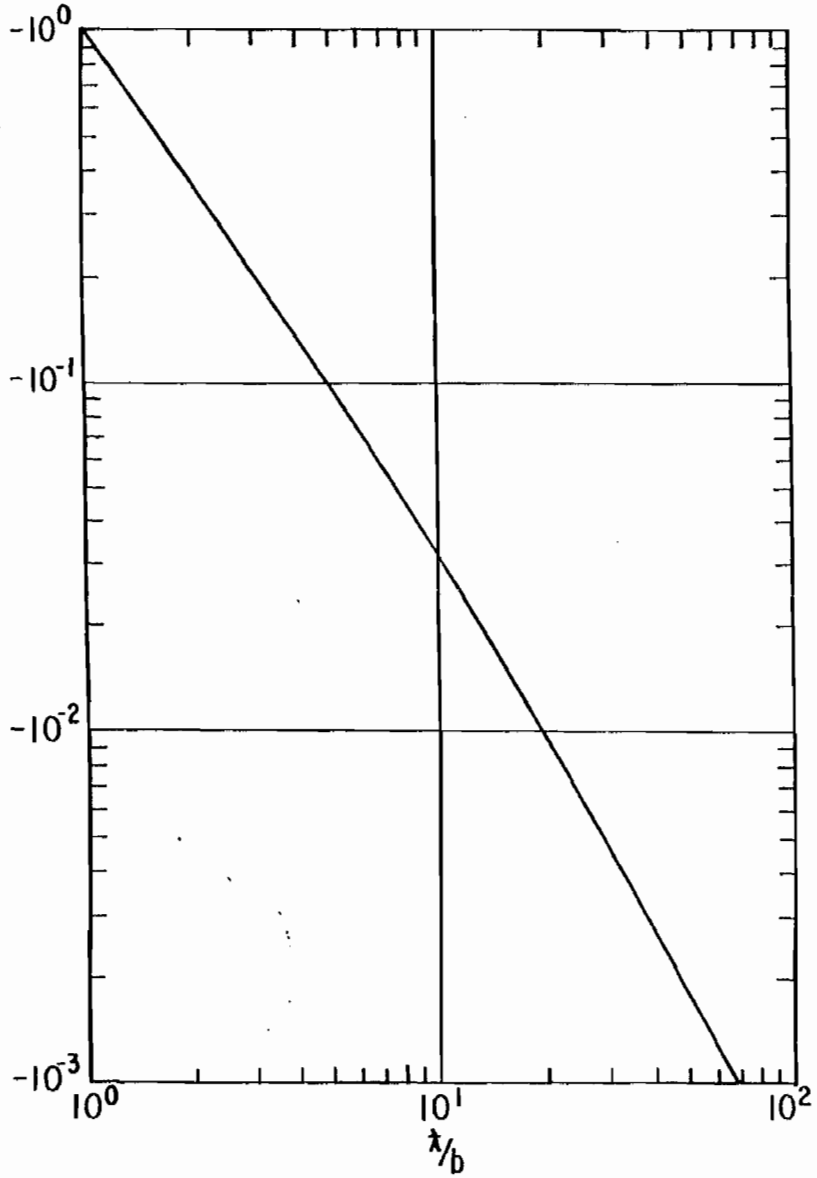

A. Re $\left[Y'_{ext}\right]\left(\frac{b}{a}\right)^2$ vs. λ/b

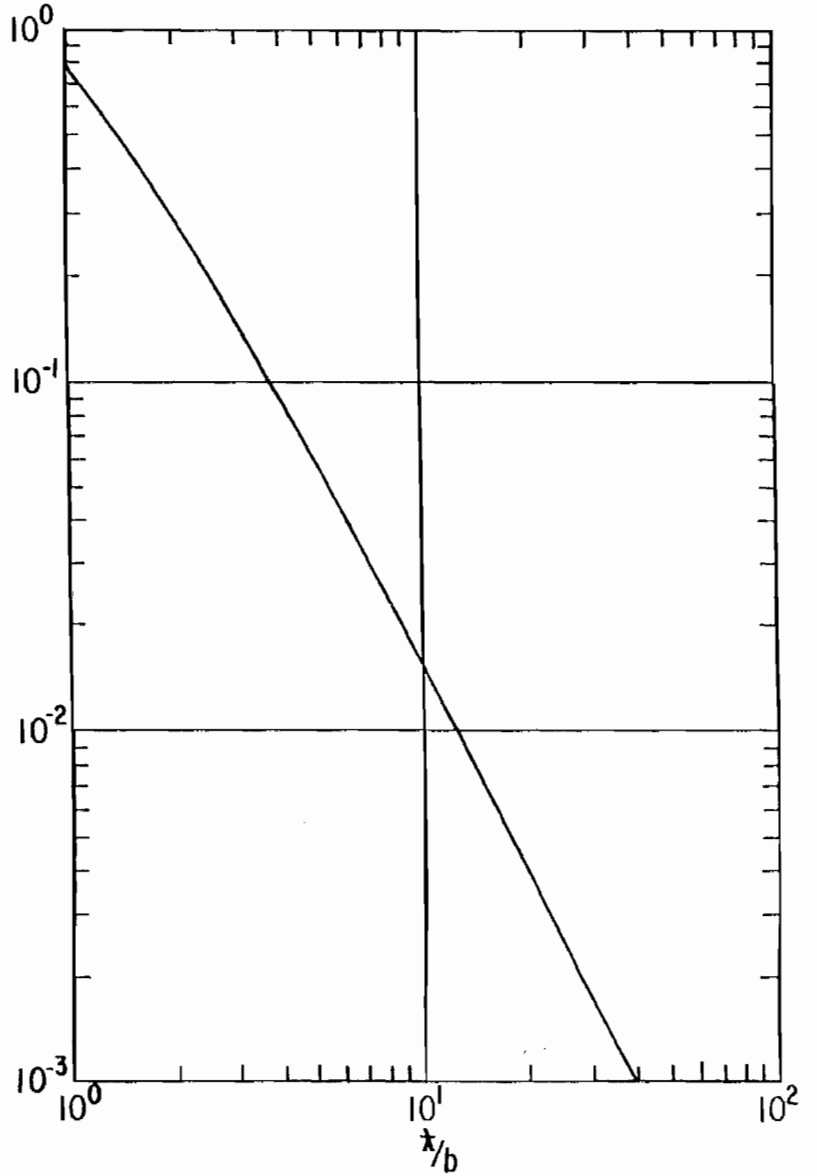

B. Im $\left[Y'_{ext}\right]\left(\frac{b}{a}\right)^2$ vs. λ/b

FIGURE 8. NORMALIZED EXTERNAL ADMITTANCE OF CYLINDRICAL LOOP BELOW GROUND PLANE WITH NO CONDUCTIVITY

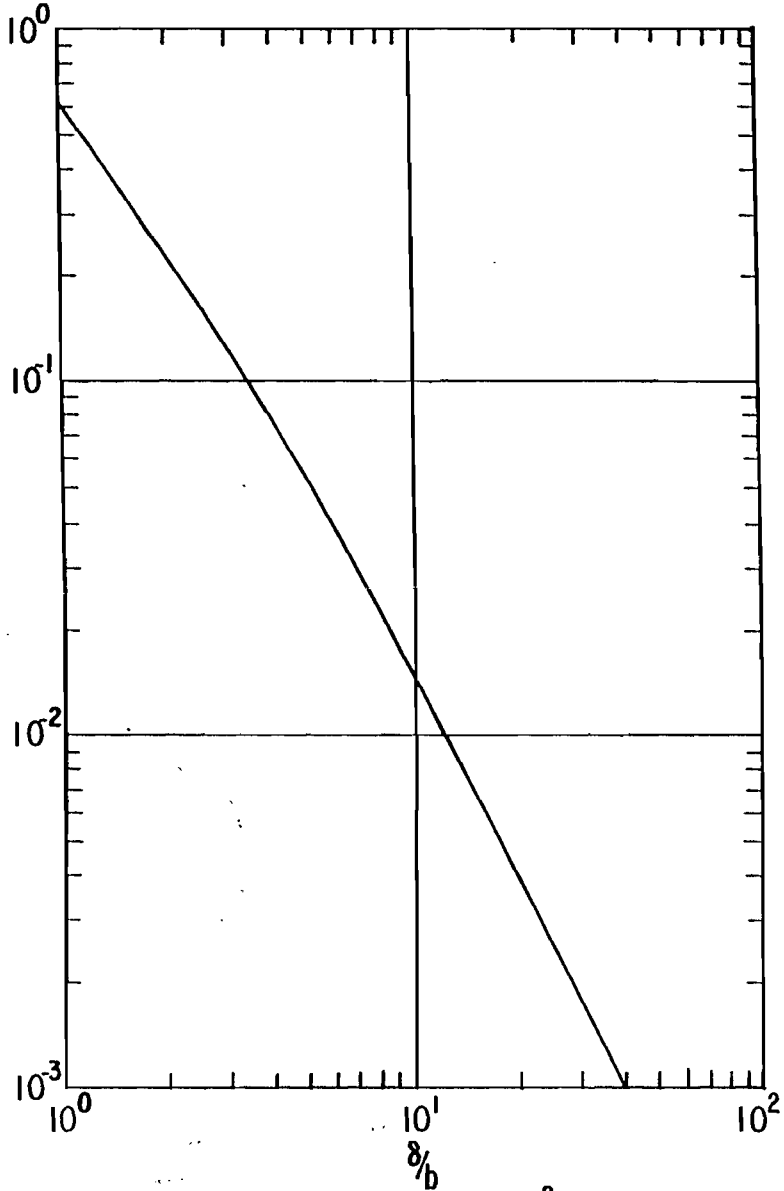

A. Re $\left[Y'_{ext}\right]\left(\frac{b}{a}\right)^2$ vs. δ/b

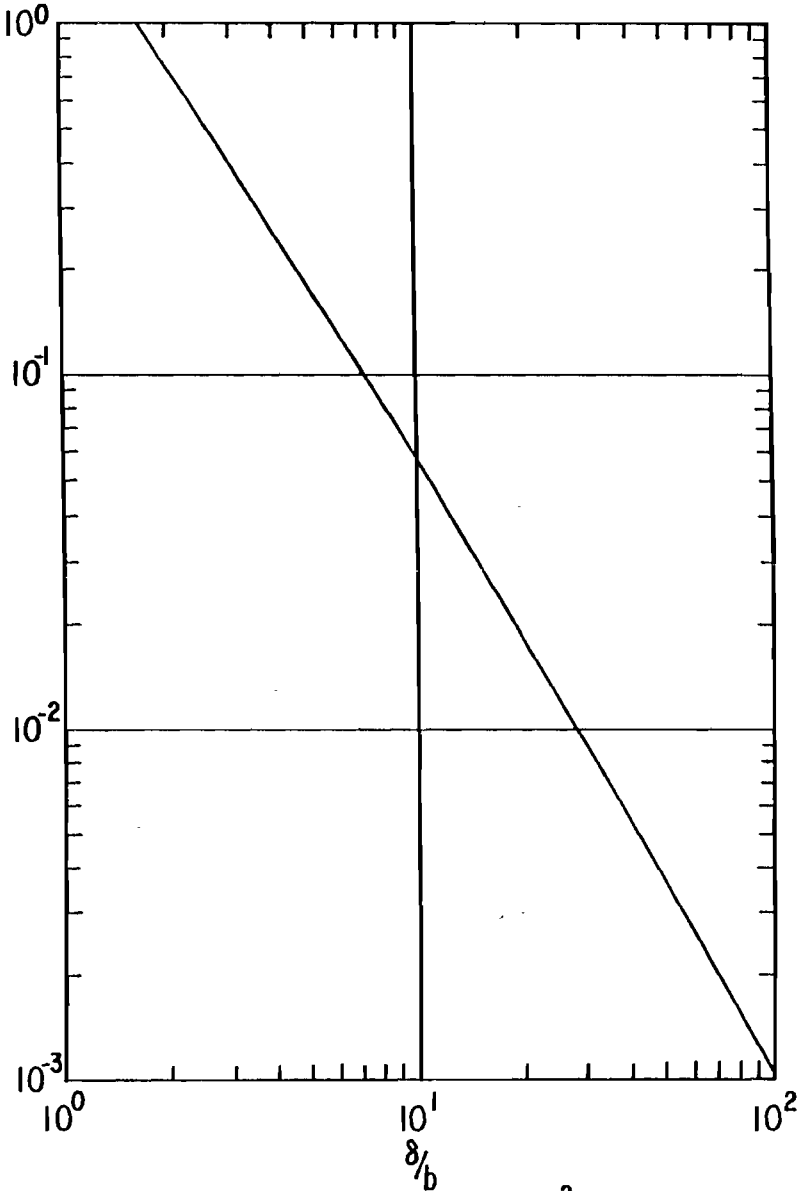

B. Im $\left[Y'_{ext}\right]\left(\frac{b}{a}\right)^2$ vs. δ/b

FIGURE 9. NORMALIZED EXTERNAL ADMITTANCE OF CYLINDRICAL LOOP BELOW GROUND PLANE WITH HIGH CONDUCTIVITY

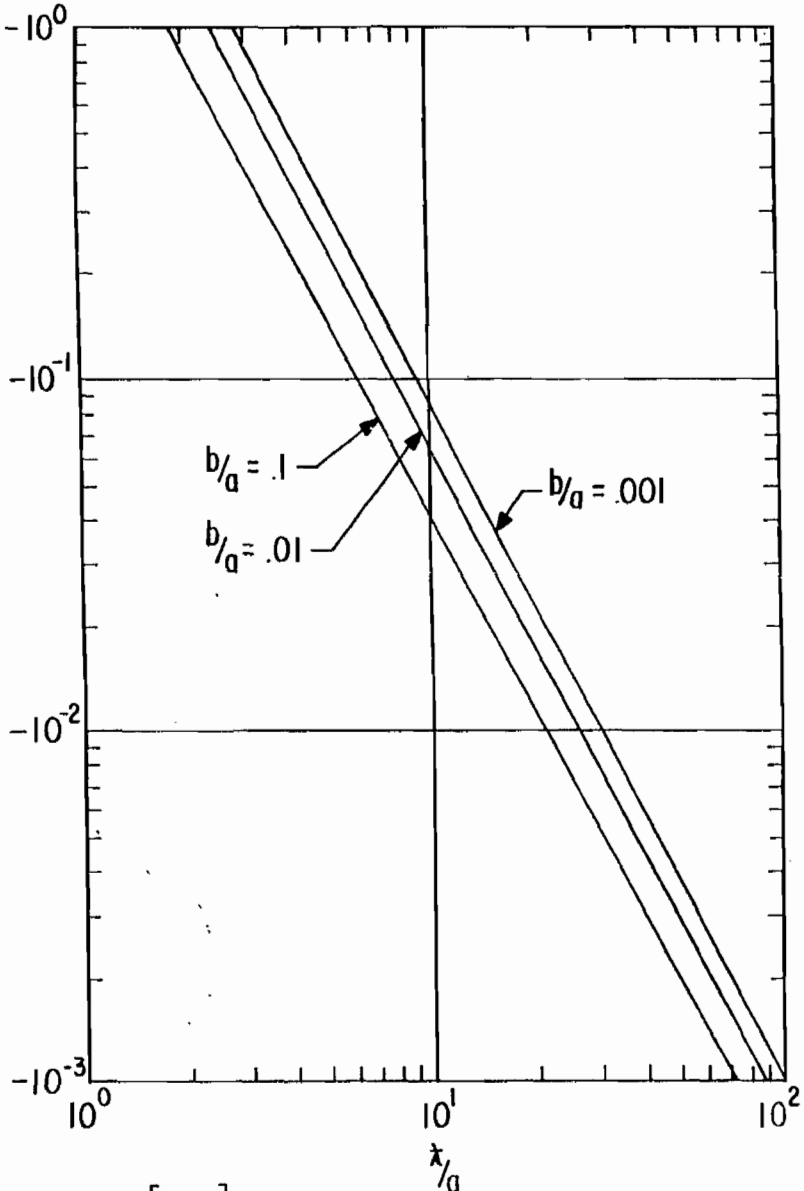

A. $\mathrm{Re}\left[Y_{ext}\right]$ vs. λ/a WITH b/a AS A PARAMETER

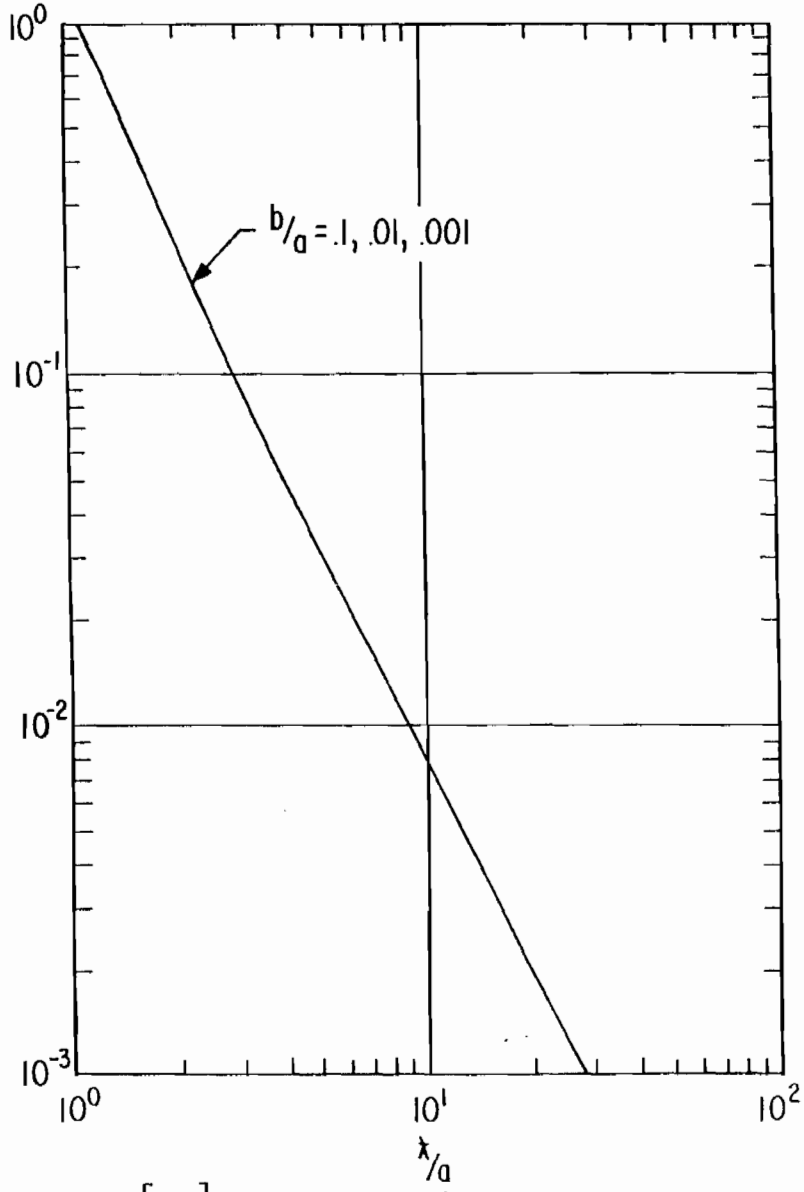

B. $\mathrm{Im}\left[Y_{ext}\right]$ vs. λ/a WITH b/a AS A PARAMETER

FIGURE 10. NORMALIZED EXTERNAL ADMITTANCE OF EXPOSED CYLINDRICAL LOOP WITH NO CONDUCTIVITY

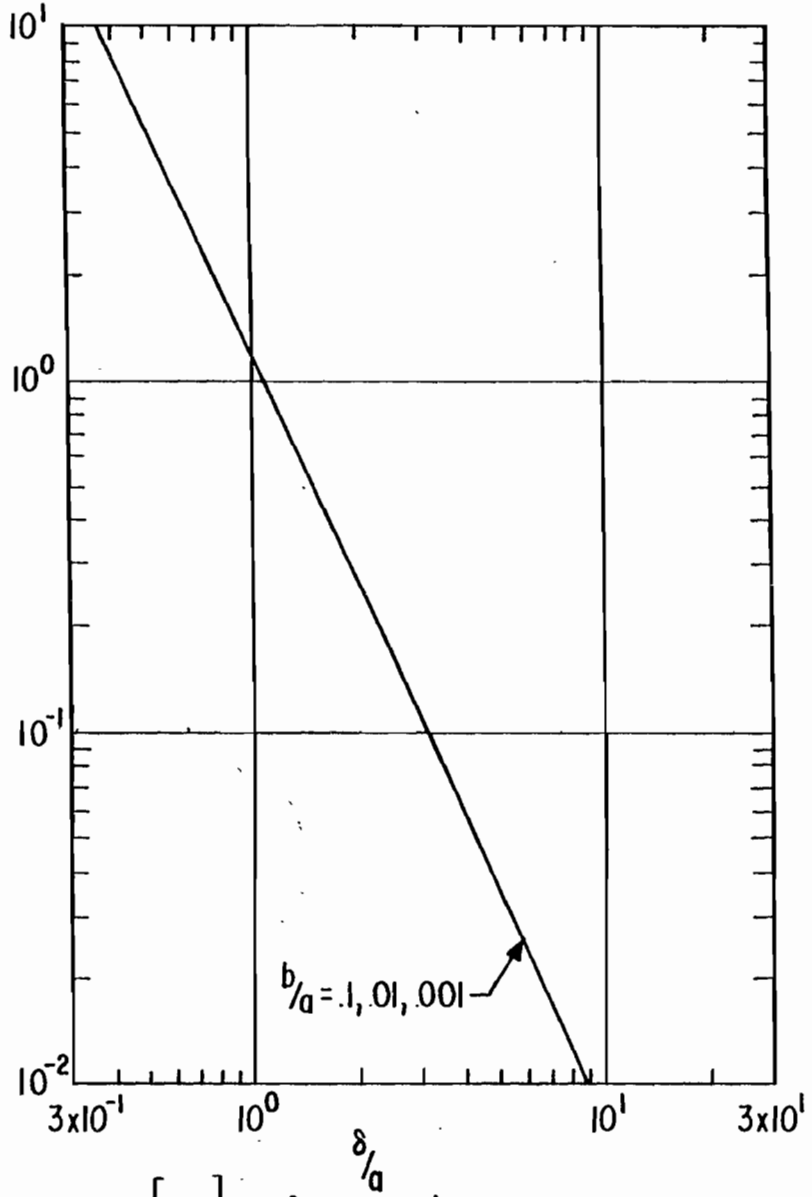

A. $\mathrm{Re}\left[Y_{ext}\right]$ vs. δ/a WITH b/a AS A PARAMETER

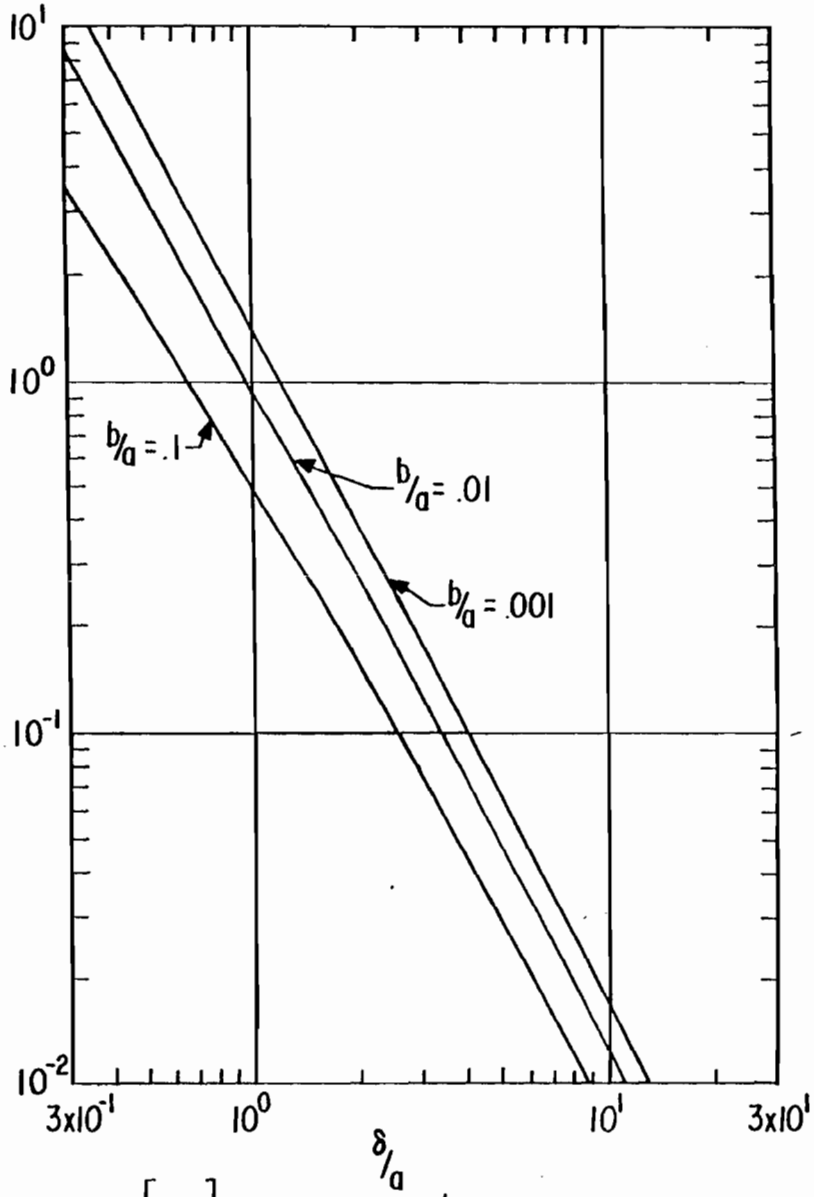

B. $\mathrm{Im}\left[Y_{ext}\right]$ vs. δ/a WITH b/a AS A PARAMETER

FIGURE 11. NORMALIZED EXTERNAL ADMITTANCE OF EXPOSED CYLINDRICAL LOOP WITH HIGH CONDUCTIVITY

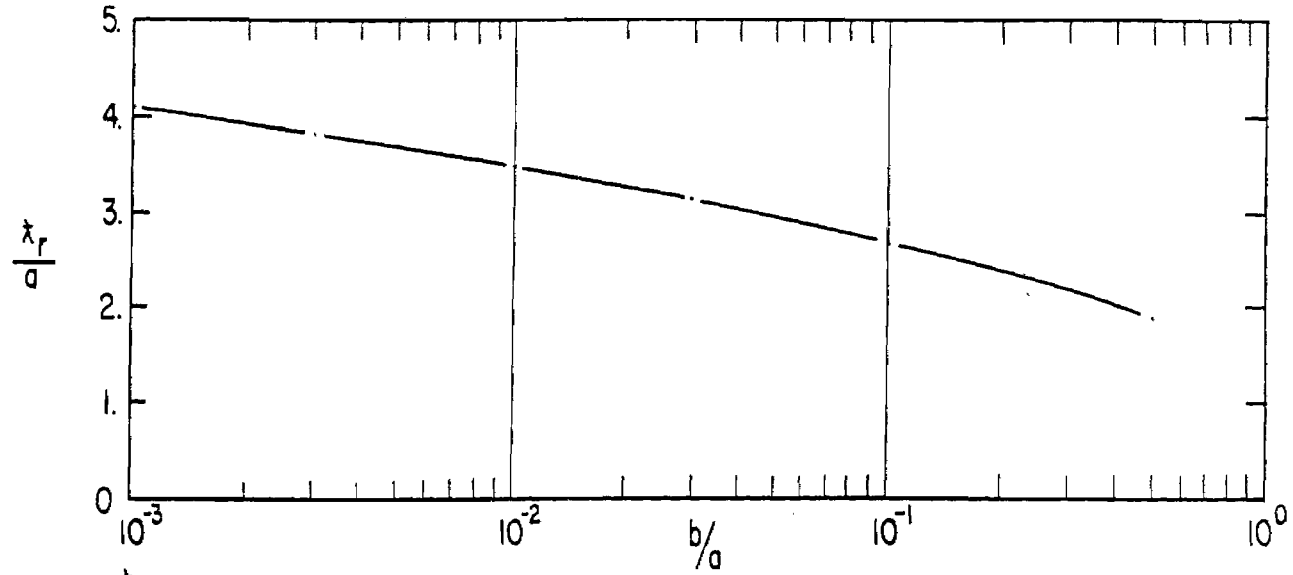

A. $\frac{\lambda_r}{a}$ vs. b/a

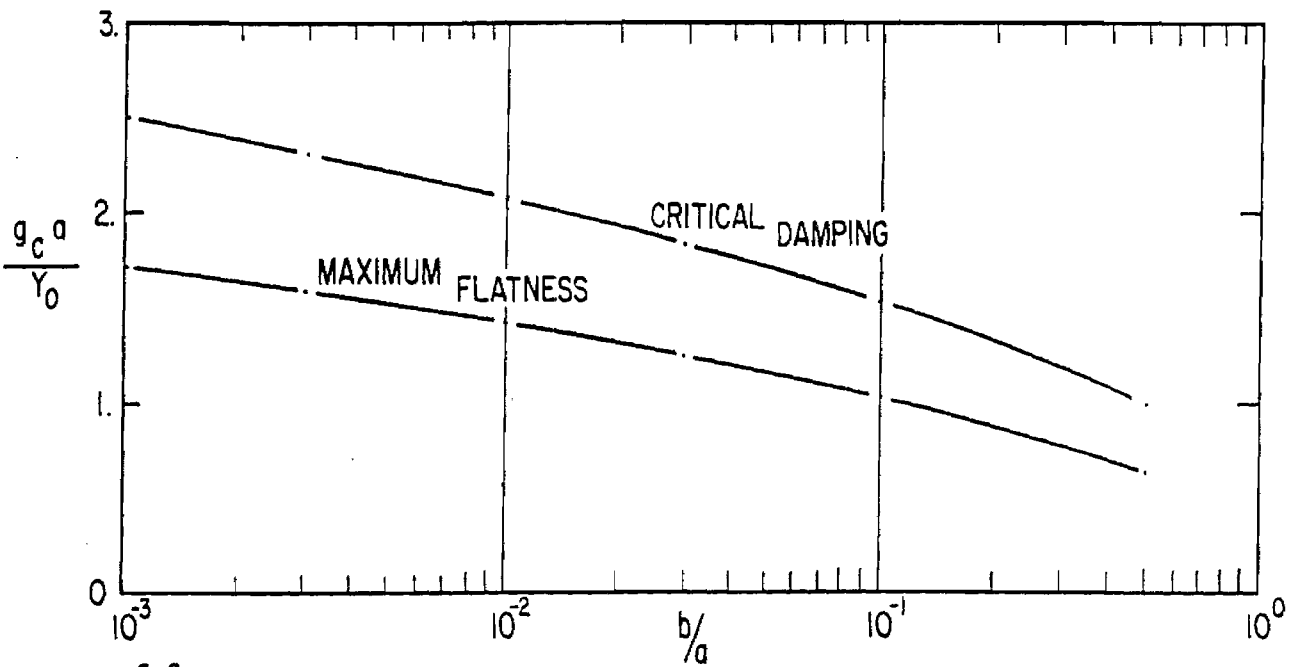

B. $\frac{g_c a}{Y_0}$ vs. b/a FOR APPROXIMATE CRITICAL DAMPING AND FOR APPROXIMATE MAXIMUM FLAT FREQUENCY RESPONSE

FIGURE 12. RESONANT FREQUENCY CHARACTERISTICS OF CYLINDRICAL LOOP BELOW GROUND PLANE WITH NO CONDUCTIVITY

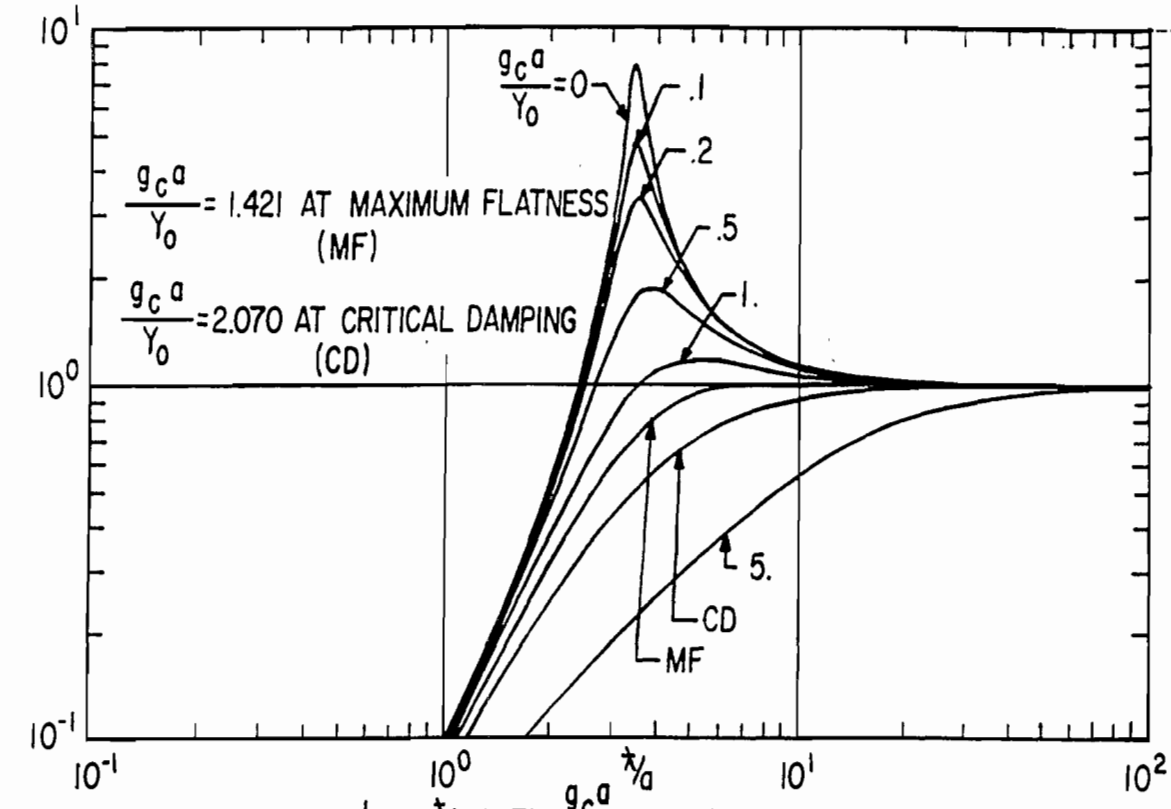

A. MAGNITUDE OF R' vs. $\frac{r}{a}$ WITH $\frac{g_c a}{Y_0}$ AS A PARAMETER

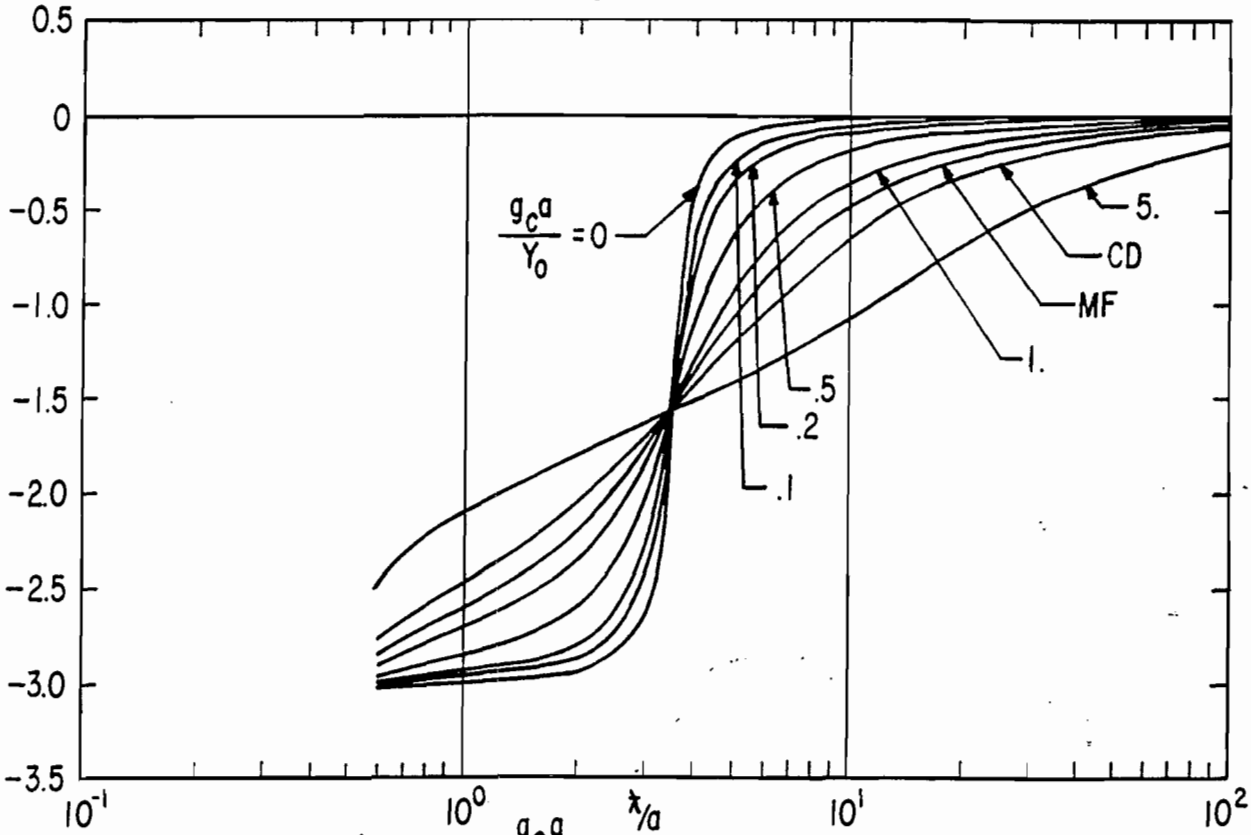

B. PHASE OF R' vs. $\frac{r}{a}$ WITH $\frac{g_c a}{Y_0}$ AS A PARAMETER

FIGURE 13. RESPONSE CHARACTERISTICS OF CYLINDRICAL LOOP BELOW GROUND PLANE WITH NO CONDUCTIVITY: $\frac{b}{a}$ =.01

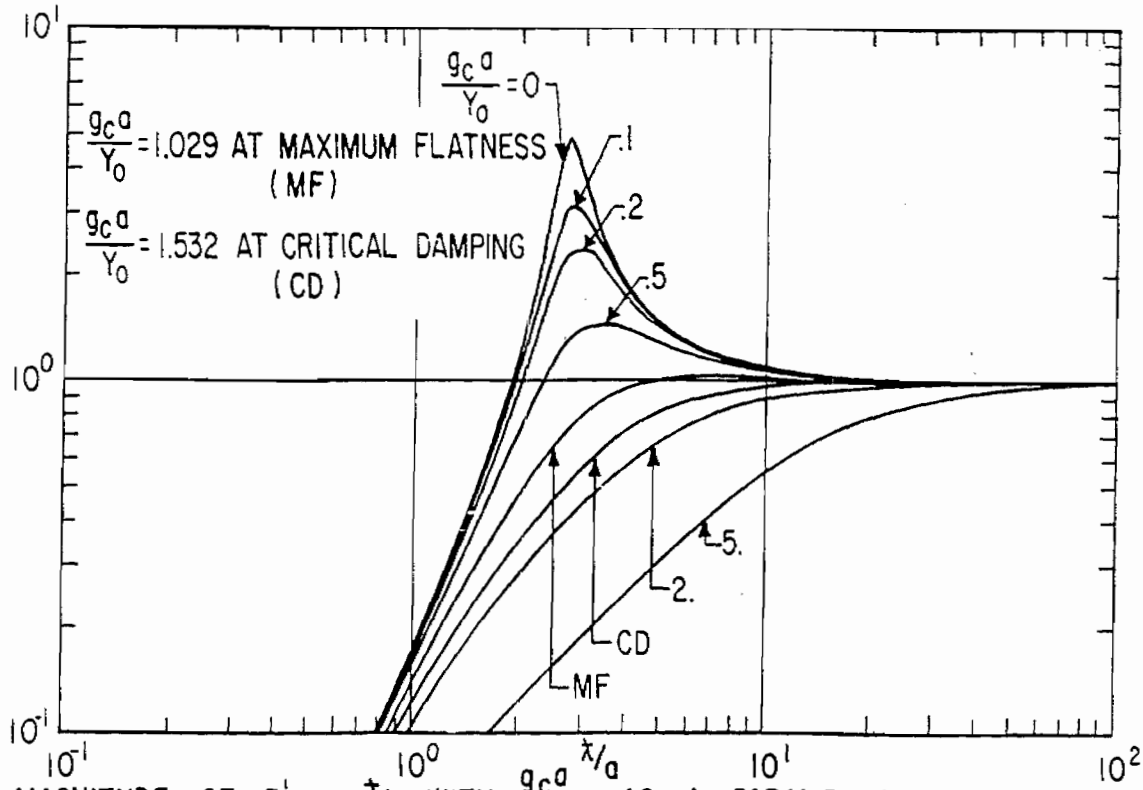

A. MAGNITUDE OF R' vs. λ/a WITH $\frac{g_c a}{Y_0}$ AS A PARAMETER

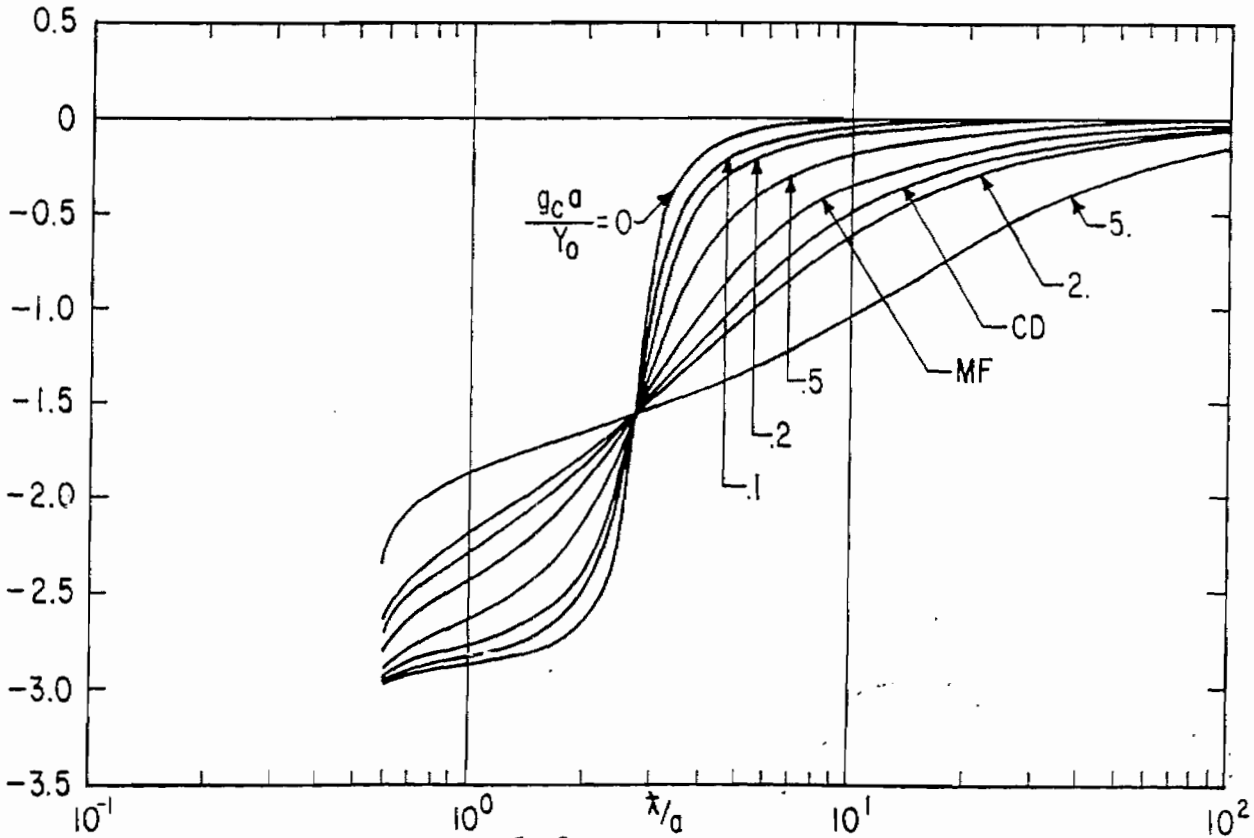

B. PHASE OF R' vs. λ/a WITH $\frac{g_c a}{Y_0}$ AS A PARAMETER

FIGURE 14. RESPONSE CHARACTERISTICS OF CYLINDRICAL LOOP BELOW GROUND PLANE WITH NO CONDUCTIVITY: b/a = .1

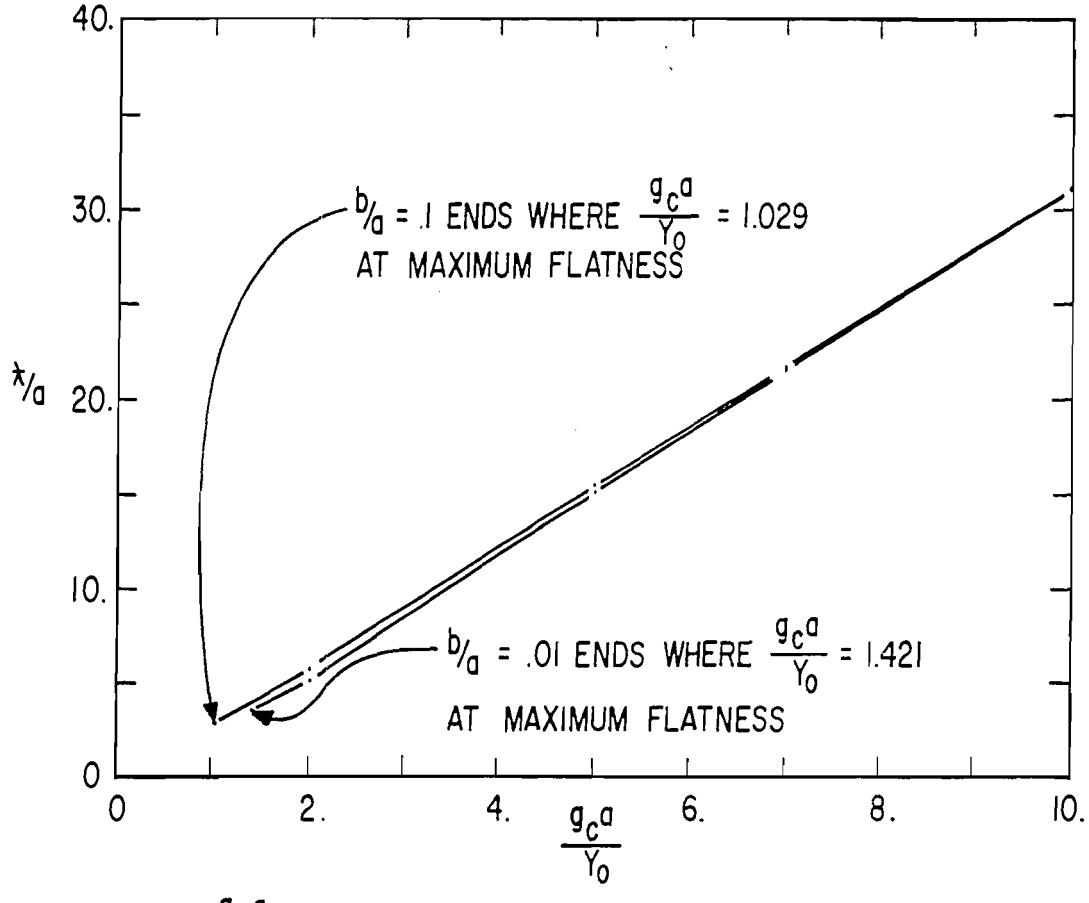

λ/a vs. $\frac{g_c a}{Y_0}$ WITH b/a AS A PARAMETER

FIGURE 15. DEPENDENCE OF FREQUENCY RESPONSE ON CABLE CONDUCTANCE FOR CYLINDRICAL LOOP BELOW GROUND PLANE WITH NO CONDUCTIVITY: $|R'| = 1/\sqrt{2}$

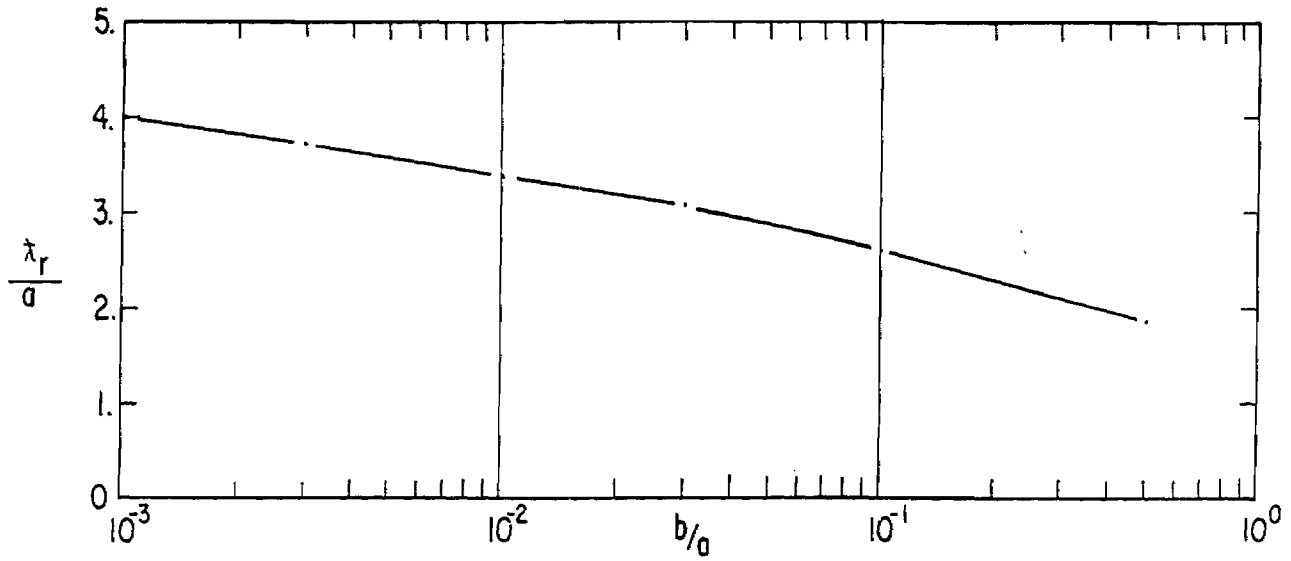

A. $\frac{\lambda_r}{a}$ vs. b/a

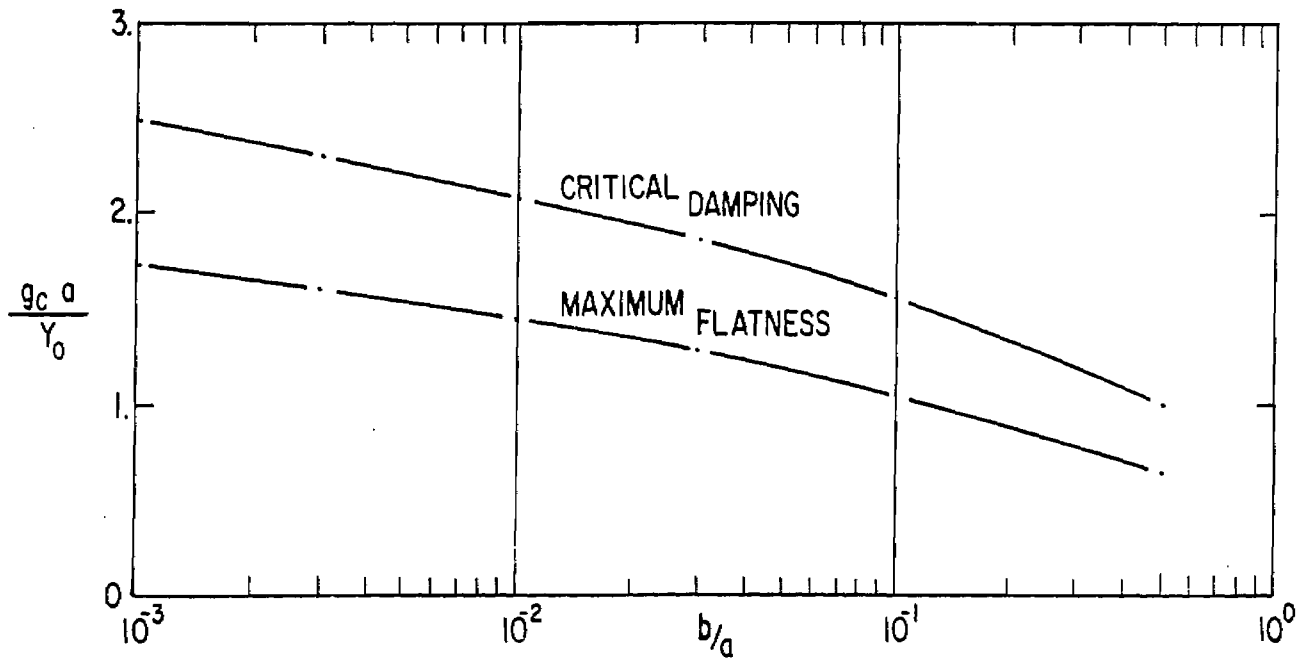

B. $\frac{g_c\, a}{Y_0}$ vs. b/a FOR APPROXIMATE CRITICAL DAMPING AND FOR APPROXIMATE MAXIMUM FLAT FREQUENCY RESPONSE

FIGURE 16. RESONANT FREQUENCY CHARACTERISTICS OF EXPOSED CYLINDRICAL LOOP WITH NO CONDUCTIVITY

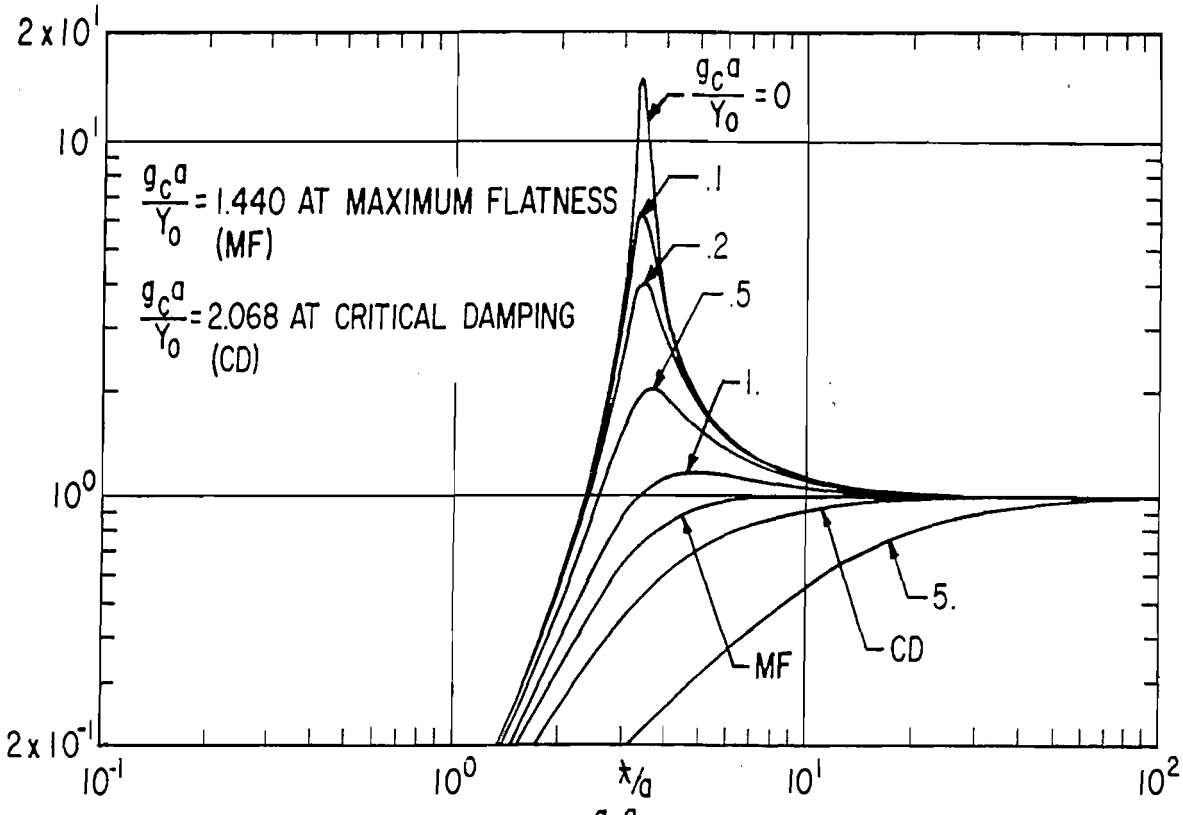

A. MAGNITUDE OF R_y vs. λ/a WITH $\frac{g_c a}{Y_0}$ AS A PARAMETER

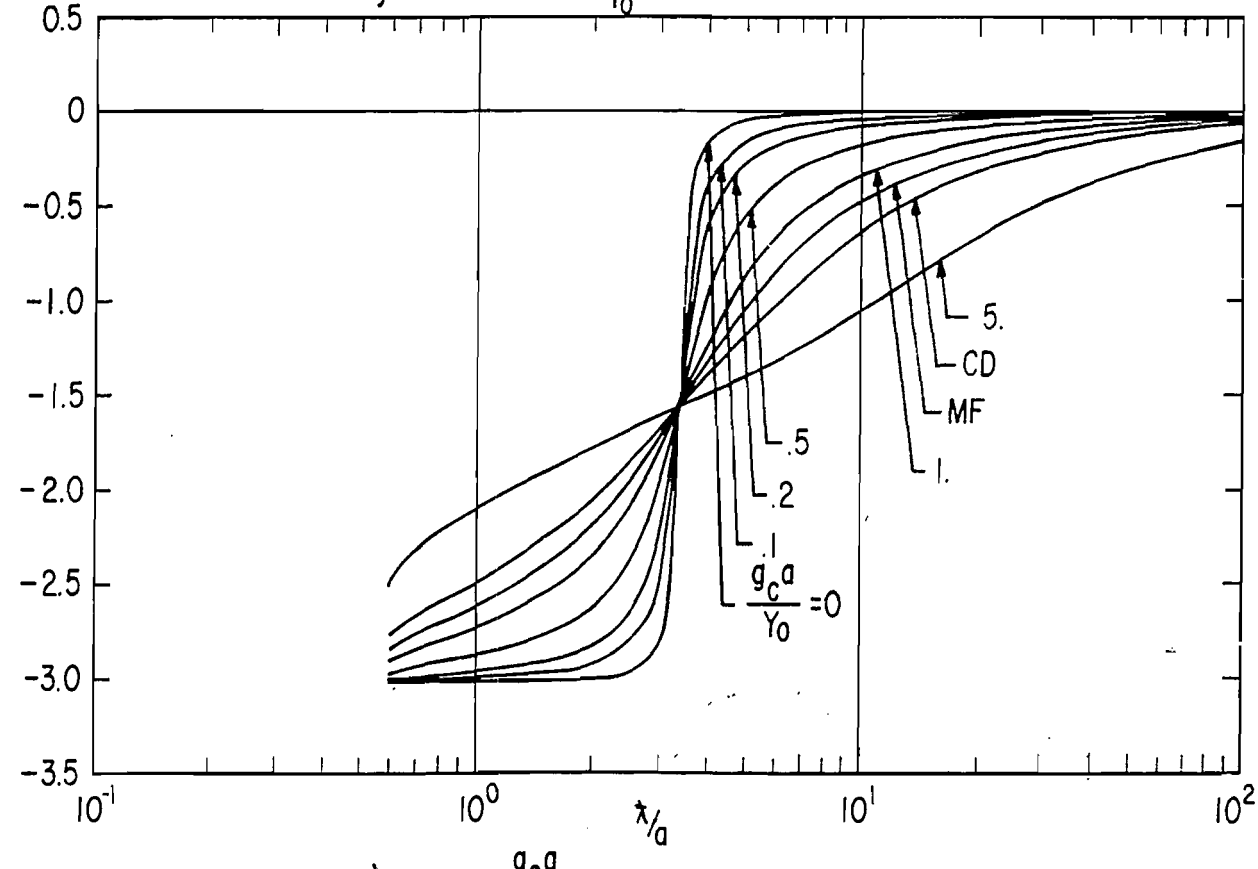

B. PHASE OF R_y vs. λ/a WITH $\frac{g_c a}{Y_0}$ AS A PARAMETER

FIGURE 17. EFFECT OF ADMITTANCES ON RESPONSE OF EXPOSED CYLINDRICAL LOOP WITH NO CONDUCTIVITY: $b/a = .01$

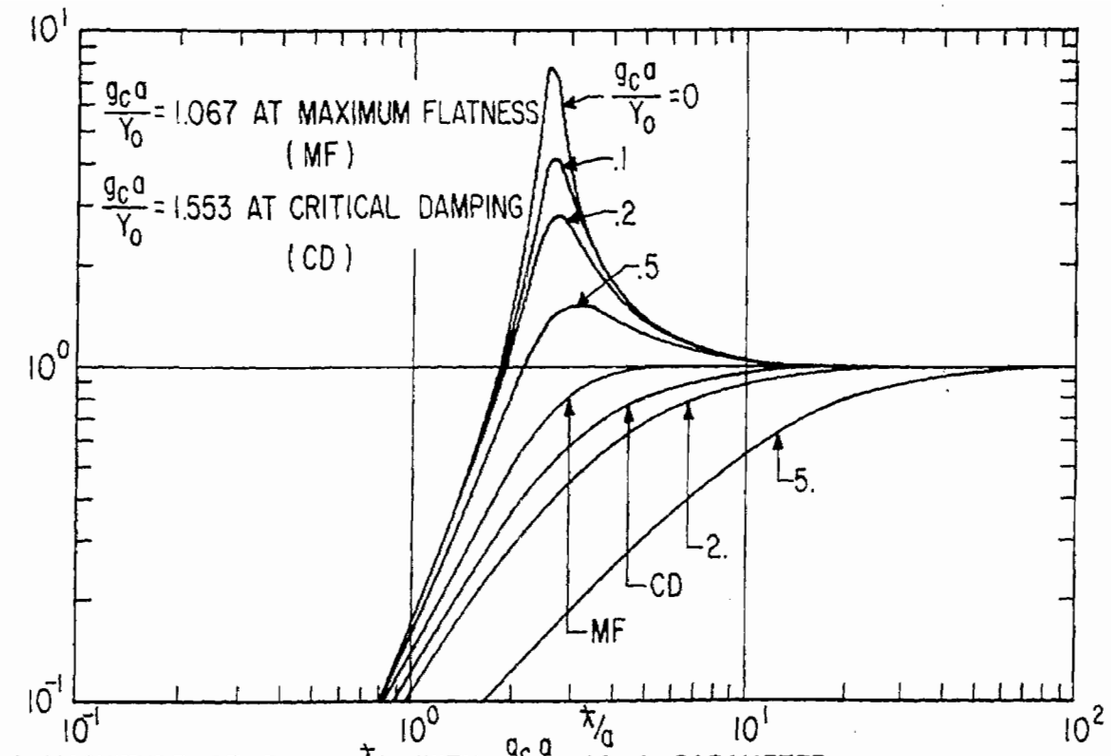

A. MAGNITUDE OF R_y vs. λ/a WITH $\frac{g_c a}{Y_0}$ AS A PARAMETER

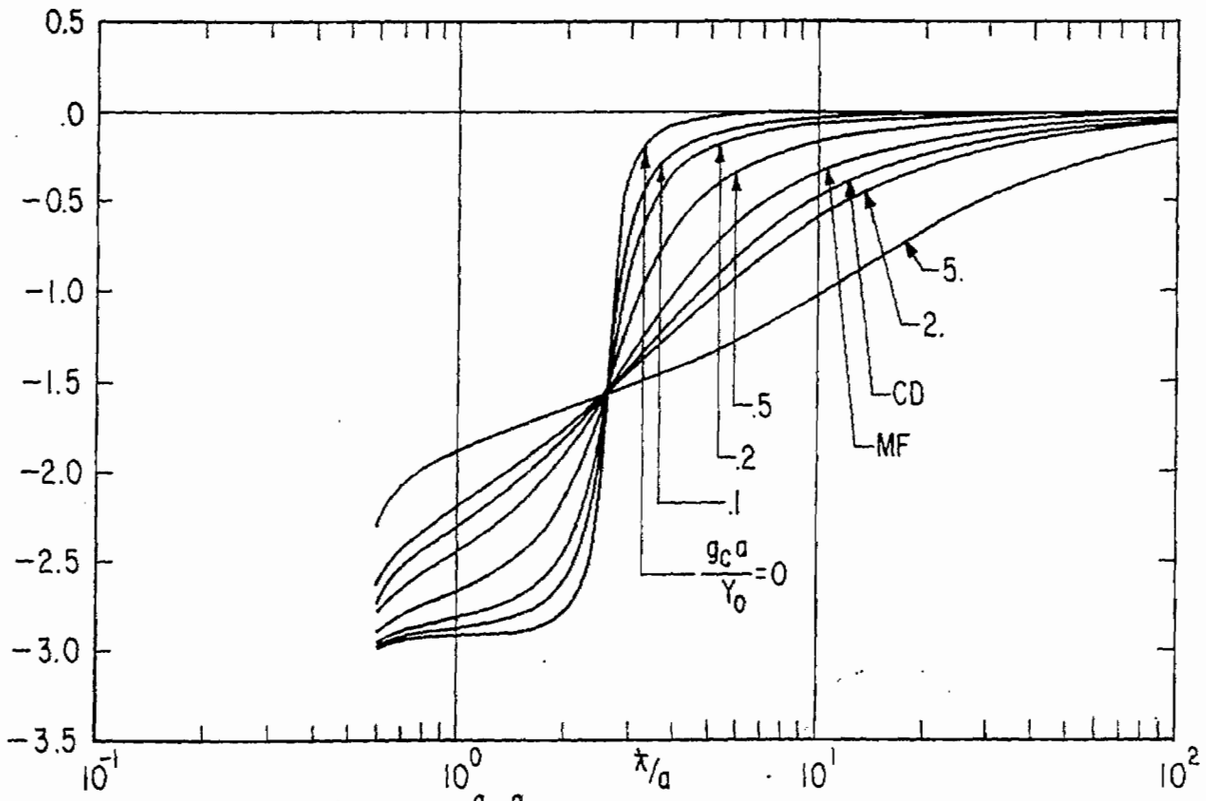

B. PHASE OF R_y vs. λ/a WITH $\frac{g_c a}{Y_0}$ AS A PARAMETER

FIGURE 18. EFFECT OF ADMITTANCES ON RESPONSE OF EXPOSED CYLINDRICAL LOOP WITH NO CONDUCTIVITY: b/a = .1

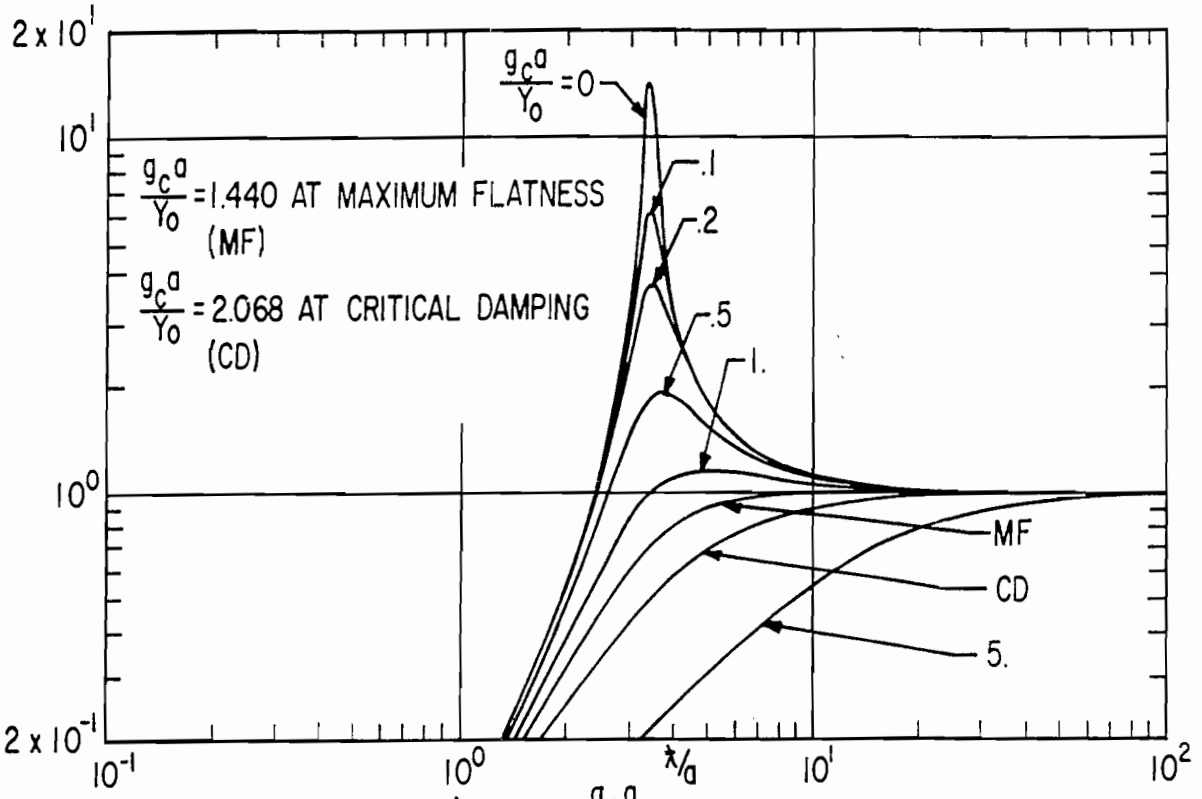

A. MAGNITUDE OF R vs. λ/a WITH $\frac{g_c a}{Y_0}$ AS A PARAMETER

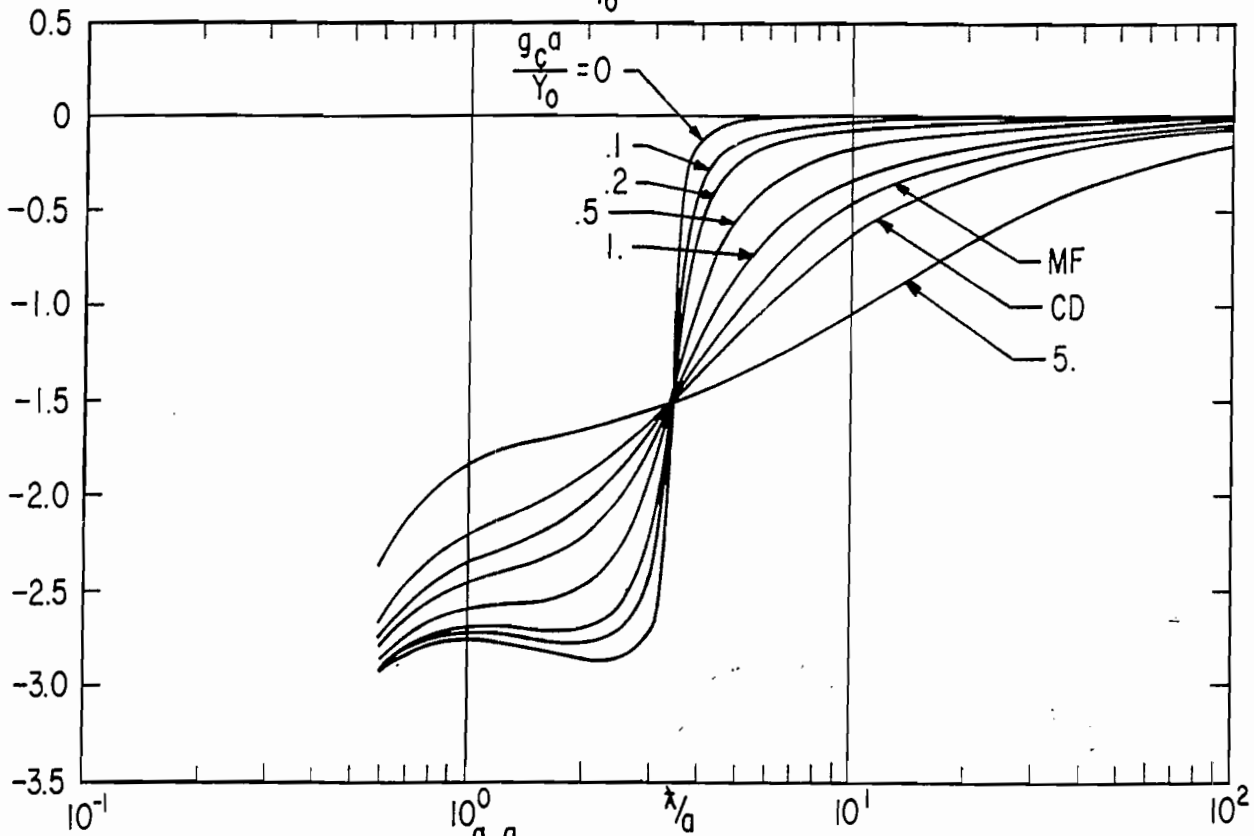

B. PHASE OF R vs. λ/a WITH $\frac{g_c a}{Y_0}$ AS A PARAMETER

FIGURE 19. RESPONSE CHARACTERISTICS OF EXPOSED CYLINDRICAL LOOP WITH NO CONDUCTIVITY: $b/a = .01$

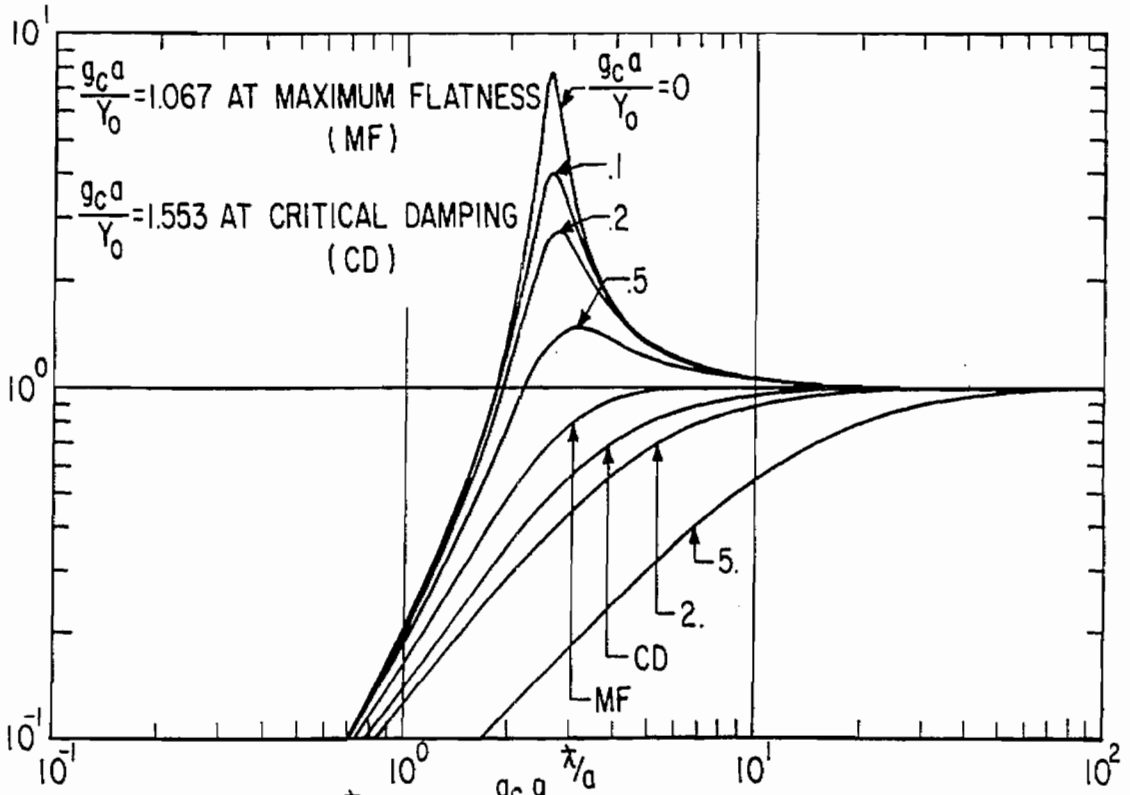

A. MAGNITUDE OF R vs. λ/a WITH $\frac{g_c a}{Y_0}$ AS A PARAMETER

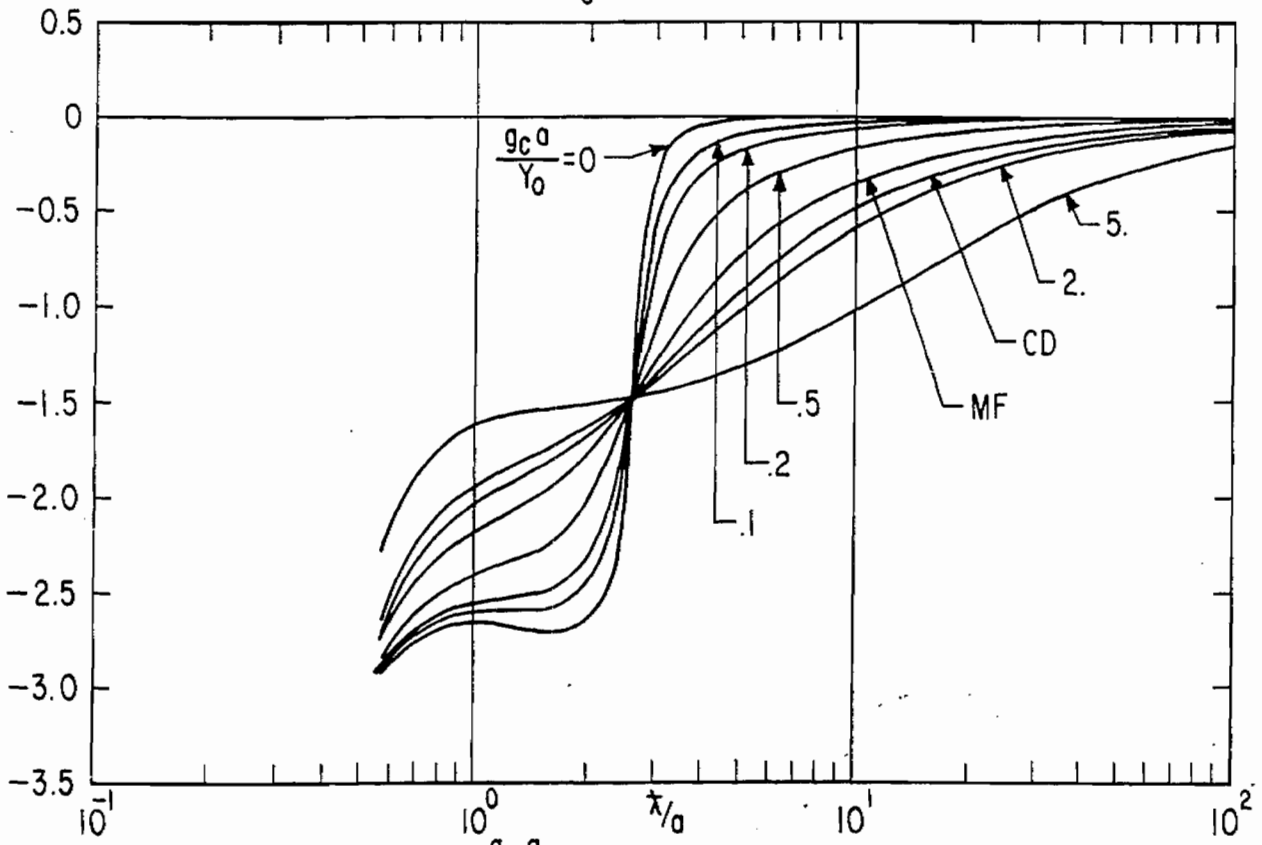

B. PHASE OF R vs. λ/a WITH $\frac{g_c a}{Y_0}$ AS A PARAMETER

FIGURE 20. RESPONSE CHARACTERISTICS OF EXPOSED CYLINDRICAL LOOP WITH NO CONDUCTIVITY: b/a = .1

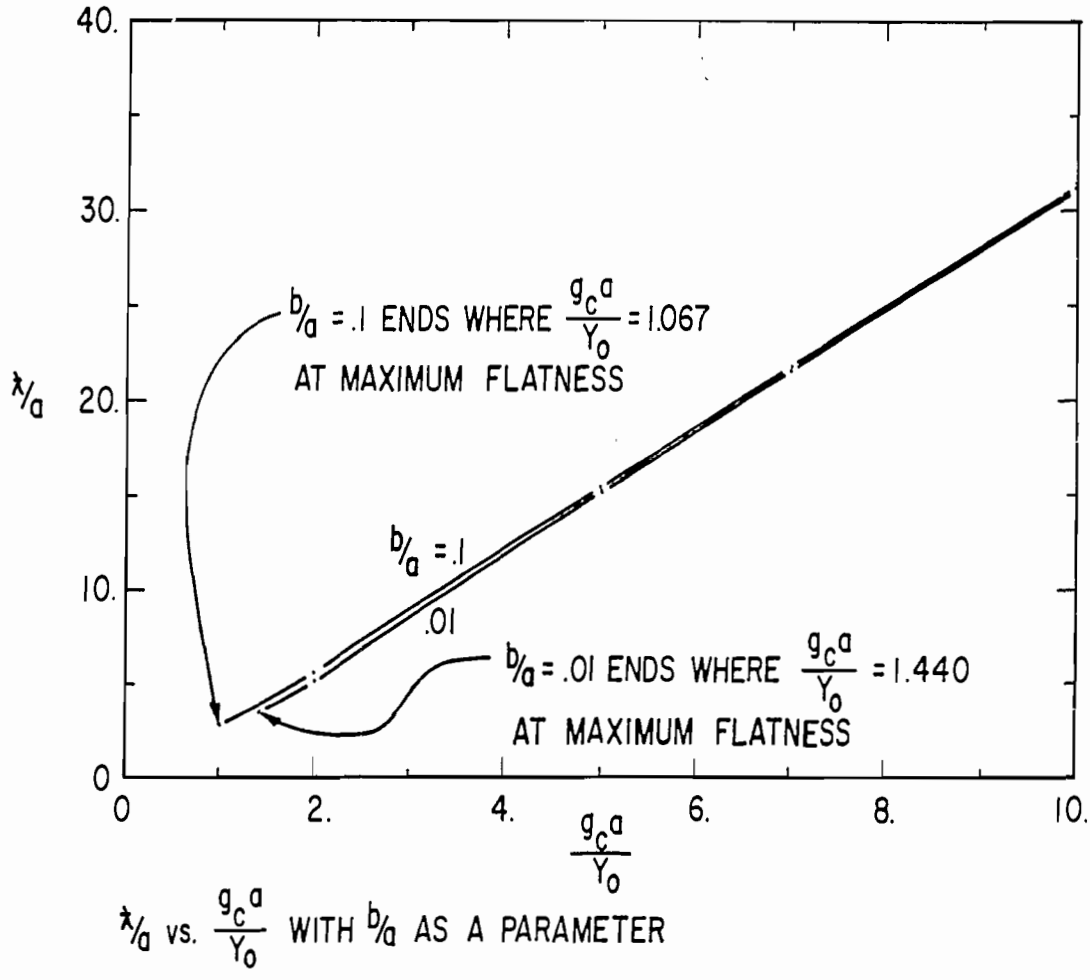

λ/a vs. $\frac{g_c a}{Y_0}$ WITH b/a AS A PARAMETER

FIGURE 21. DEPENDENCE OF FREQUENCY RESPONSE ON CABLE CONDUCTANCE FOR EXPOSED CYLINDRICAL LOOP WITH NO CONDUCTIVITY: $|R| = 1/\sqrt{2}$

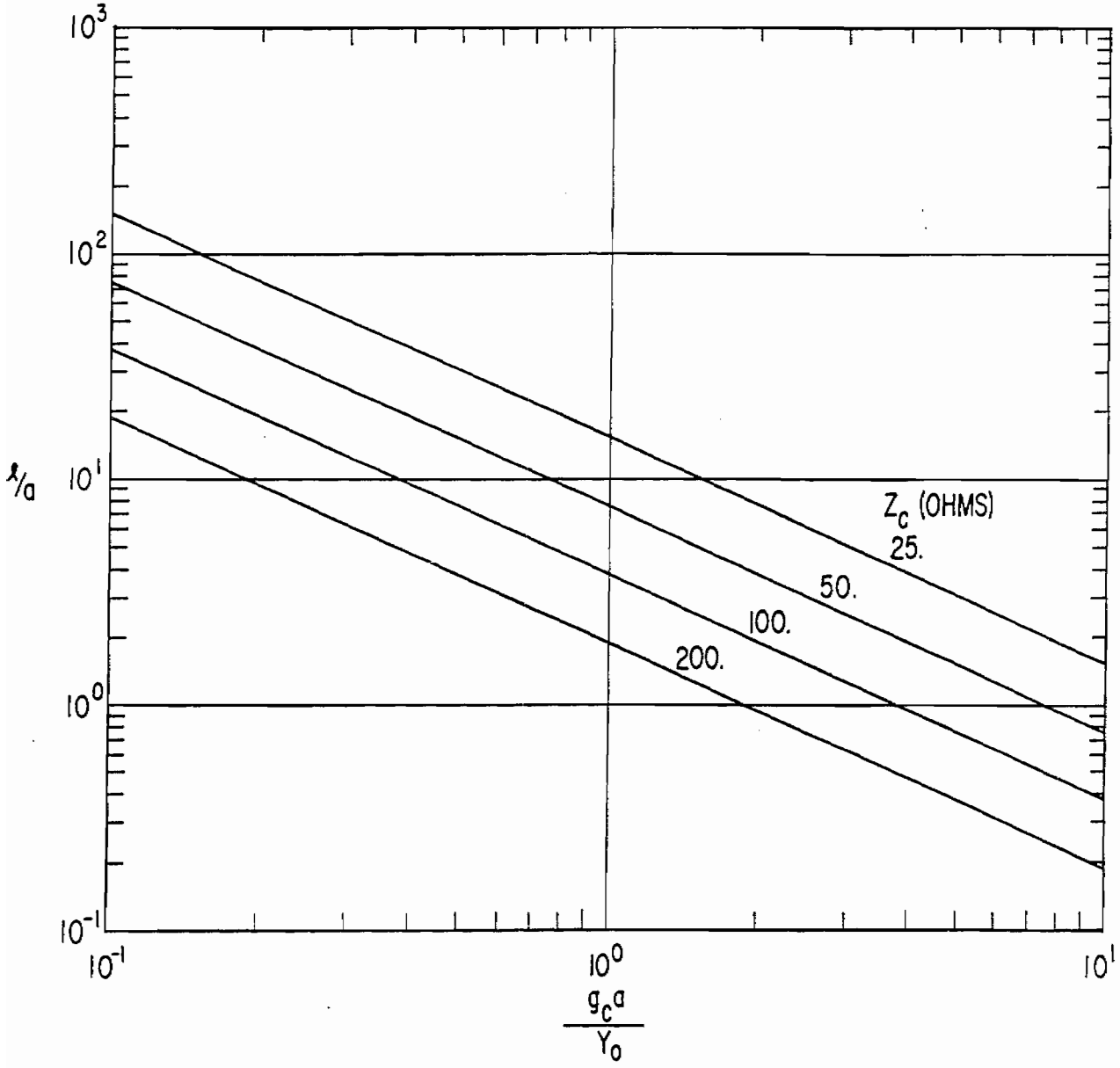

ℓ/a vs. $\frac{g_c a}{Y_0}$ WITH Z_c AS A PARAMETER

FIGURE 22. DEPENDENCE OF CYLINDRICAL LOOP LENGTH ON CABLE CONDUCTANCE

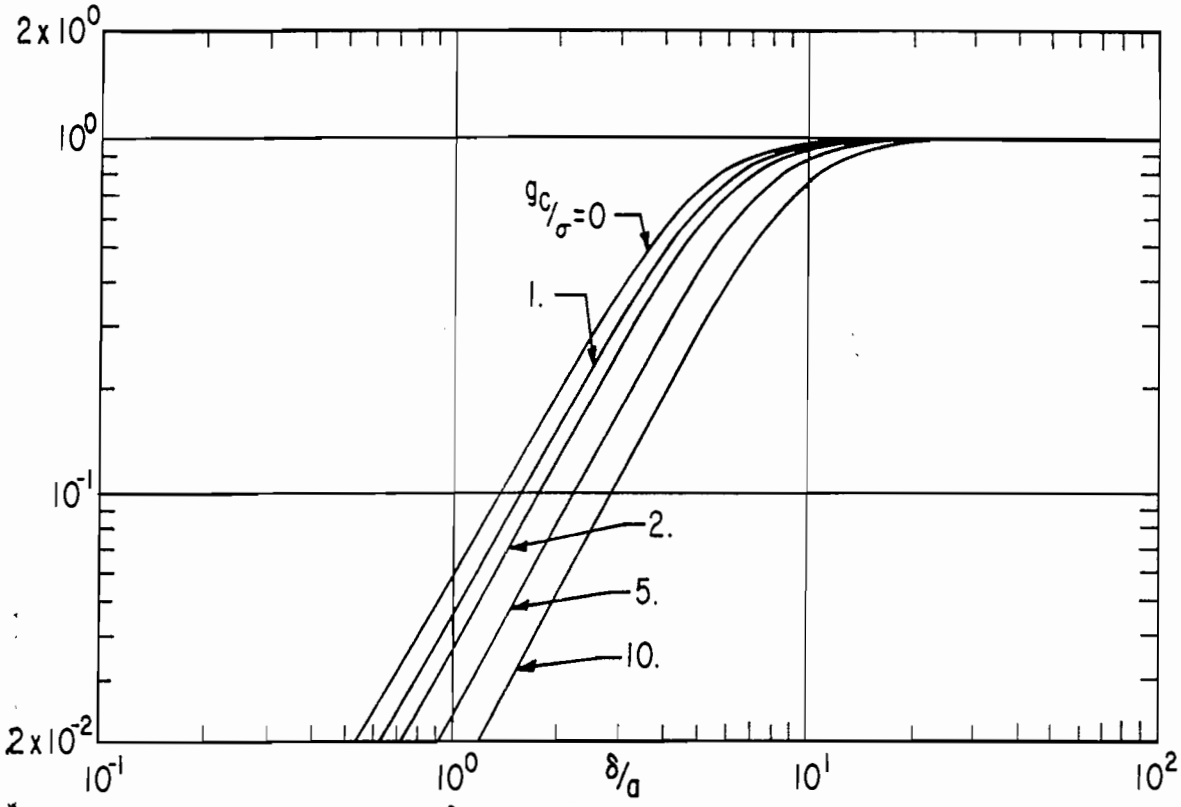

A. MAGNITUDE OF R' vs. δ/a WITH g_c/σ AS A PARAMETER

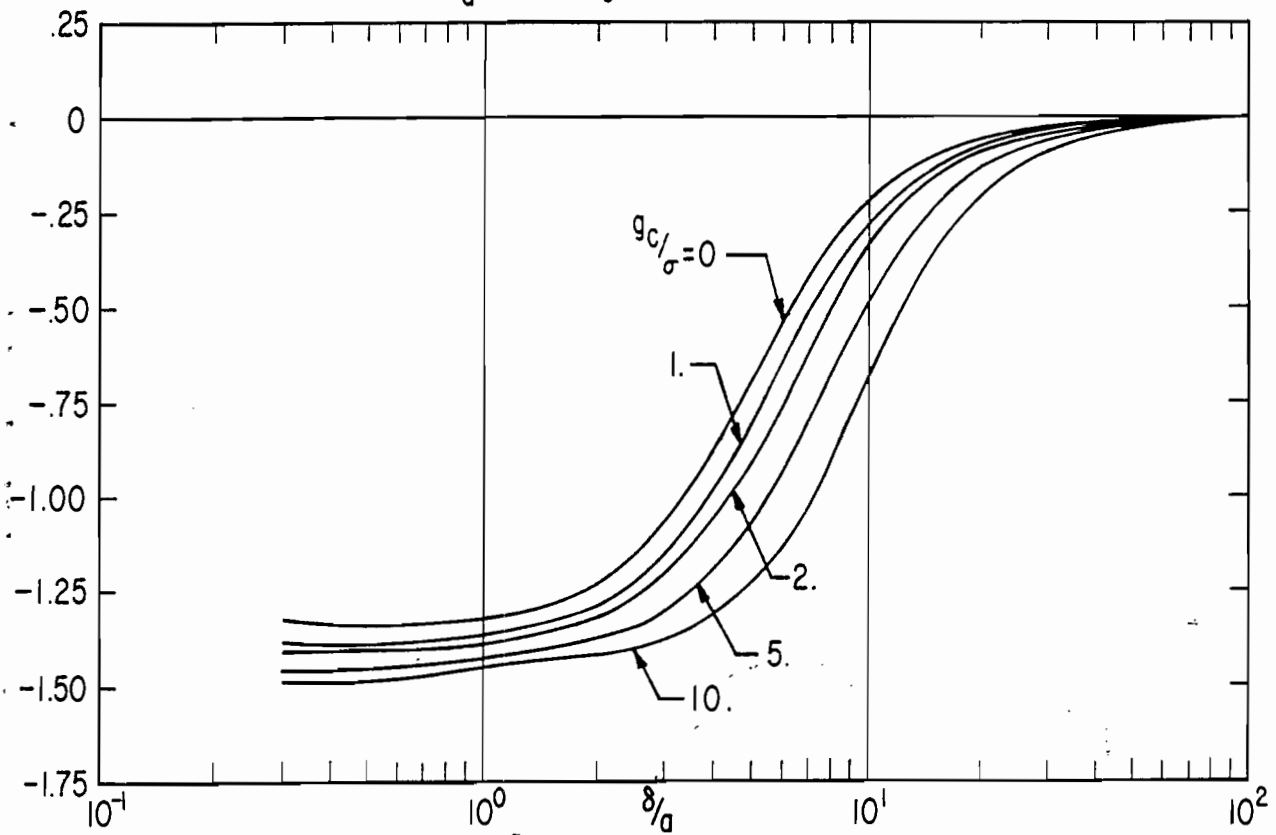

B. PHASE OF R' vs. δ/a WITH g_c/σ AS A PARAMETER

FIGURE 23. RESPONSE CHARACTERISTICS OF CYLINDRICAL LOOP BELOW GROUND PLANE WITH HIGH, EQUAL CONDUCTIVITIES BOTH INSIDE & OUTSIDE OF LOOP: $b/a = .01$

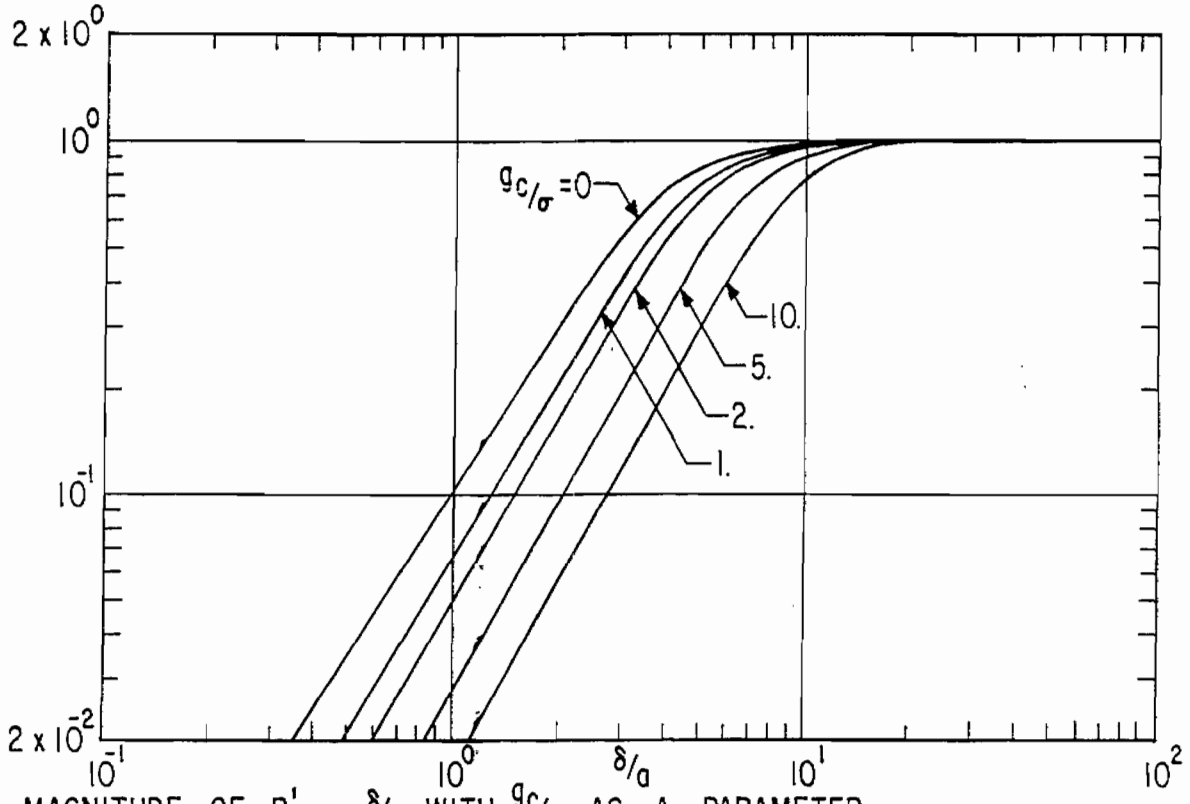

A. MAGNITUDE OF R' vs. δ/a WITH $g_{c/\sigma}$ AS A PARAMETER

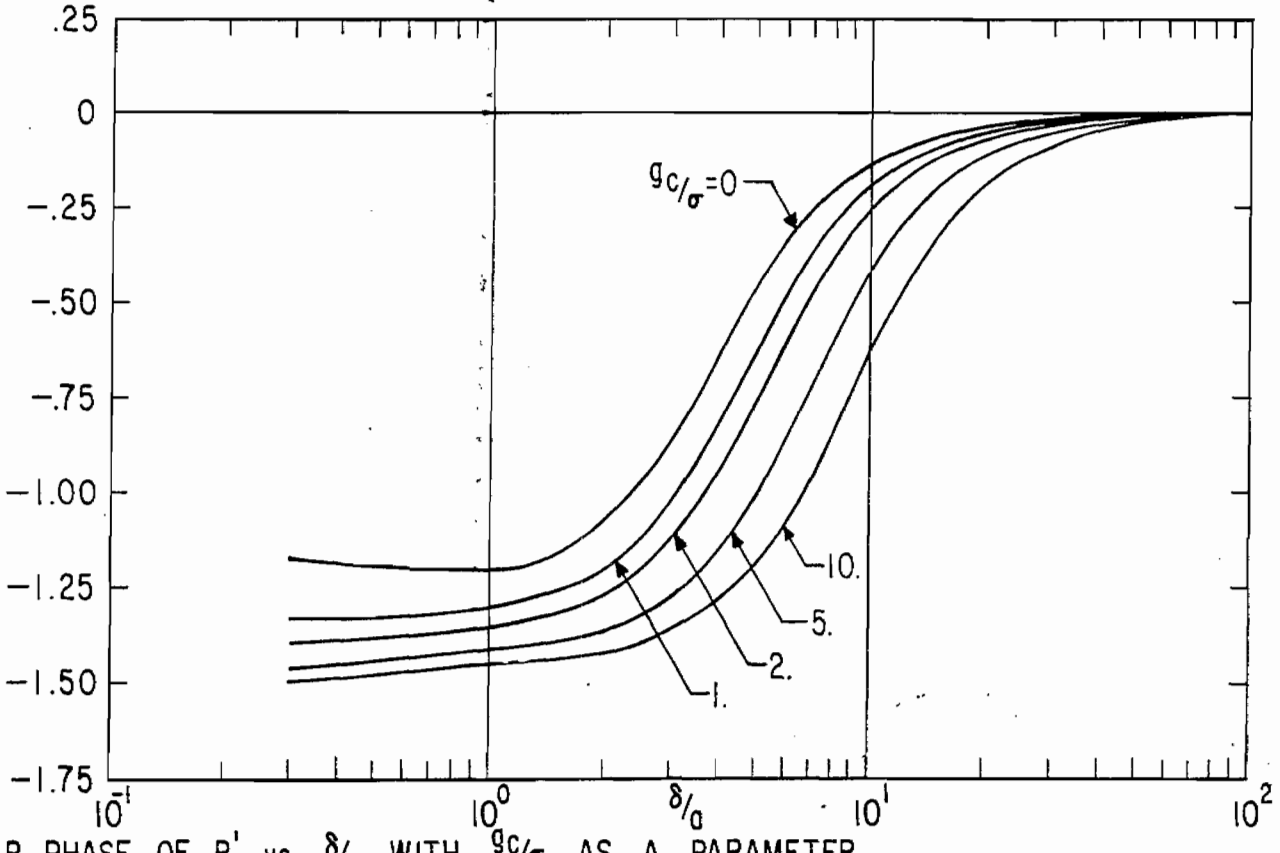

B. PHASE OF R' vs. δ/a WITH $g_{c/\sigma}$ AS A PARAMETER

FIGURE 24. RESPONSE CHARACTERISTICS OF CYLINDRICAL LOOP BELOW GROUND PLANE WITH HIGH, EQUAL CONDUCTIVITIES BOTH INSIDE AND OUTSIDE OF LOOP: $b/a = .1$

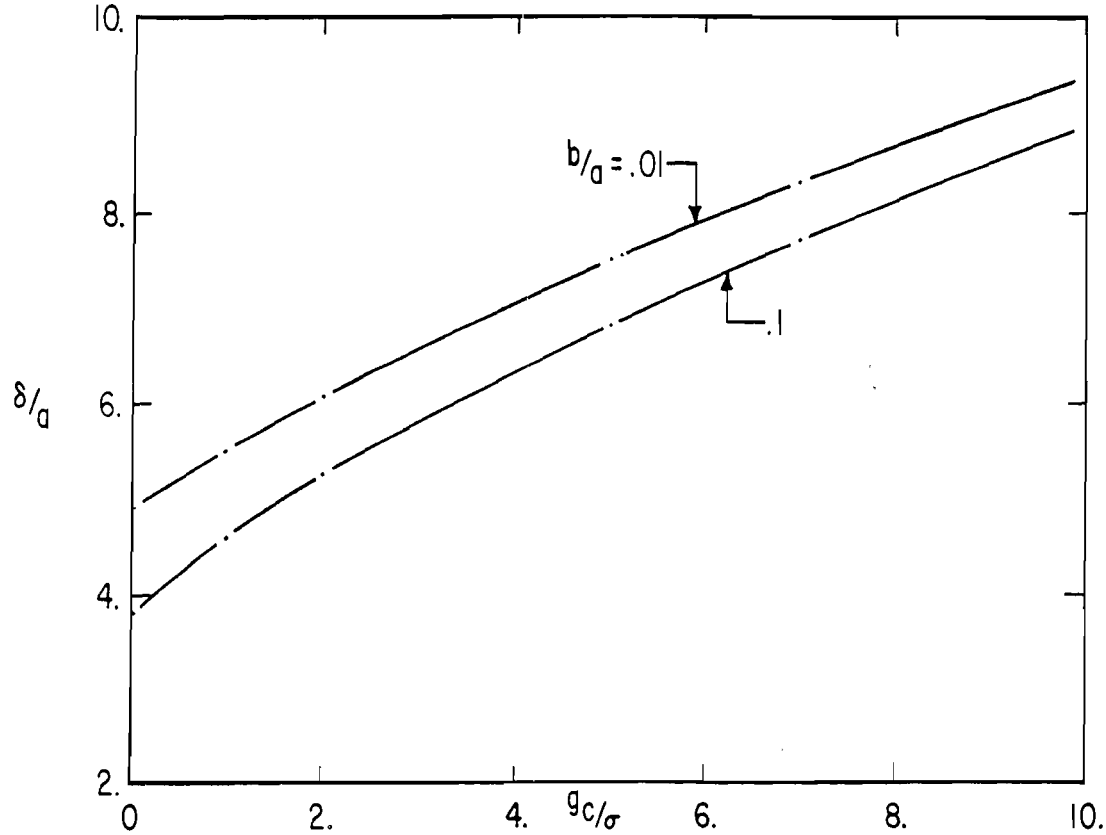

A. δ/a vs. g_c/σ WITH b/a AS A PARAMETER

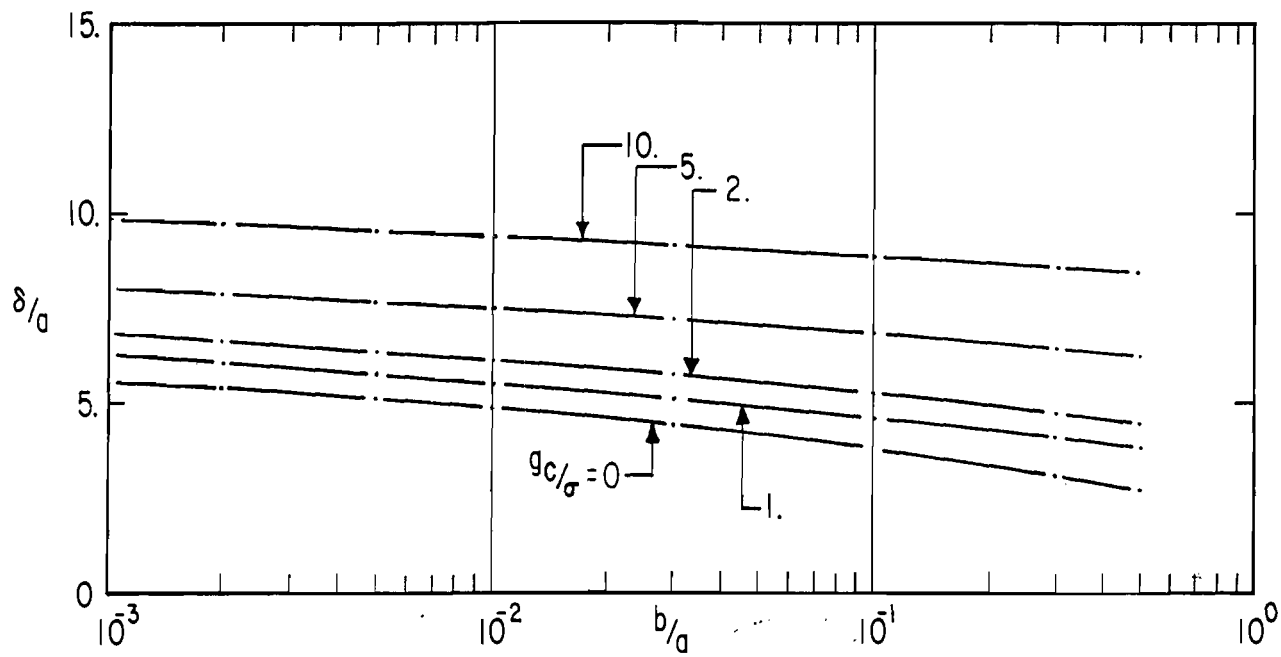

B. δ/a vs. b/a WITH g_c/σ AS A PARAMETER

FIGURE 25. DEPENDENCE OF FREQUENCY RESPONSE ON CABLE CONDUCTANCE FOR CYLINDRICAL LOOP BELOW GROUND PLANE WITH HIGH, EQUAL CONDUCTIVITIES BOTH INSIDE & OUTSIDE OF LOOP : $|R'| = 1/\sqrt{2}$

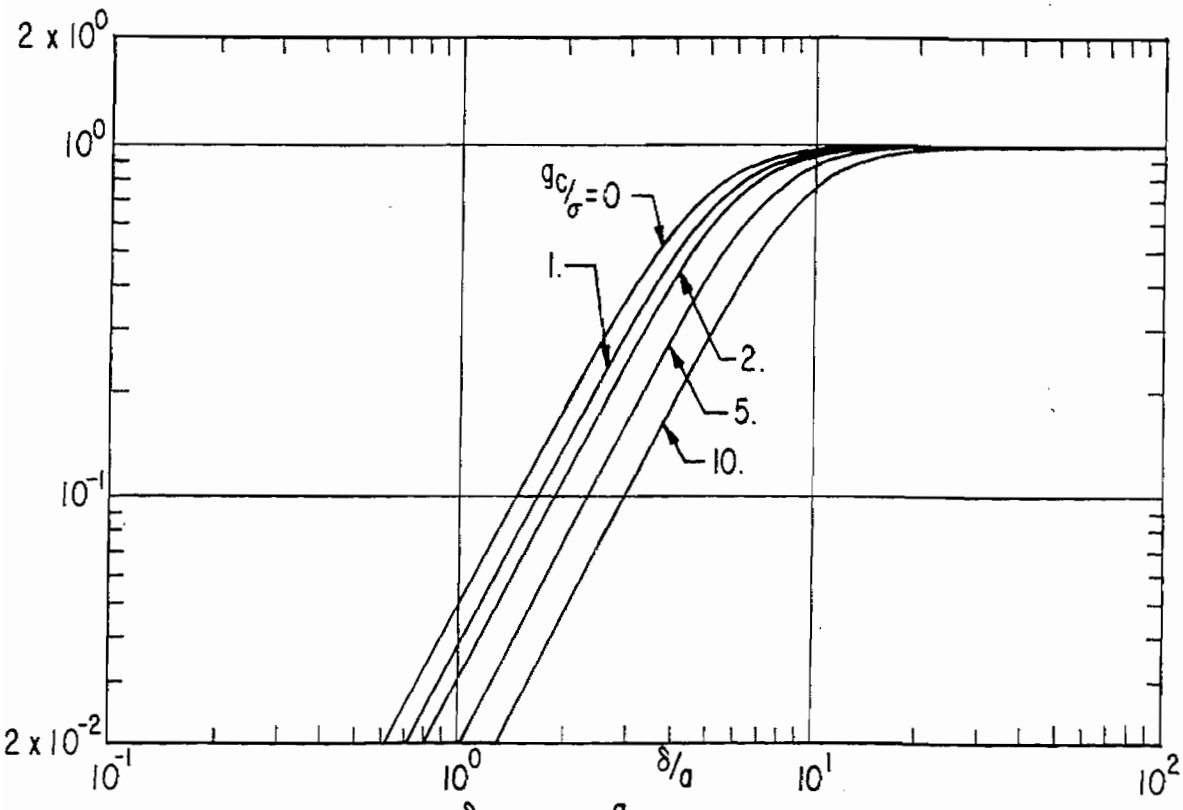

A. MAGNITUDE OF R_y vs. δ/a WITH g_c/σ AS A PARAMETER

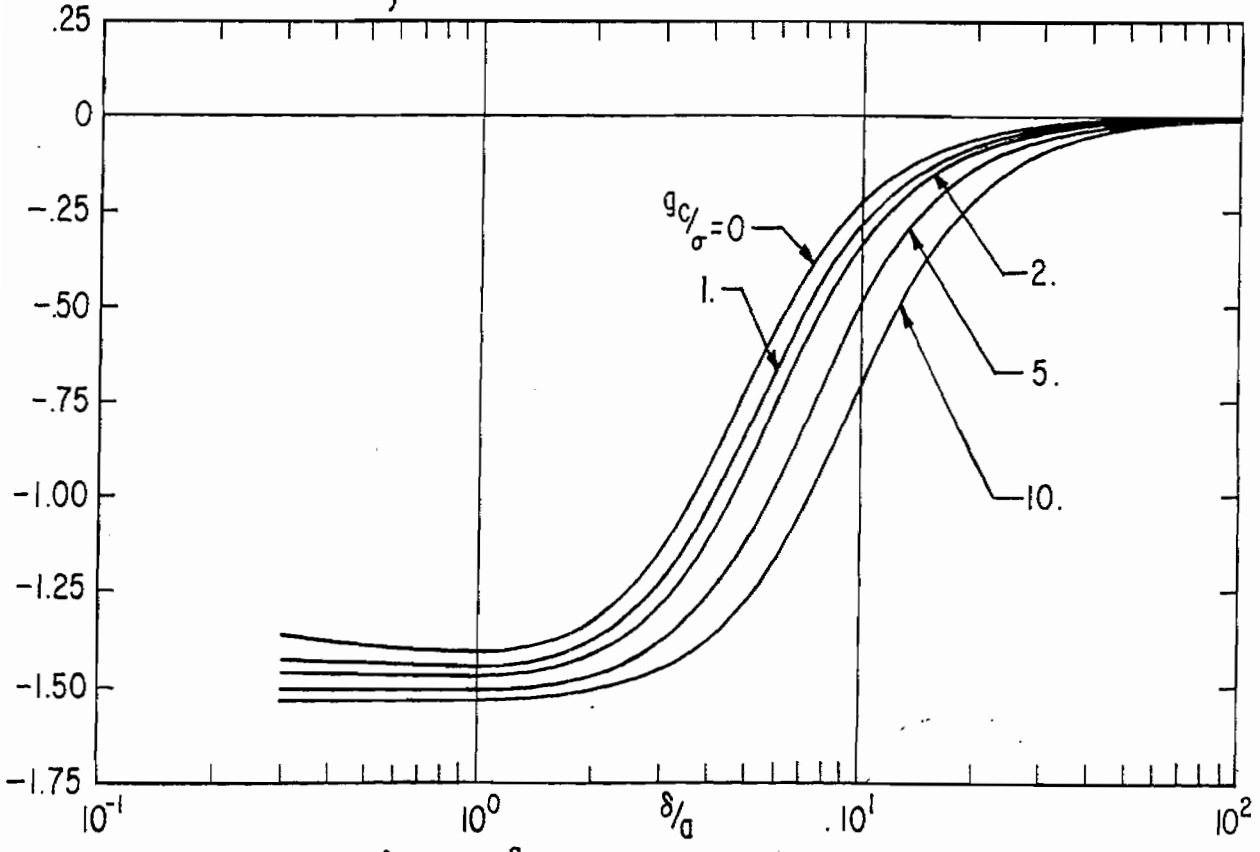

B. PHASE OF R_y vs. δ/a WITH g_c/σ AS A PARAMETER

FIGURE 26. EFFECT OF ADMITTANCES ON RESPONSE OF EXPOSED CYLINDRICAL LOOP WITH HIGH, EQUAL CONDUCTIVITIES BOTH INSIDE & OUTSIDE OF LOOP: $b/a = .01$

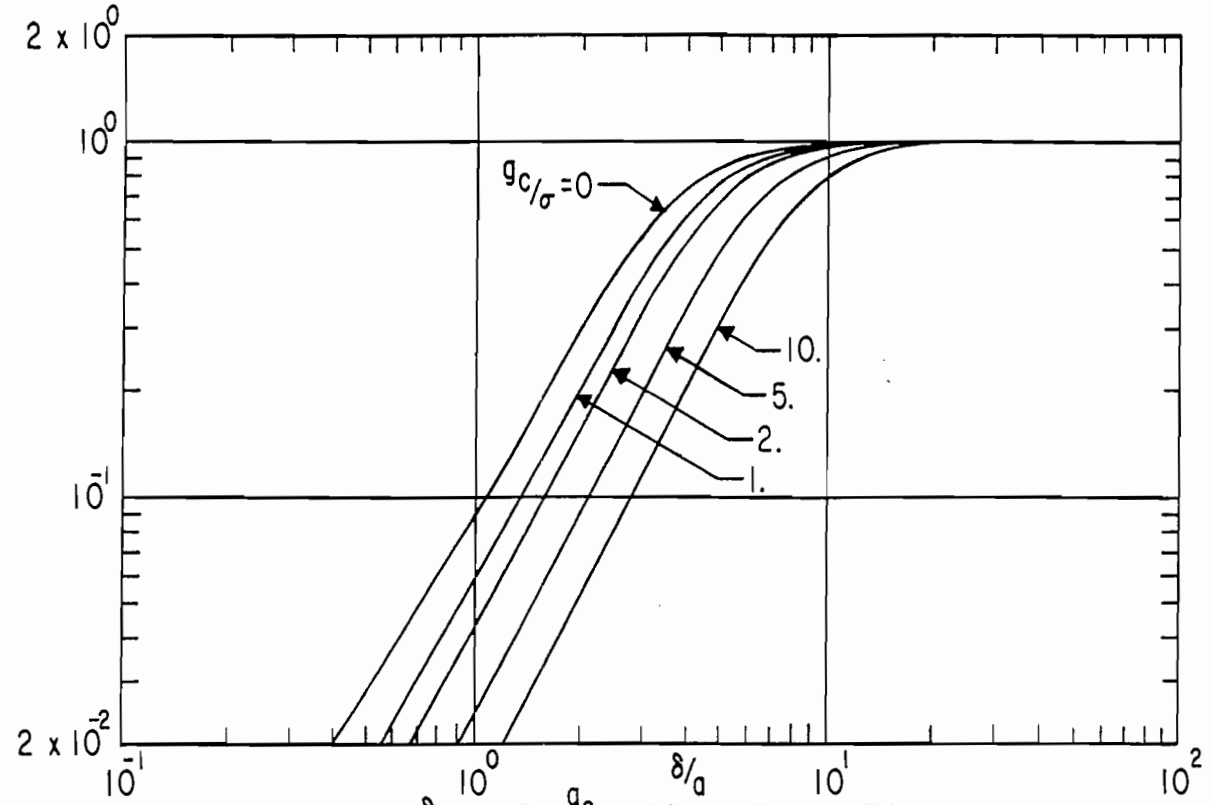

A. MAGNITUDE OF R_y vs. δ/a WITH g_c/σ AS A PARAMETER

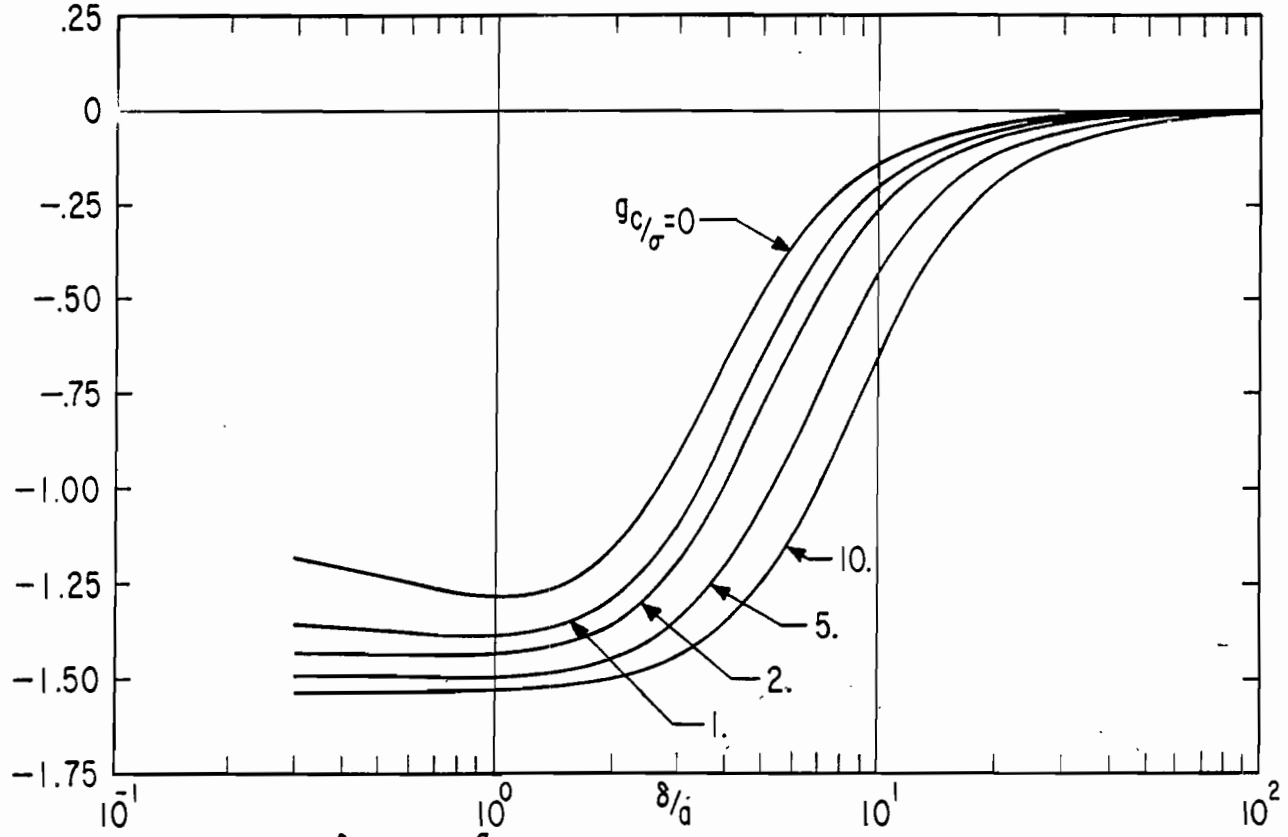

B. PHASE OF R_y vs. δ/a WITH g_c/σ AS A PARAMETER

FIGURE 27. EFFECT OF ADMITTANCES ON RESPONSE OF EXPOSED CYLINDRICAL LOOP WITH HIGH, EQUAL CONDUCTIVITIES BOTH INSIDE & OUTSIDE OF LOOP: $b/a = .1$

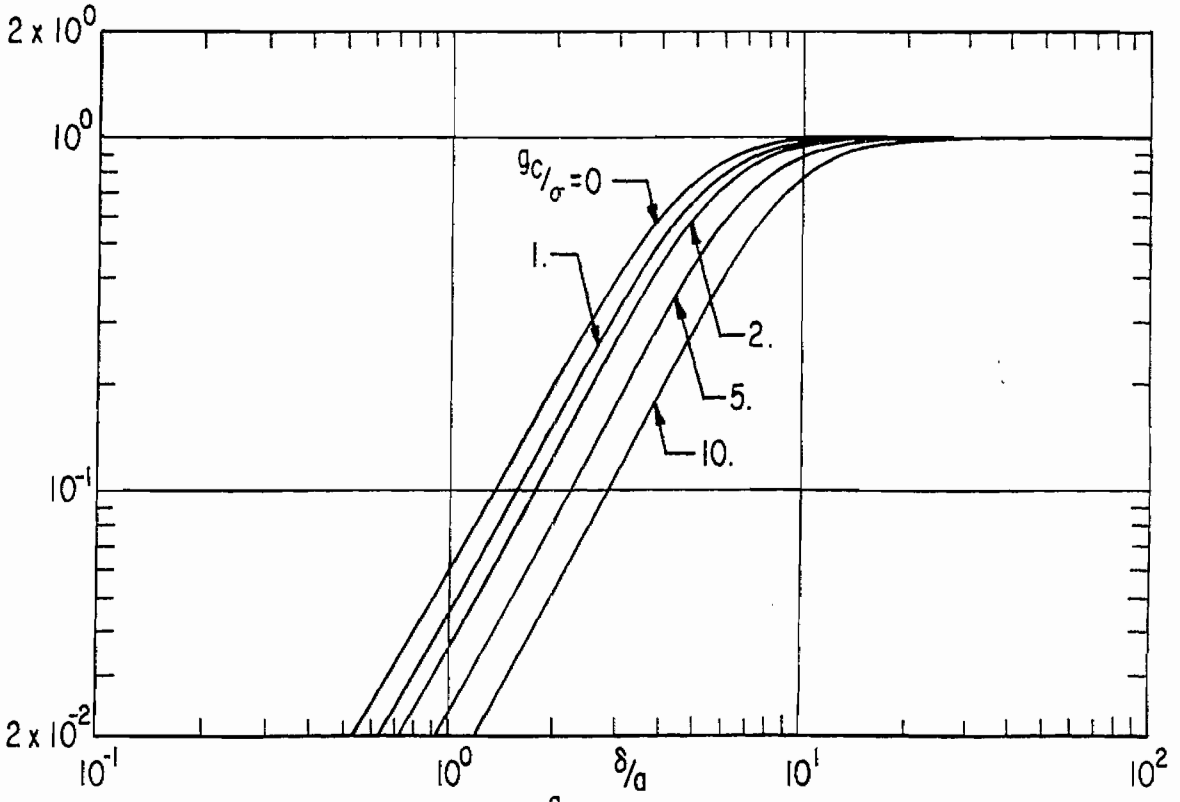

A. MAGNITUDE OF R vs. δ/a WITH g_c/σ AS A PARAMETER

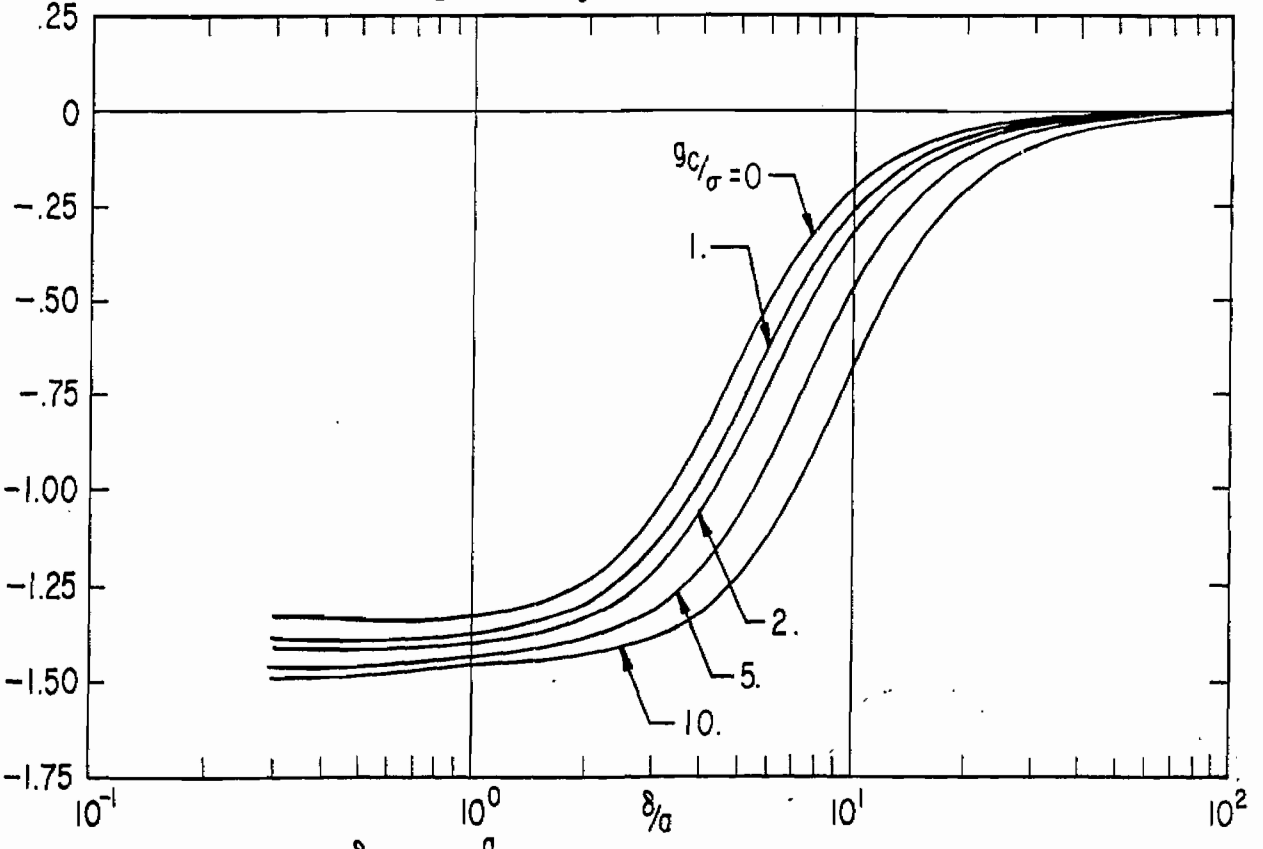

B. PHASE OF R vs. δ/a WITH g_c/σ AS A PARAMETER

FIGURE 28. RESPONSE CHARACTERISTICS OF EXPOSED CYLINDRICAL LOOP WITH HIGH, EQUAL CONDUCTIVITIES BOTH INSIDE & OUTSIDE OF LOOP: $b/a = .01$

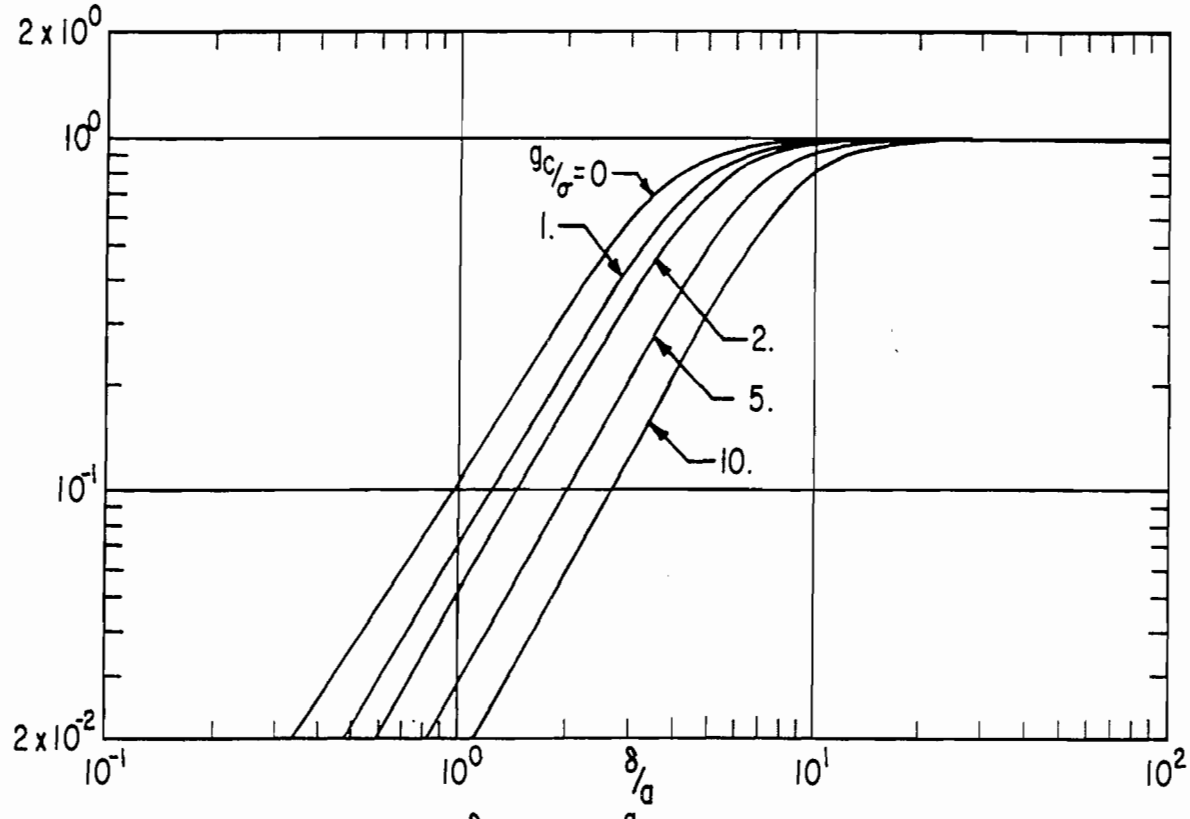

A. MAGNITUDE OF R vs. δ/a WITH gc/σ AS A PARAMETER

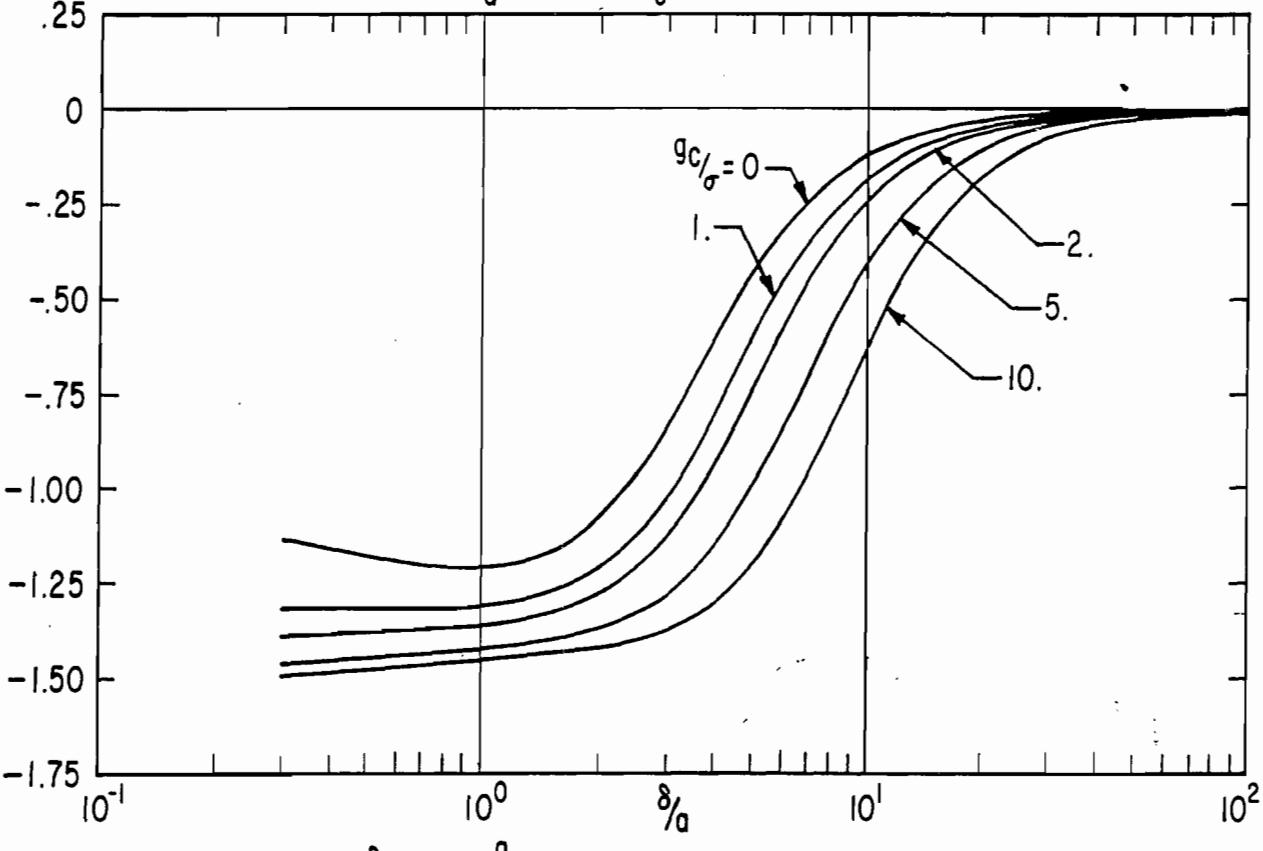

B. PHASE OF R vs. δ/a WITH gc/σ AS A PARAMETER

FIGURE 29. RESPONSE CHARACTERISTICS OF EXPOSED CYLINDRICAL LOOP WITH HIGH, EQUAL CONDUCTIVITIES BOTH INSIDE & OUTSIDE OF LOOP: $b/a = .1$

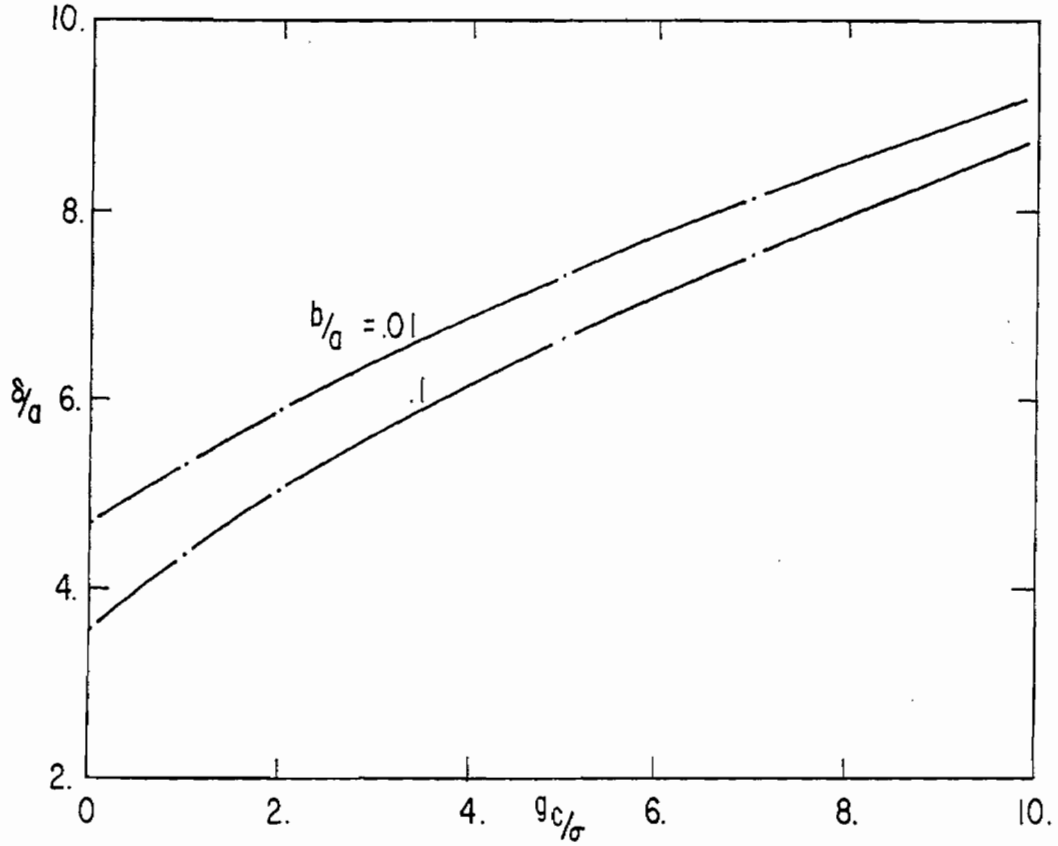

A. δ/a vs. g_c/σ WITH b/a AS A PARAMETER

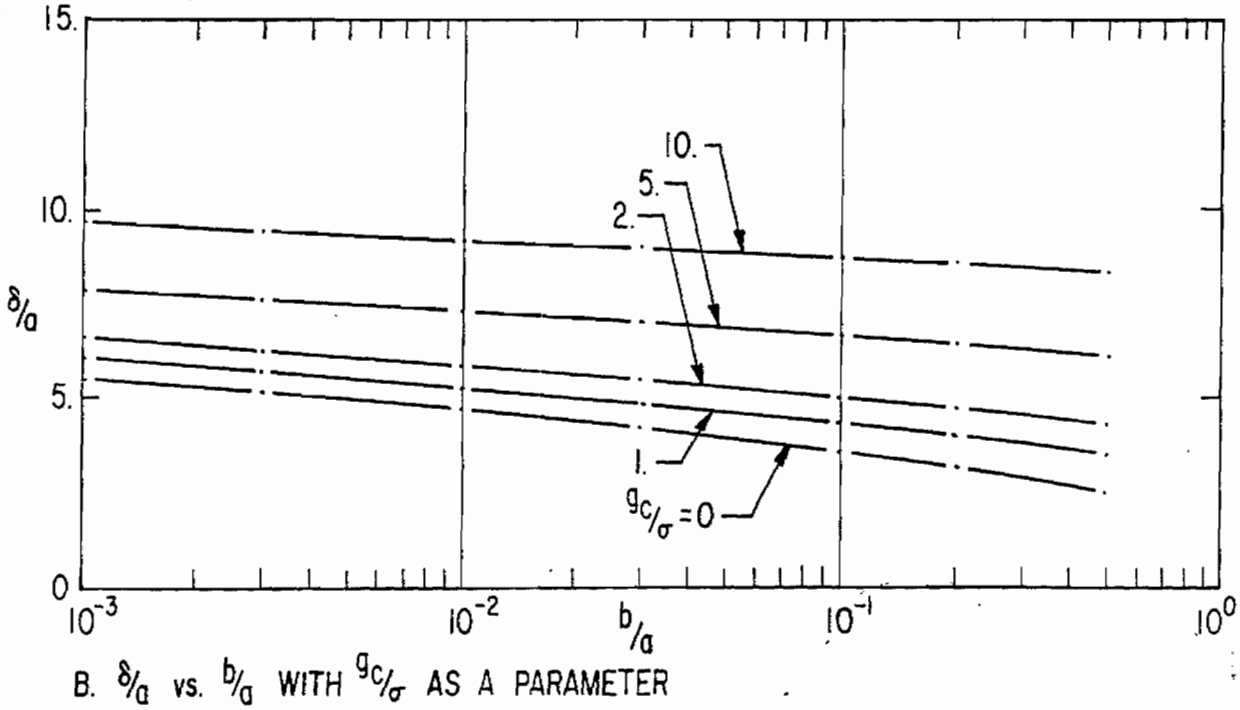

B. δ/a vs. b/a WITH g_c/σ AS A PARAMETER

FIGURE 30. DEPENDENCE OF FREQUENCY RESPONSE ON CABLE CONDUCTANCE FOR EXPOSED CYLINDRICAL LOOP WITH HIGH, EQUAL CONDUCTIVITIES BOTH INSIDE & OUTSIDE OF LOOP: $|R| = 1/\sqrt{2}$

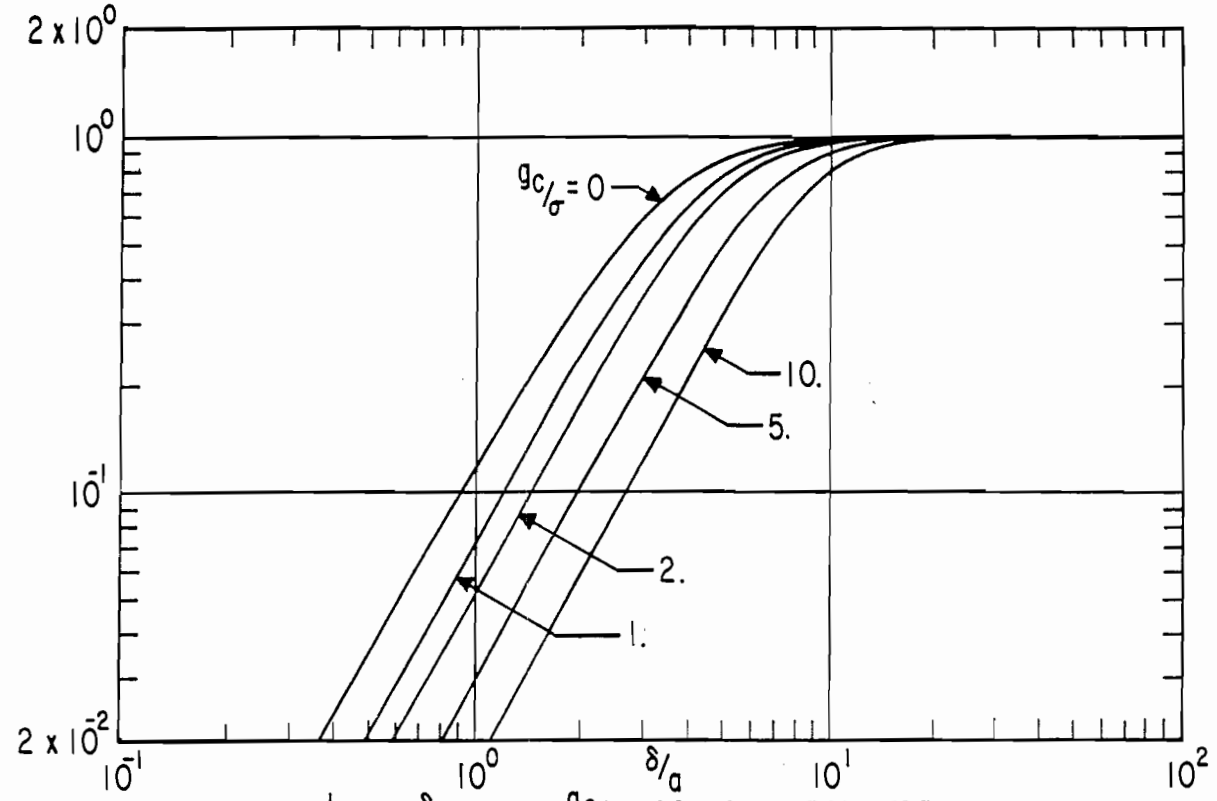

A. MAGNITUDE OF R' vs. δ/a WITH gc/σ AS A PARAMETER

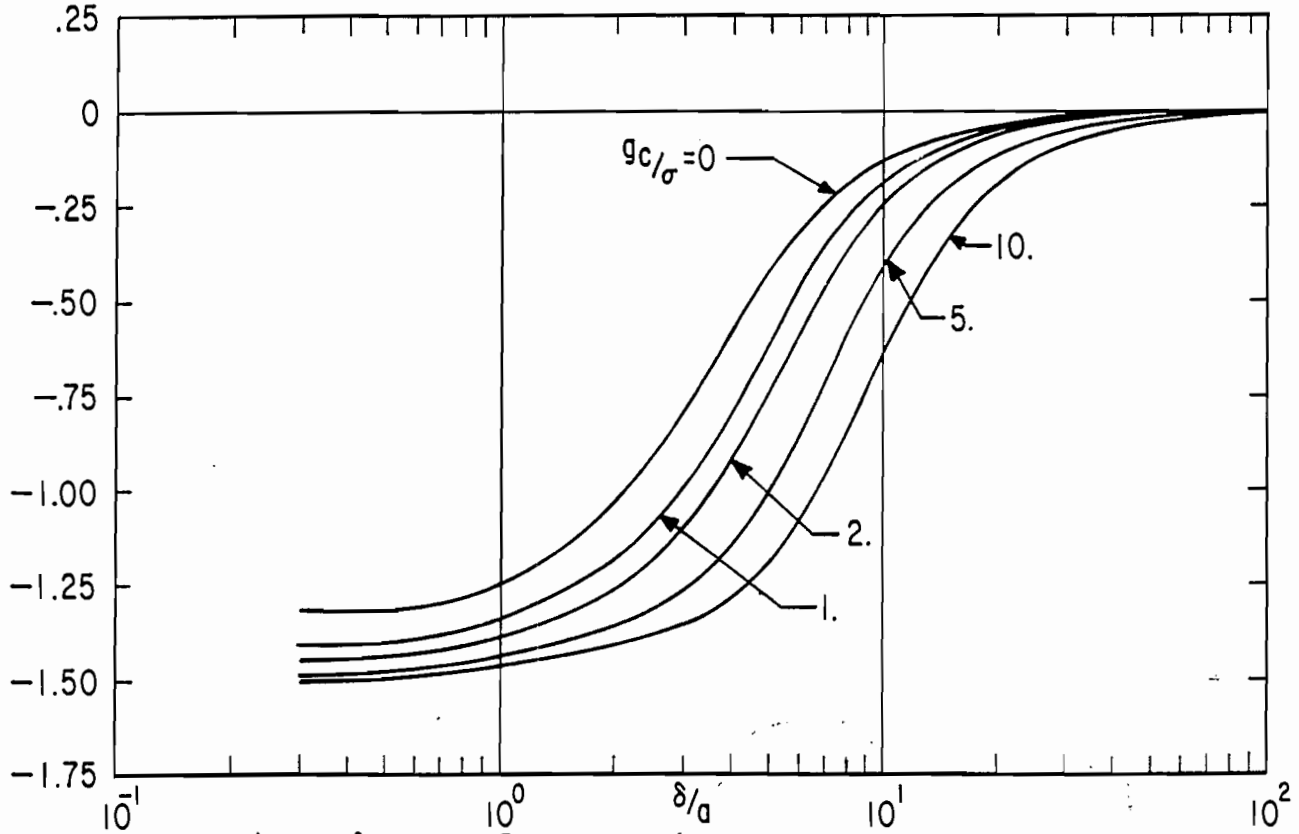

B. PHASE OF R' vs. δ/a WITH gc/σ AS A PARAMETER

FIGURE 31. RESPONSE CHARACTERISTICS OF CYLINDRICAL LOOP BELOW GROUND PLANE WITH HIGH CONDUCTIVITY OUTSIDE & NO CONDUCTIVITY INSIDE OF LOOP : $b/a = .01$

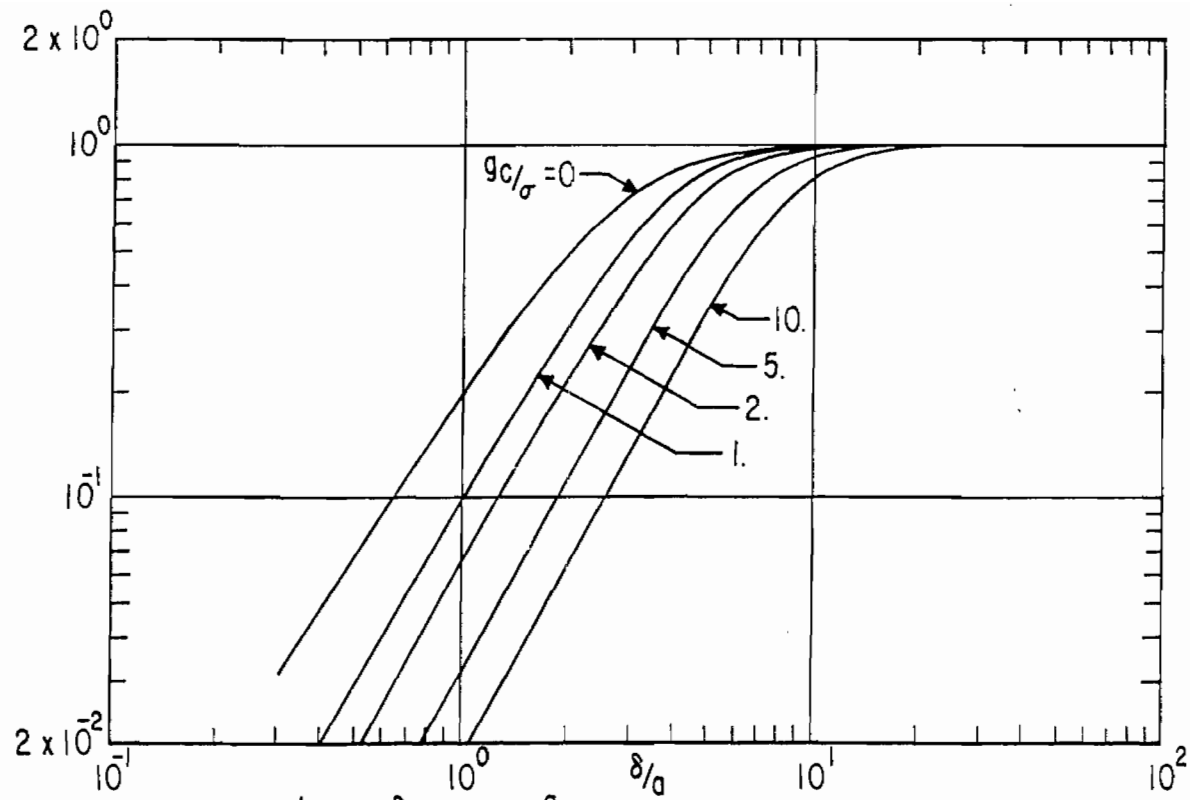

A. MAGNITUDE OF R' vs. δ/a WITH g_c/σ AS A PARAMETER

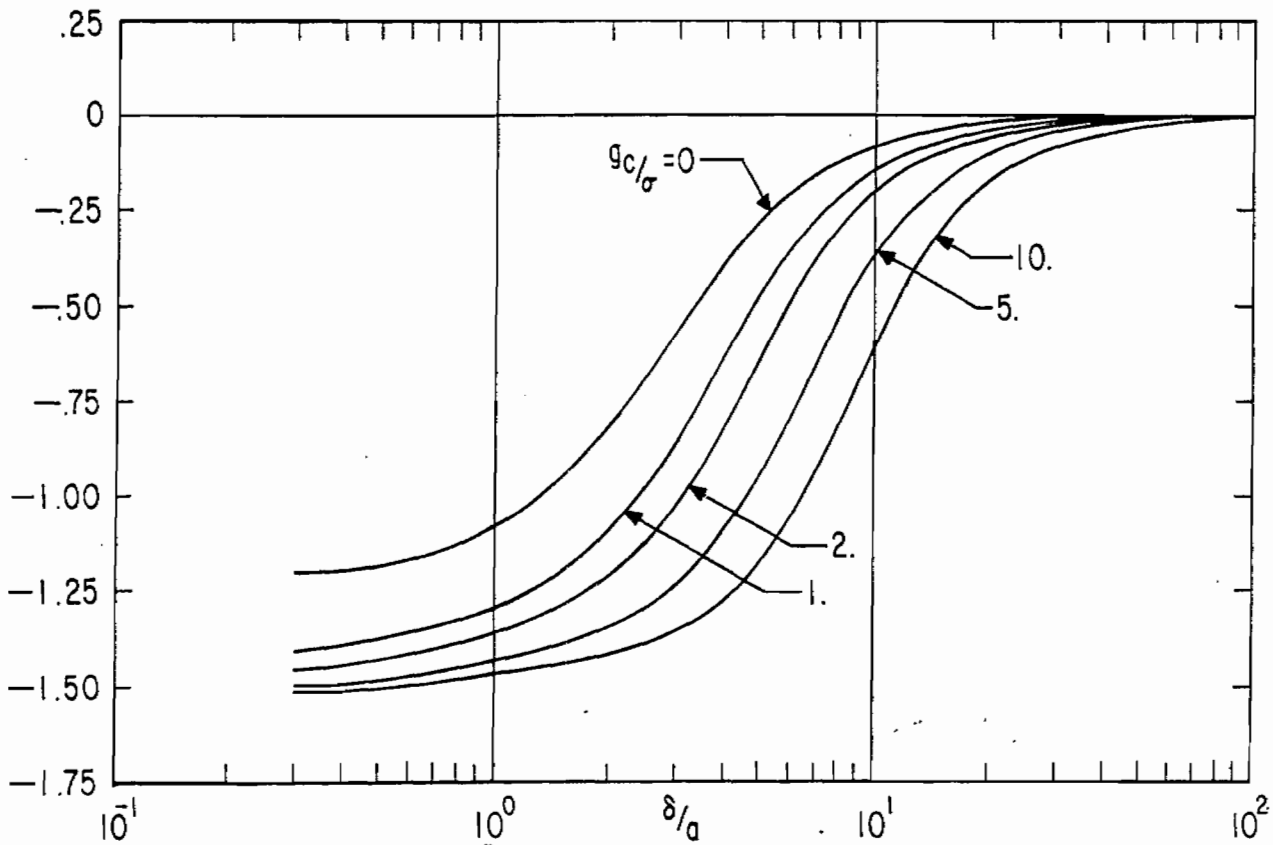

B. PHASE OF R' vs. δ/a WITH g_c/σ AS A PARAMETER

FIGURE 32. RESPONSE CHARACTERISTICS OF CYLINDRICAL LOOP BELOW GROUND PLANE WITH HIGH CONDUCTIVITY OUTSIDE & NO CONDUCTIVITY INSIDE OF LOOP: $b/a = .1$

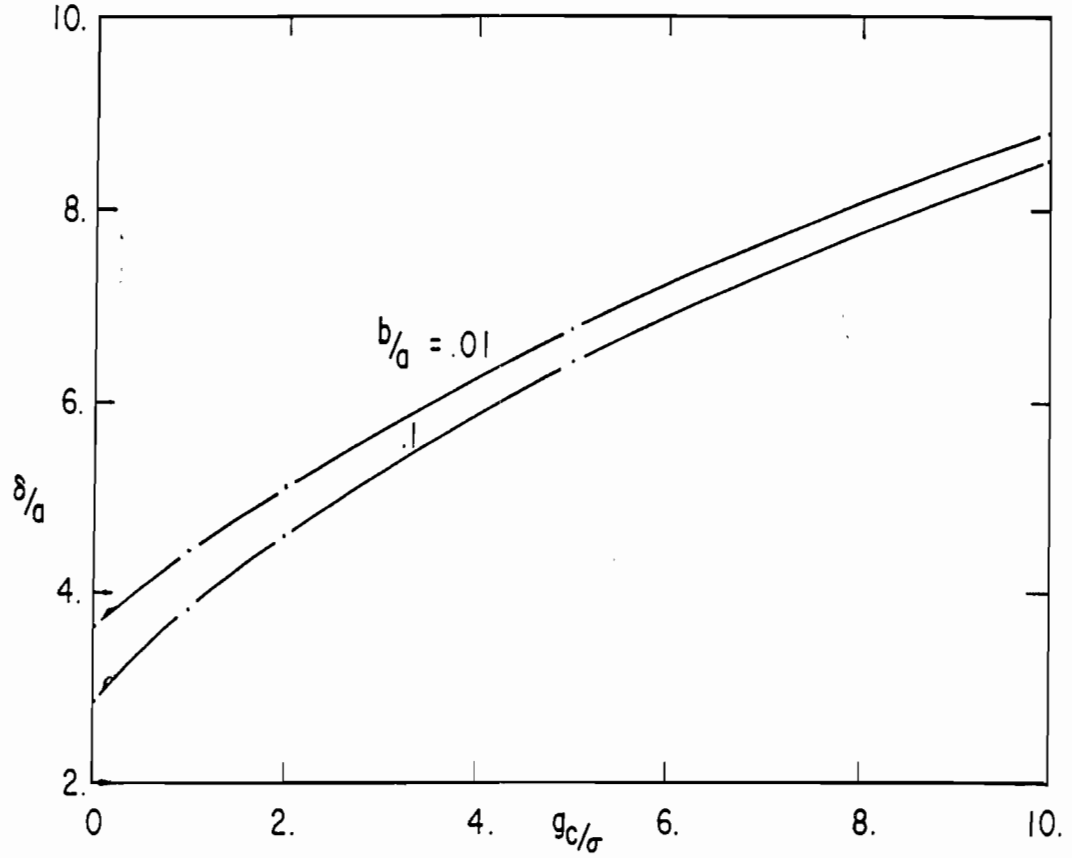

A. δ/a vs. $g_{c/\sigma}$ WITH b/a AS A PARAMETER

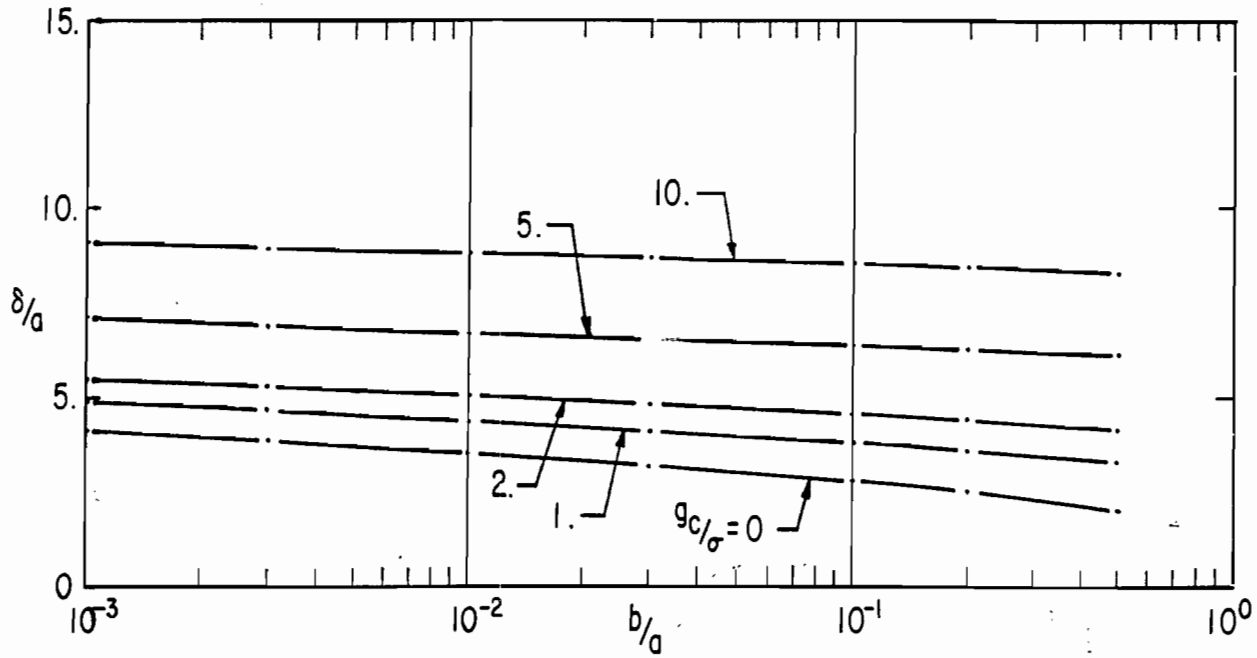

B. δ/a vs. b/a WITH $g_{c/\sigma}$ AS A PARAMETER

FIGURE 33. DEPENDENCE OF FREQUENCY RESPONSE ON CABLE CONDUCTANCE FOR CYLINDRICAL LOOP BELOW GROUND PLANE WITH HIGH CONDUCTIVITY OUTSIDE AND NO CONDUCTIVITY INSIDE OF LOOP: $|R'| = 1/\sqrt{2}$

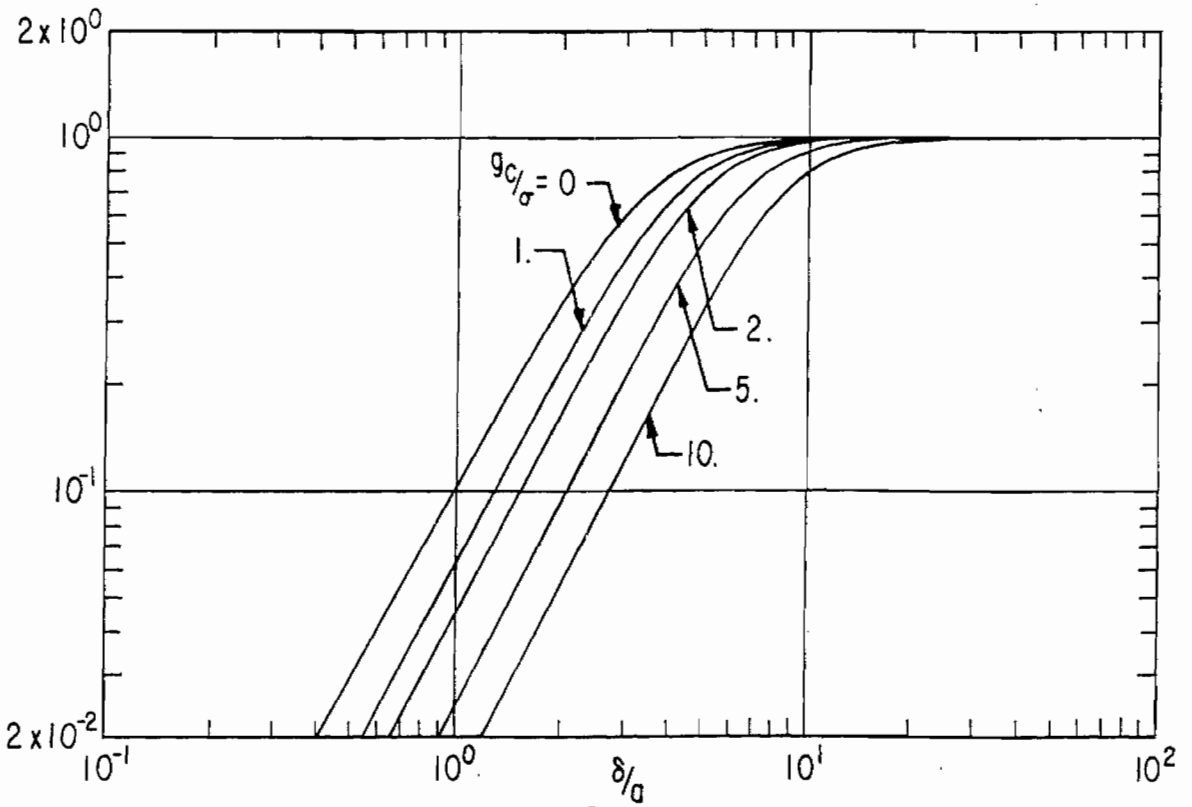

A. MAGNITUDE OF R_y vs. δ/a WITH g_c/σ AS A PARAMETER

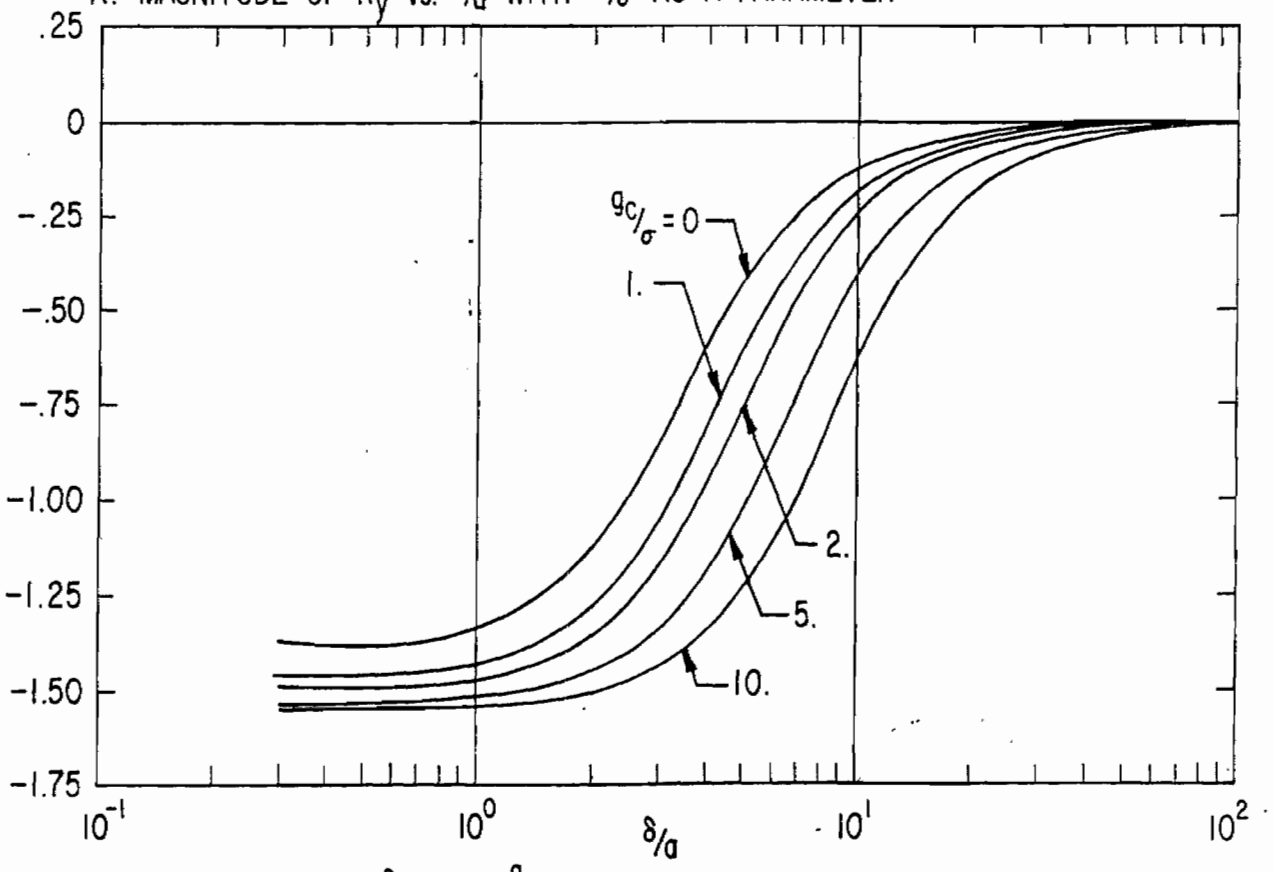

B. PHASE OF R_y vs. δ/a WITH g_c/σ AS A PARAMETER

FIGURE 34. EFFECT OF ADMITTANCES ON RESPONSE OF EXPOSED CYLINDRICAL LOOP WITH HIGH CONDUCTIVITY OUTSIDE & NO CONDUCTIVITY INSIDE OF LOOP: $b/a = .01$

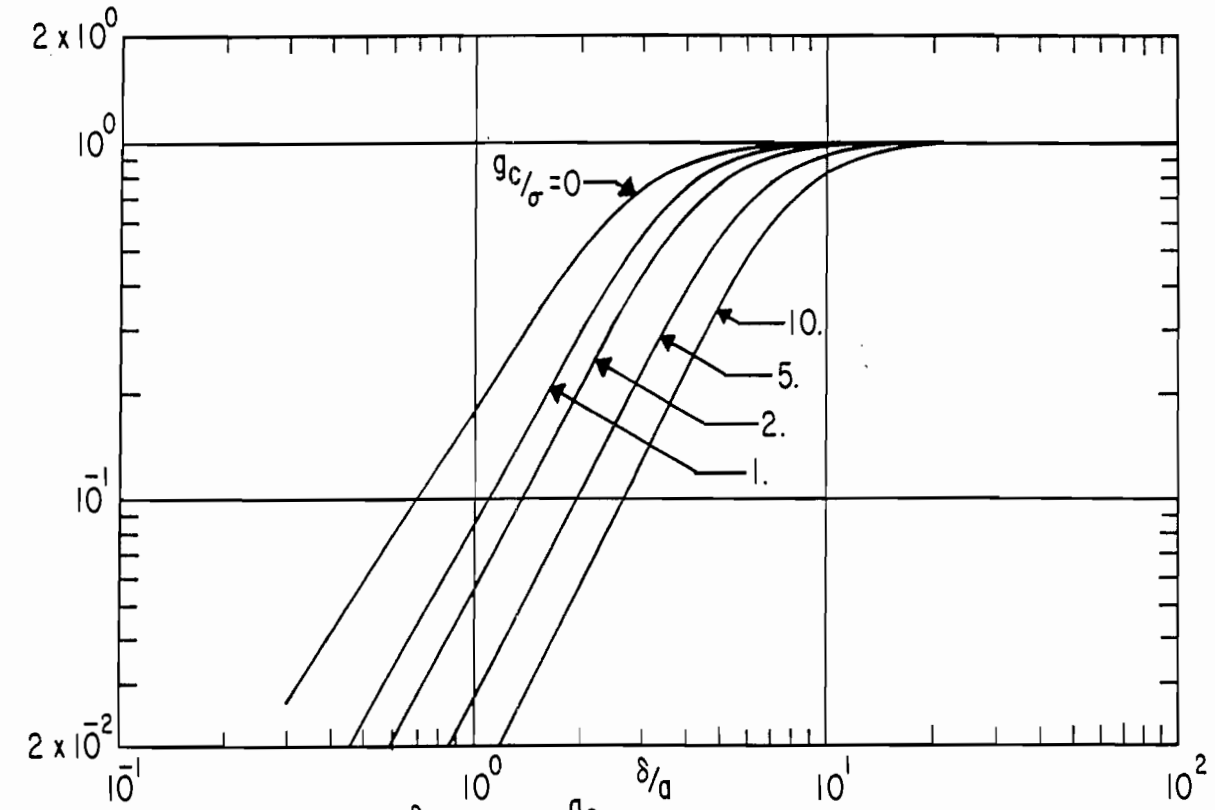

A. MAGNITUDE OF R_y vs. δ/a WITH g_c/σ AS A PARAMETER

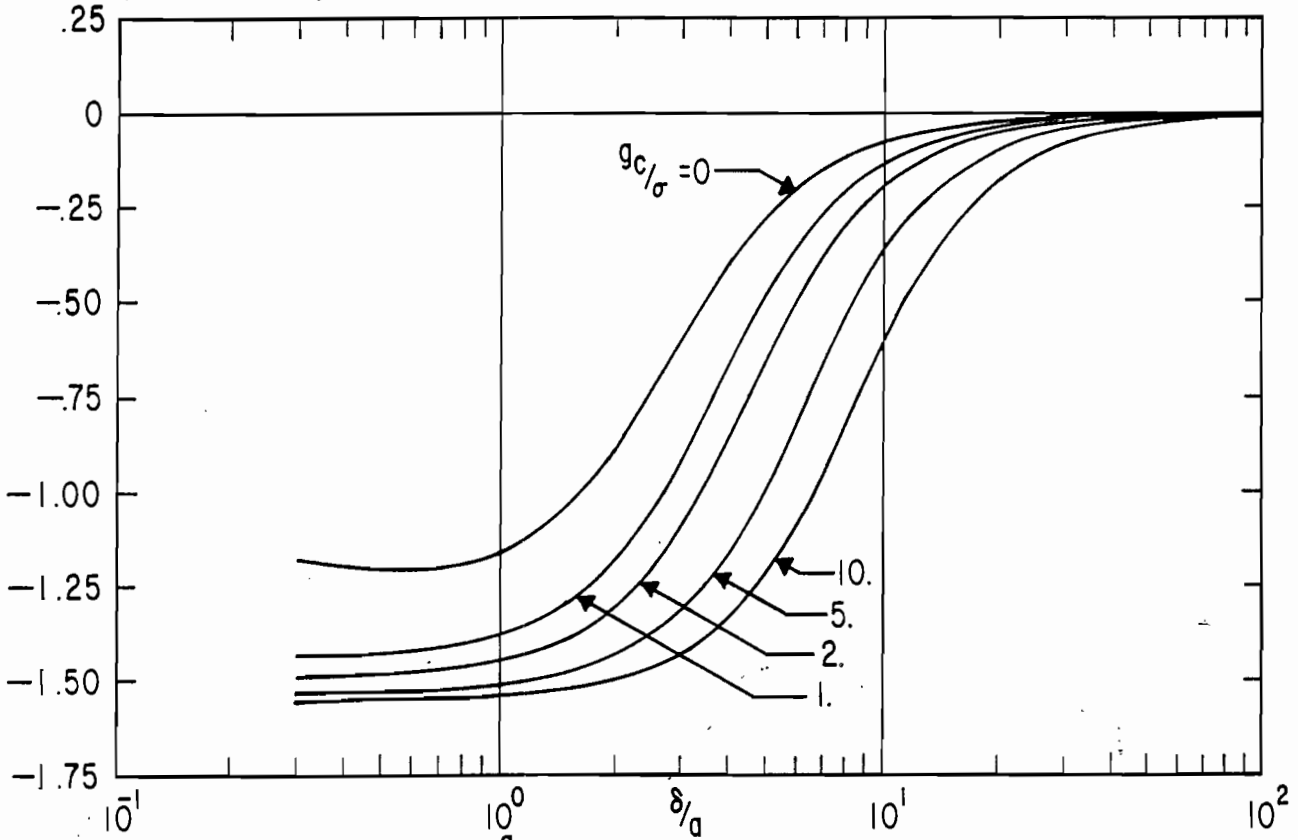

B. PHASE OF R_y vs. δ/a WITH g_c/σ AS A PARAMETER

FIGURE 35. EFFECT OF ADMITTANCES ON RESPONSE OF EXPOSED CYLINDRICAL LOOP WITH HIGH CONDUCTIVITY OUTSIDE & NO CONDUCTIVITY INSIDE OF LOOP : $b/a = .1$

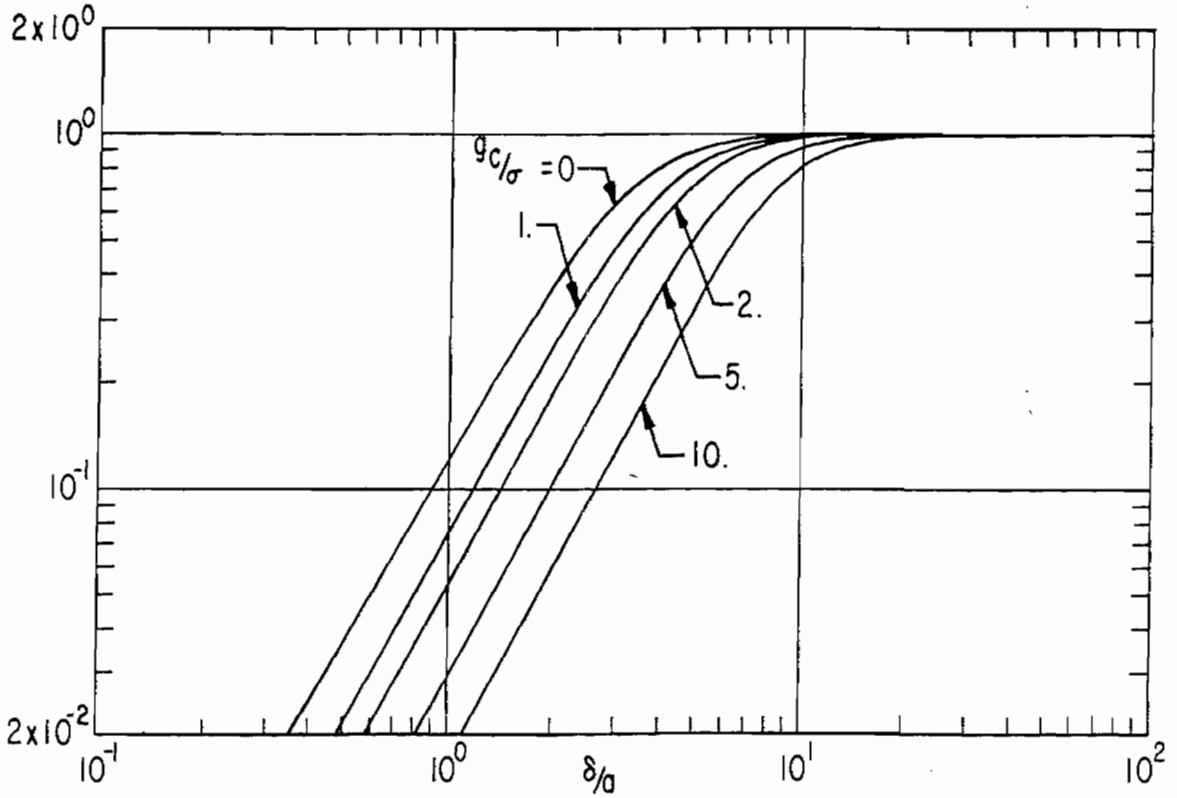

A. MAGNITUDE OF R vs. δ/a WITH g_c/σ AS A PARAMETER

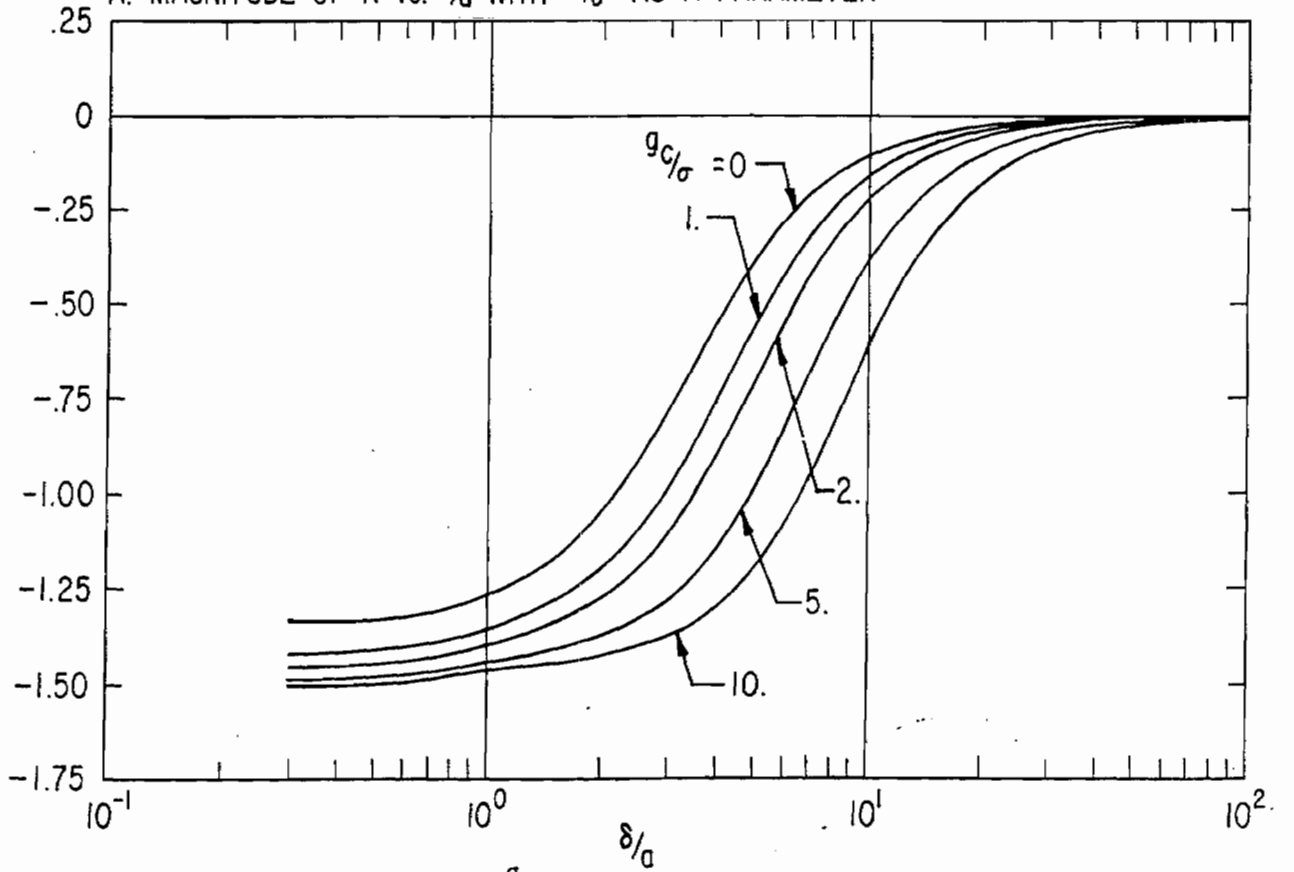

B. PHASE OF R vs. δ/a WITH g_c/σ AS A PARAMETER

FIGURE 36. RESPONSE CHARACTERISTICS OF EXPOSED CYLINDRICAL LOOP WITH HIGH CONDUCTIVITY OUTSIDE & NO CONDUCTIVITY INSIDE OF LOOP: $b/a = .01$

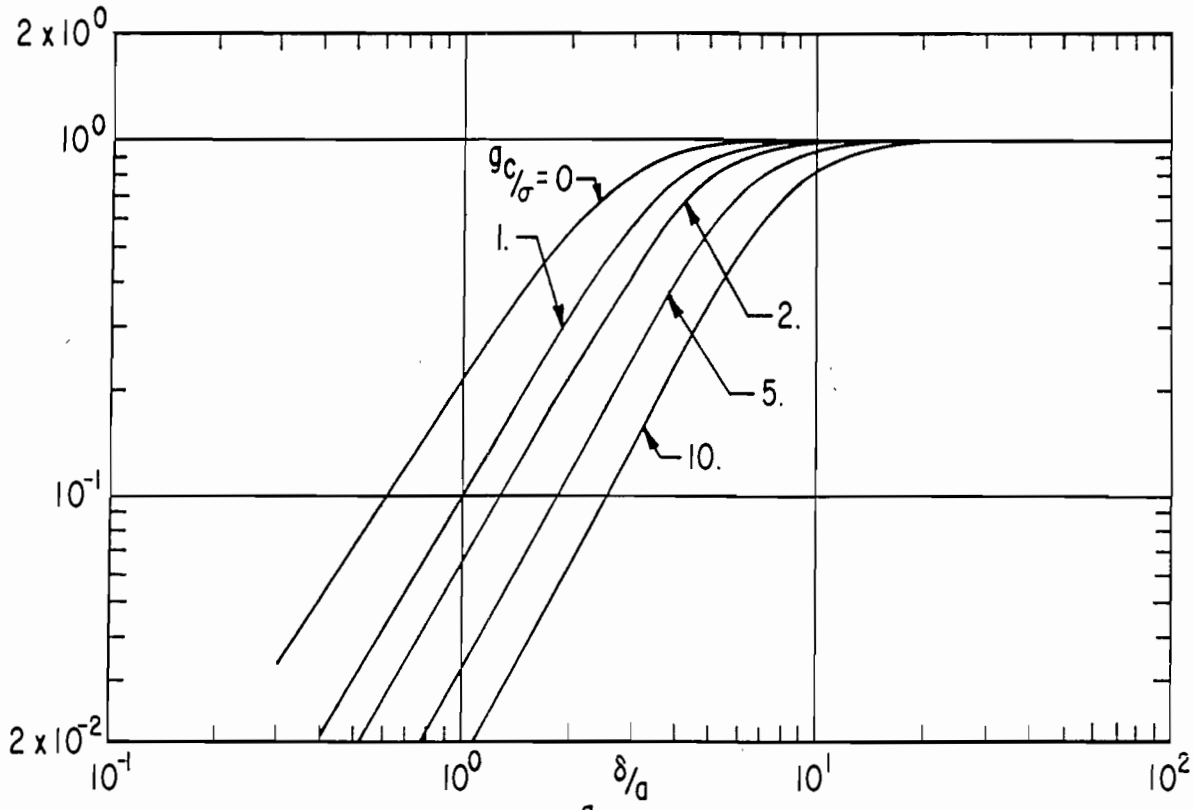

A. MAGNITUDE OF R vs. δ/a WITH g_c/σ AS A PARAMETER

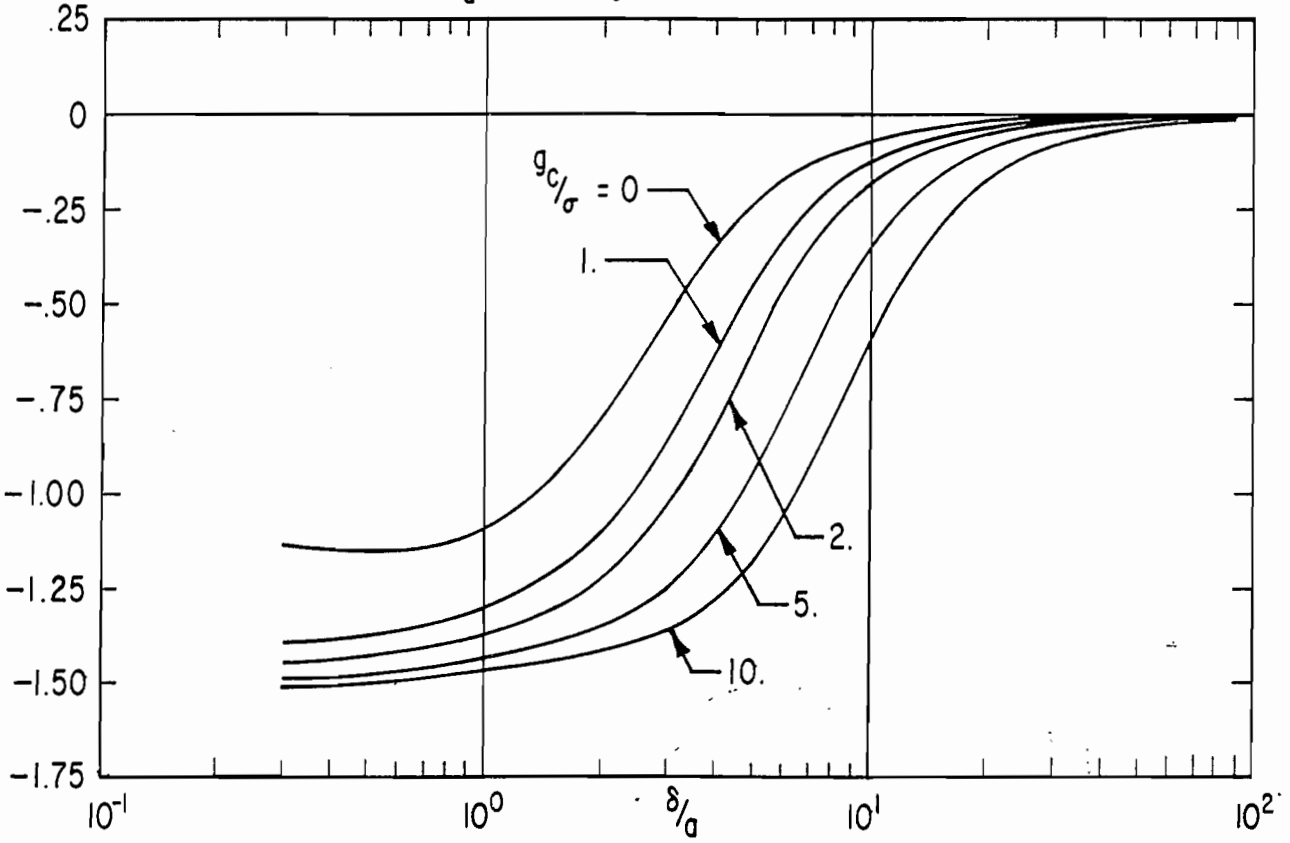

B. PHASE OF R vs. δ/a WITH g_c/σ AS A PARAMETER

FIGURE 37. RESPONSE CHARACTERISTICS OF EXPOSED CYLINDRICAL LOOP WITH HIGH CONDUCTIVITY OUTSIDE & NO CONDUCTIVITY INSIDE OF LOOP: $b/a = .1$

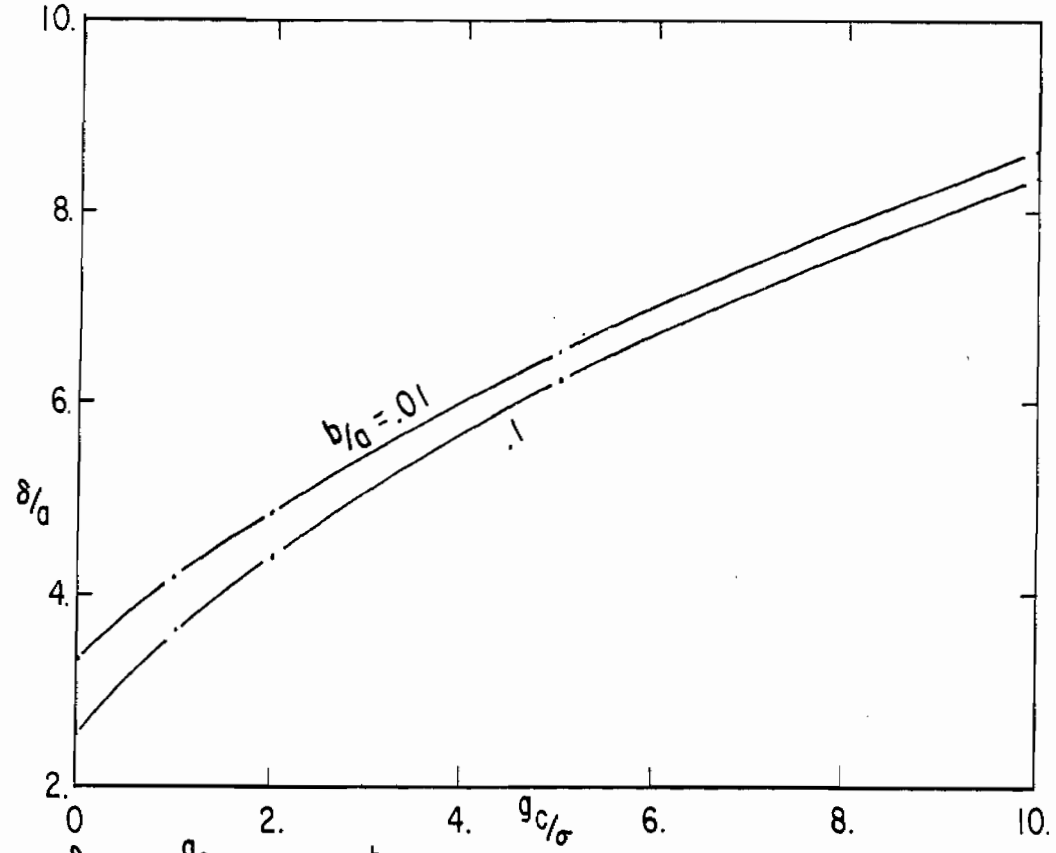

A. δ/a vs. $g_{c/\sigma}$ WITH b/a AS A PARAMETER

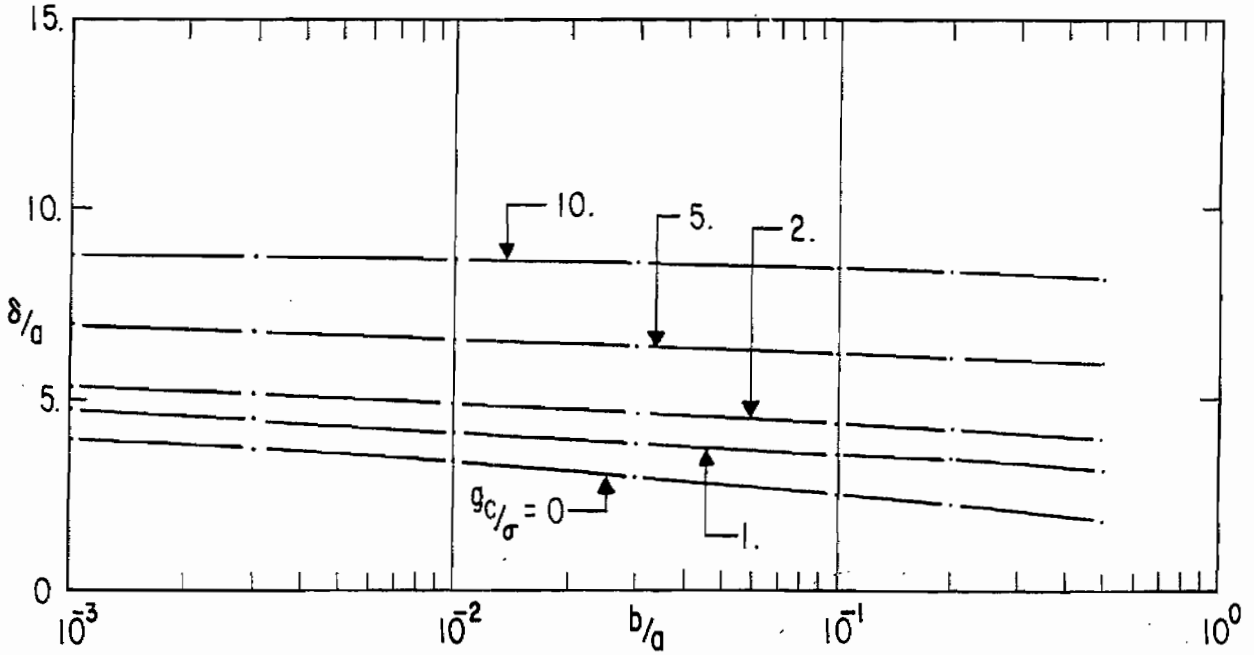

B. δ/a vs. b/a WITH $g_{c/\sigma}$ AS A PARAMETER

FIGURE 38. DEPENDENCE OF FREQUENCY RESPONSE ON CABLE CONDUCTANCE FOR EXPOSED CYLINDRICAL LOOP WITH HIGH CONDUCTIVITY OUTSIDE & NO CONDUCTIVITY INSIDE OF LOOP : $|R| = 1/\sqrt{2}$

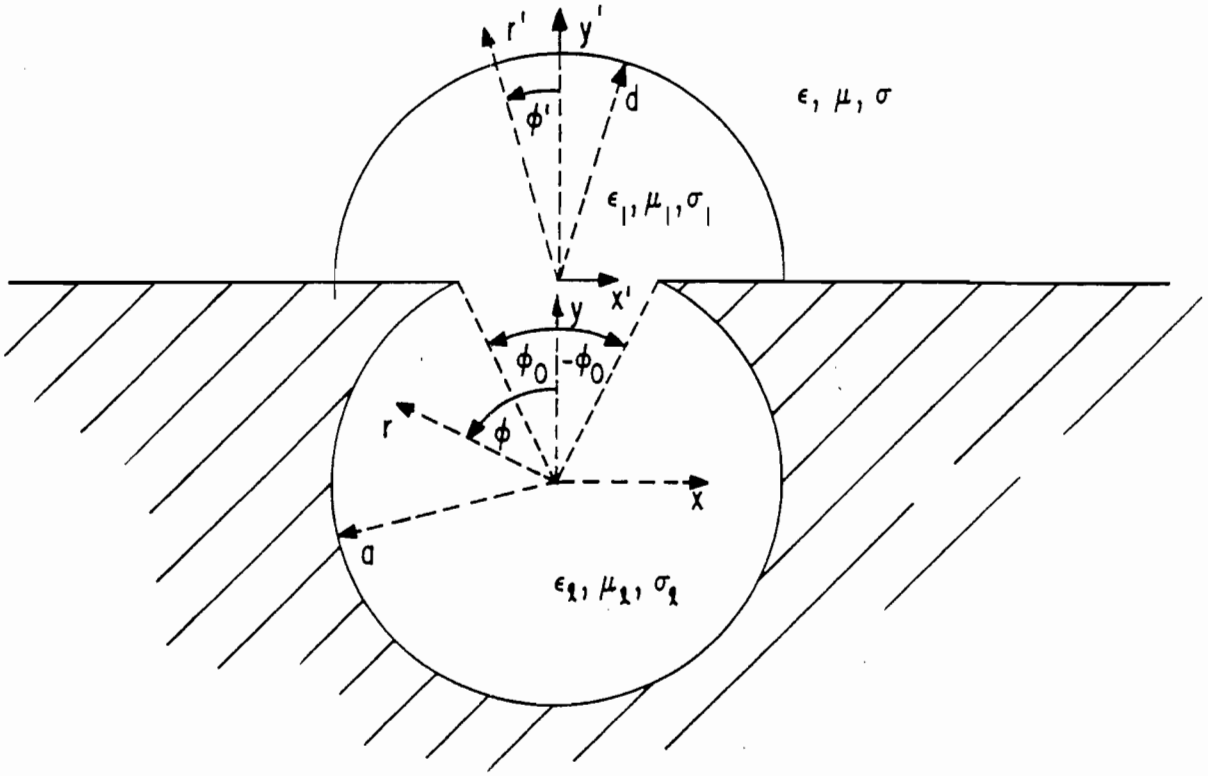

A. CYLINDRICAL LOOP BELOW GROUND PLANE

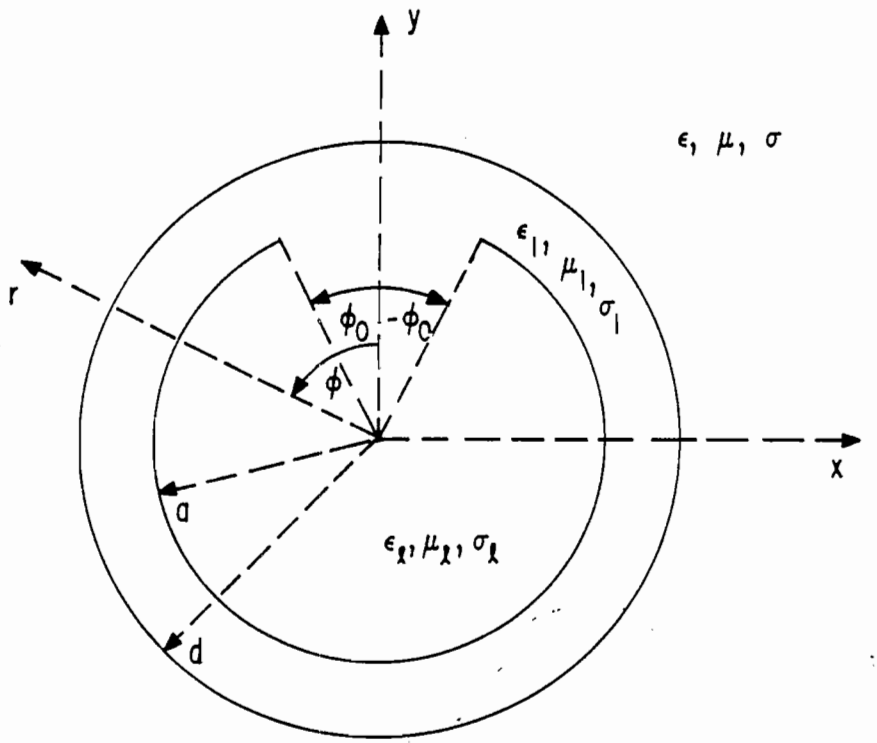

B. EXPOSED CYLINDRICAL LOOP

FIGURE 39. CYLINDRICAL LOOPS WITH AN ADDITIONAL DISTINCT EXTERNAL MEDIUM

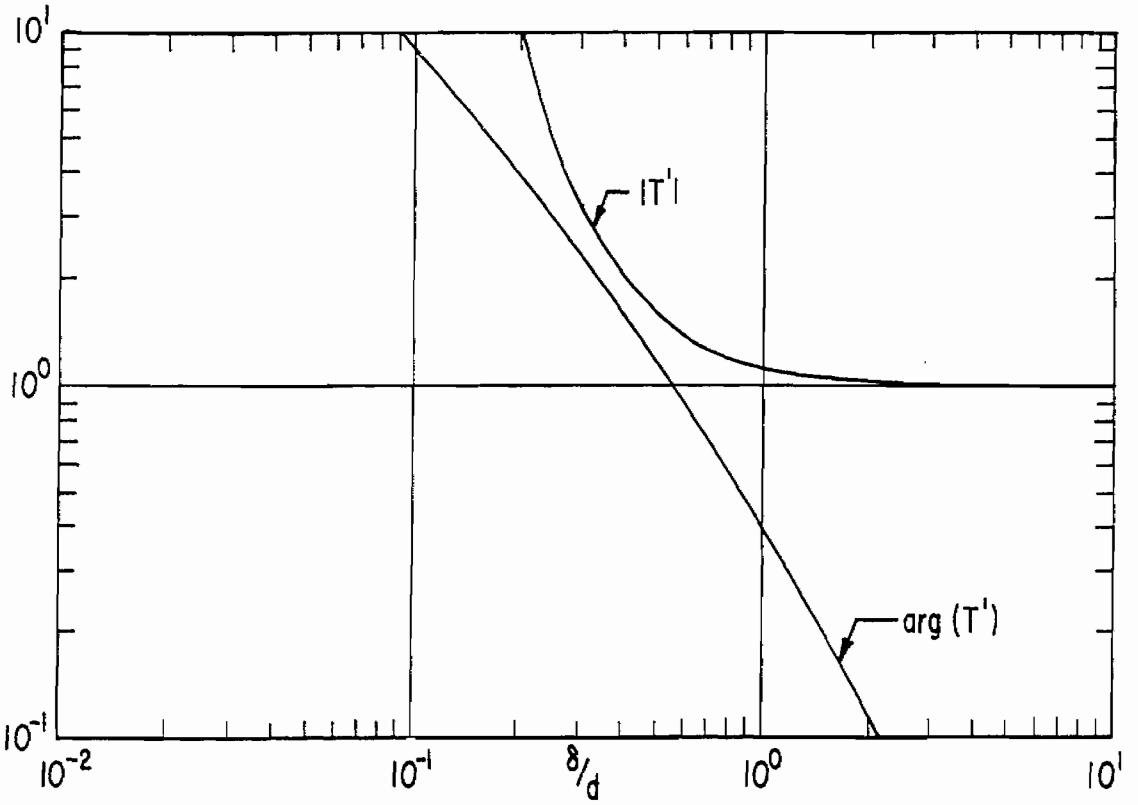

A. MAGNITUDE & PHASE OF T' vs. δ/d

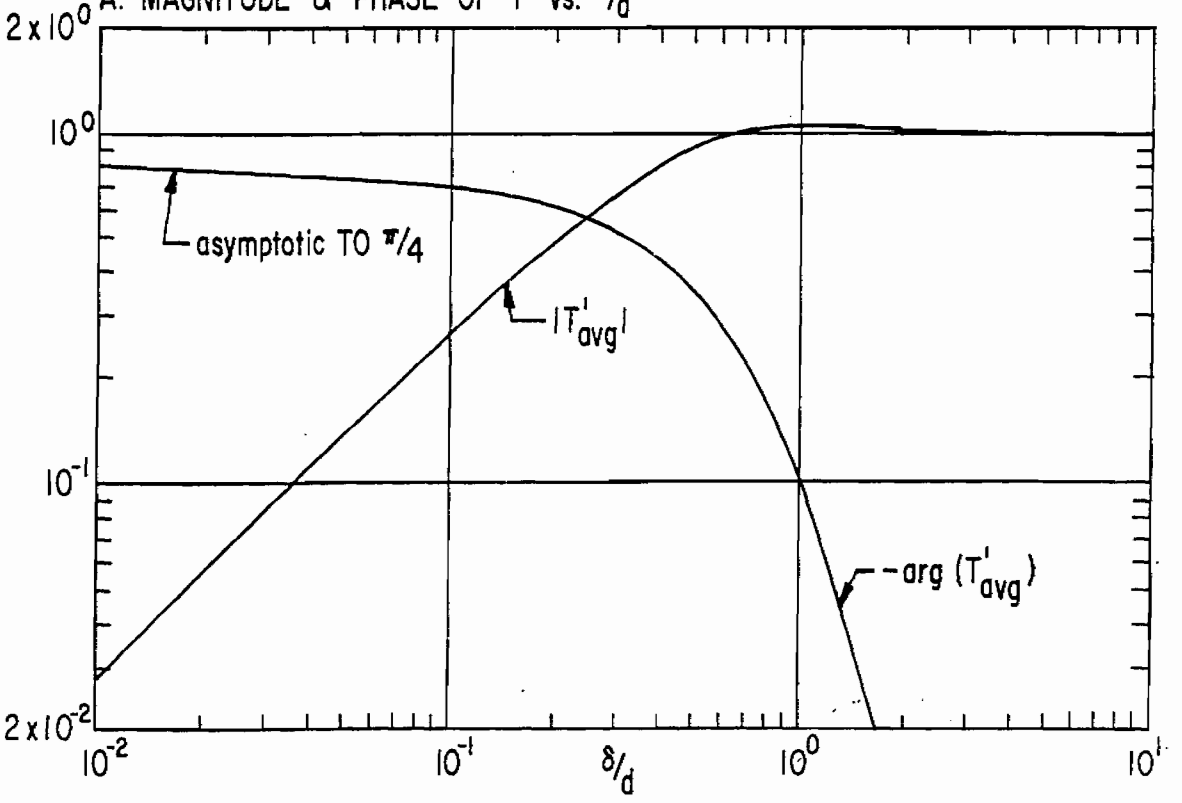

B. MAGNITUDE & PHASE OF T'_{avg} vs. δ/d

FIGURE 40. SHORT CIRCUIT CURRENT TRANSFER FUNCTION FOR CYLINDRICAL LOOP BELOW GROUND PLANE, WITH INSULATING DIELECTRIC, & WITH HIGH EXTERNAL CONDUCTIVITY.

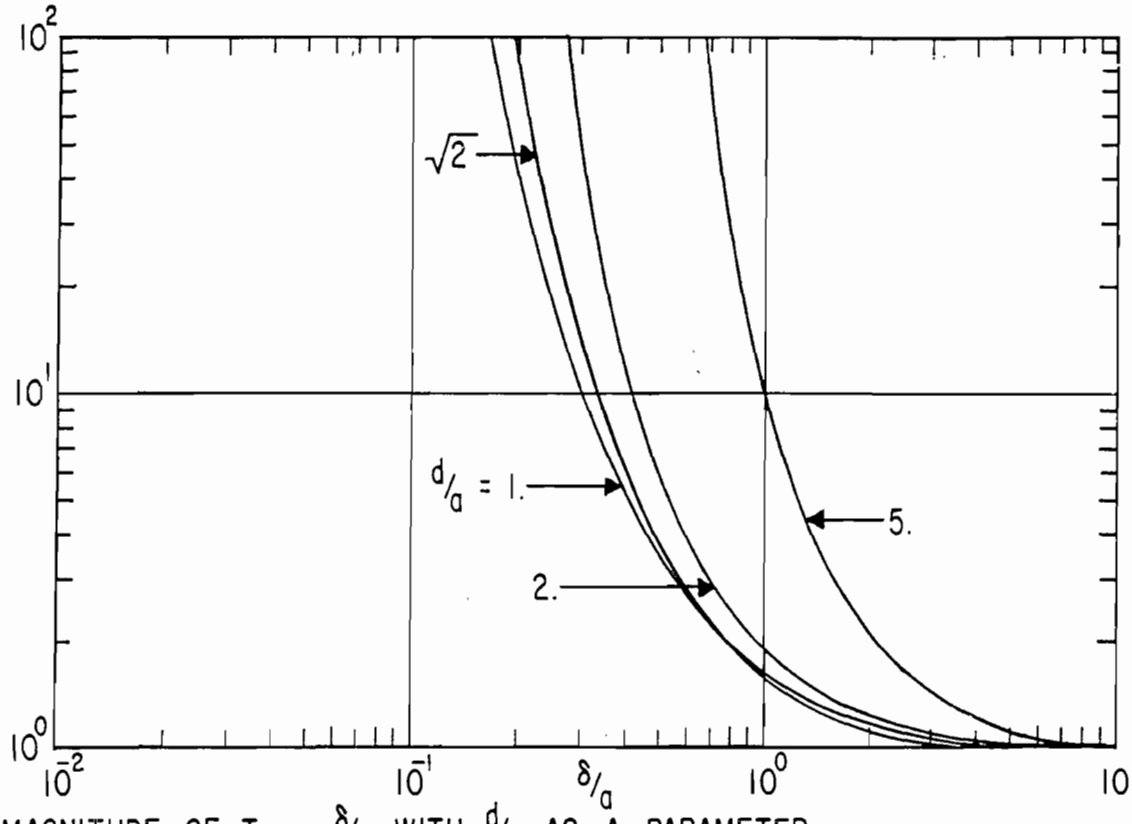

A. MAGNITUDE OF T vs. δ/a WITH d/a AS A PARAMETER

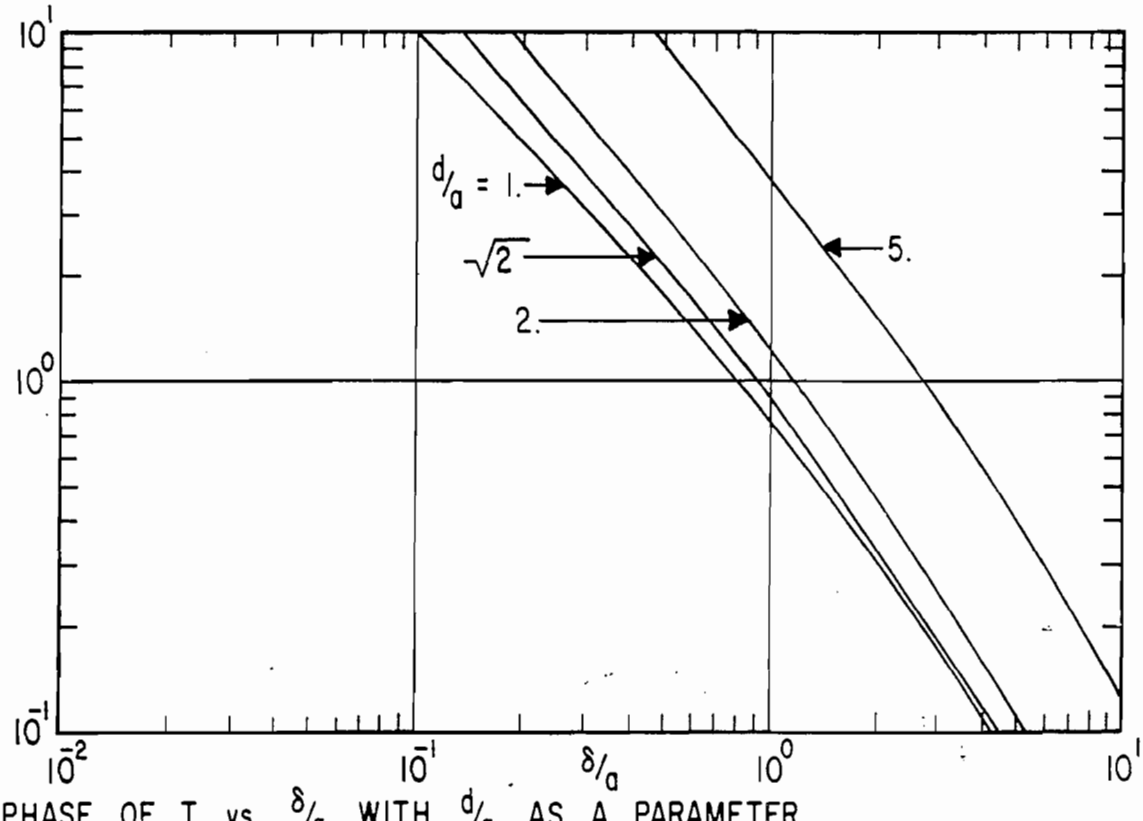

B. PHASE OF T vs. δ/a WITH d/a AS A PARAMETER

FIGURE 41. SHORT CIRCUIT CURRENT TRANSFER FUNCTION FOR EXPOSED CYLINDRICAL LOOP, COVERED WITH INSULATING DIELECTRIC, & WITH HIGH EXTERNAL CONDUCTIVITY

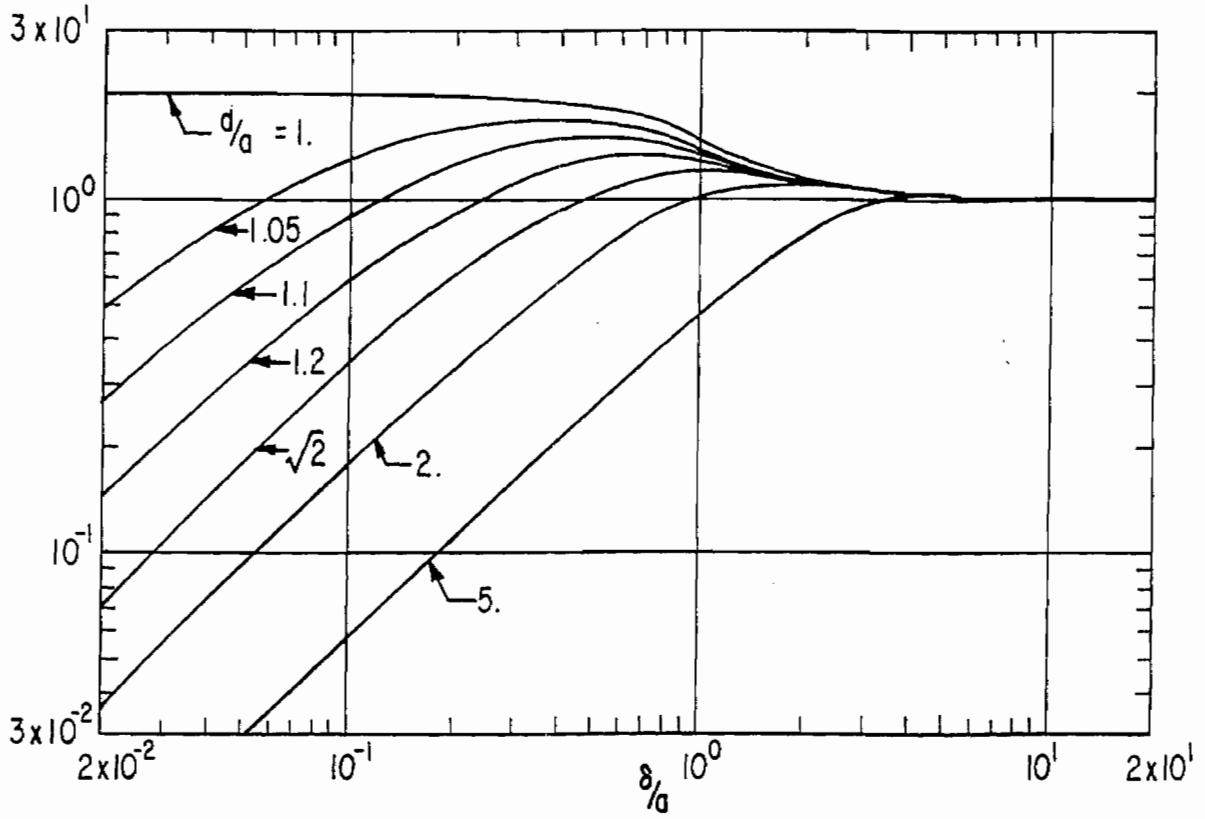

A. MAGNITUDE OF T_{avg} vs. δ/a WITH d/a AS A PARAMETER

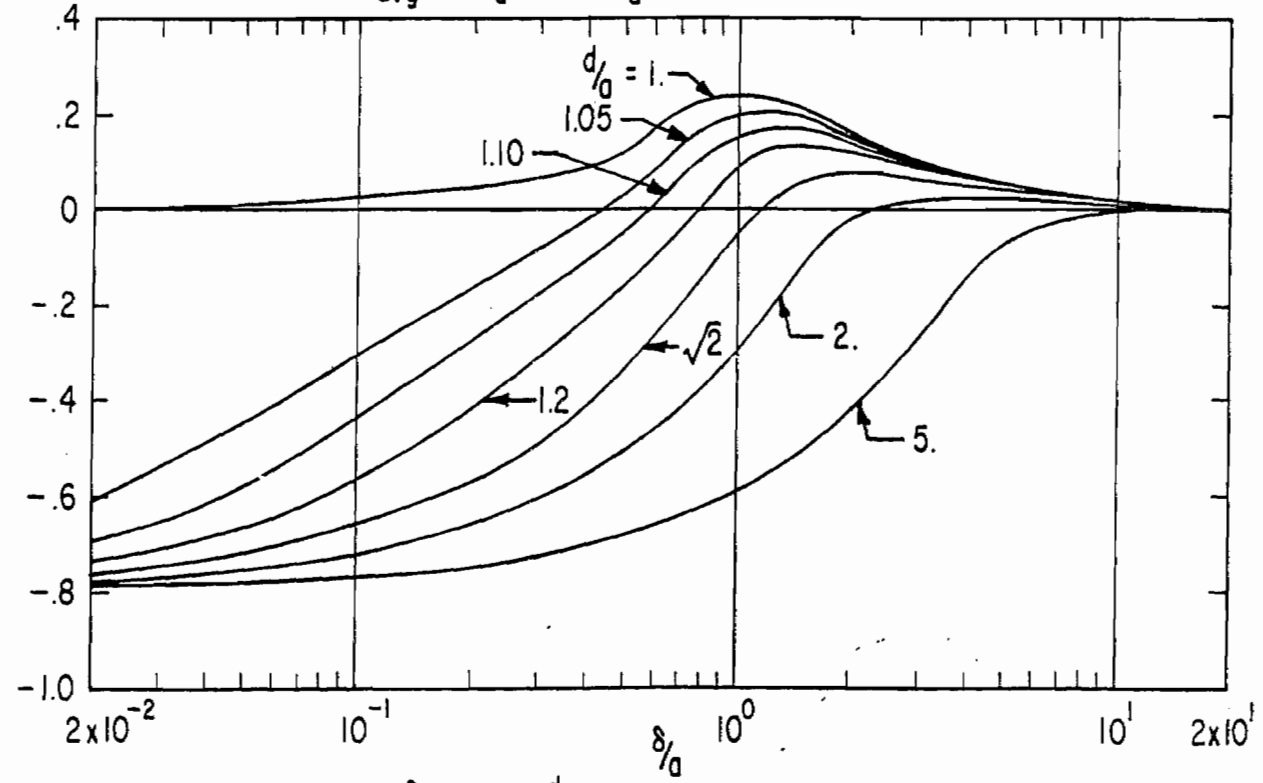

B. PHASE OF T_{avg} vs. δ/a WITH d/a AS A PARAMETER

FIGURE 42. SHORT CIRCUIT CURRENT TRANSFER FUNCTION FOR EXPOSED CYLINDRICAL LOOP, COVERED WITH INSULATING DIELECTRIC, AND WITH HIGH EXTERNAL CONDUCTIVITY

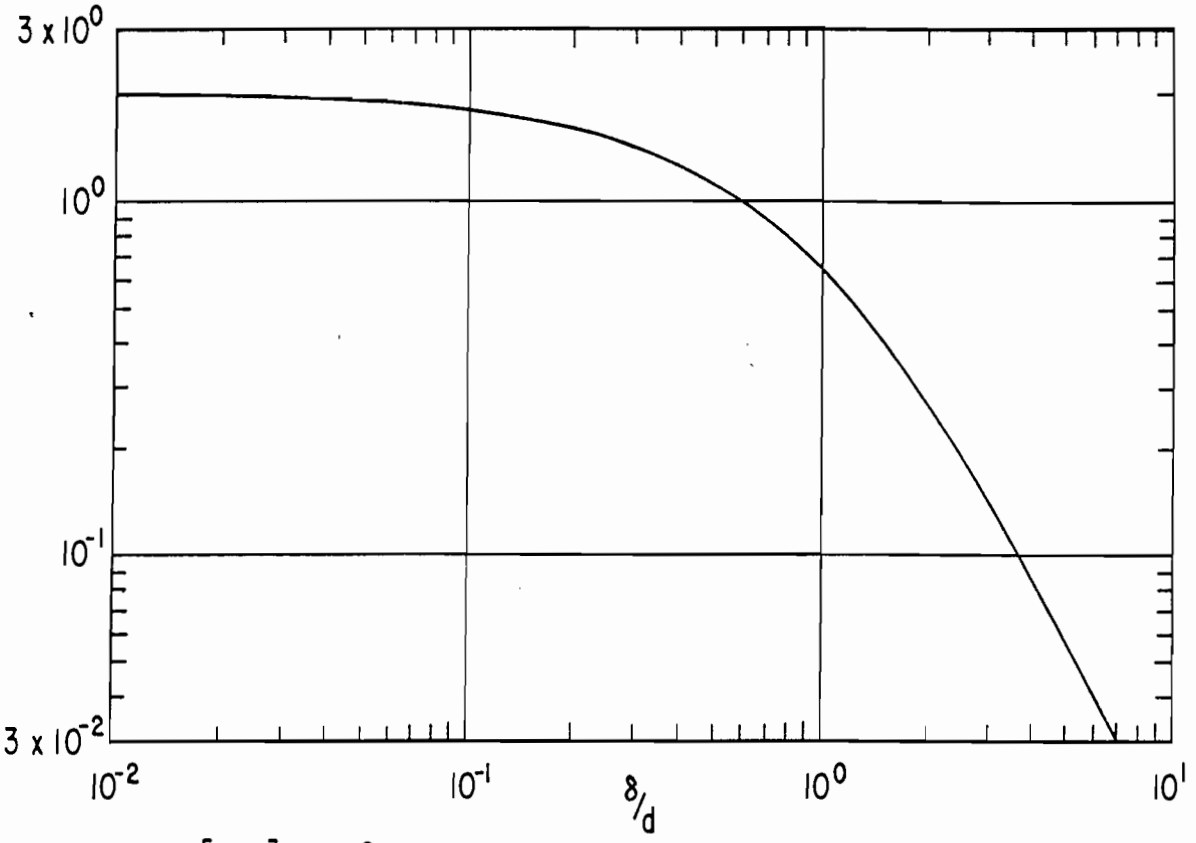

A. Re $\left[Y'_{ext}\right] \left(d/a\right)^2$ vs. δ/d

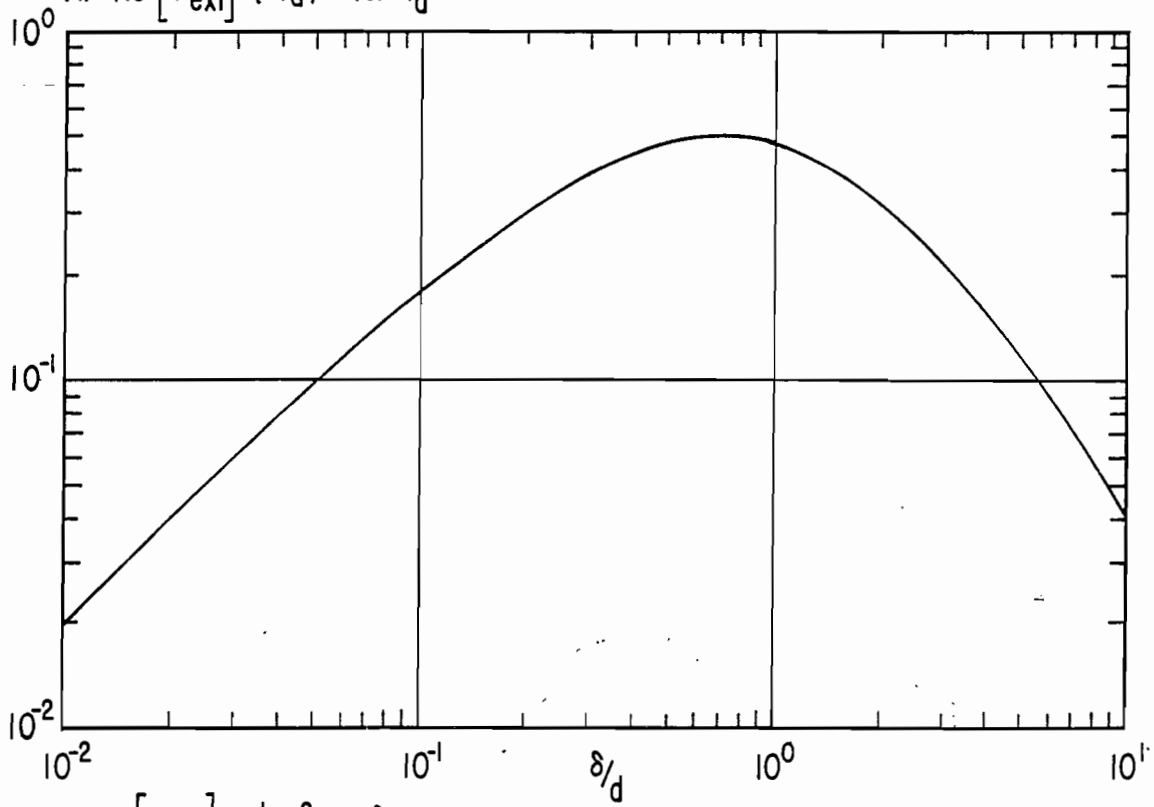

B. Im $\left[Y'_{ext}\right] \left(d/a\right)^2$ vs. δ/d

FIGURE 43. NORMALIZED EXTERNAL ADMITTANCE OF CYLINDRICAL LOOP BELOW GROUND PLANE, COVERED WITH INSULATING DIELECTRIC, & WITH HIGH EXTERNAL CONDUCTIVITY

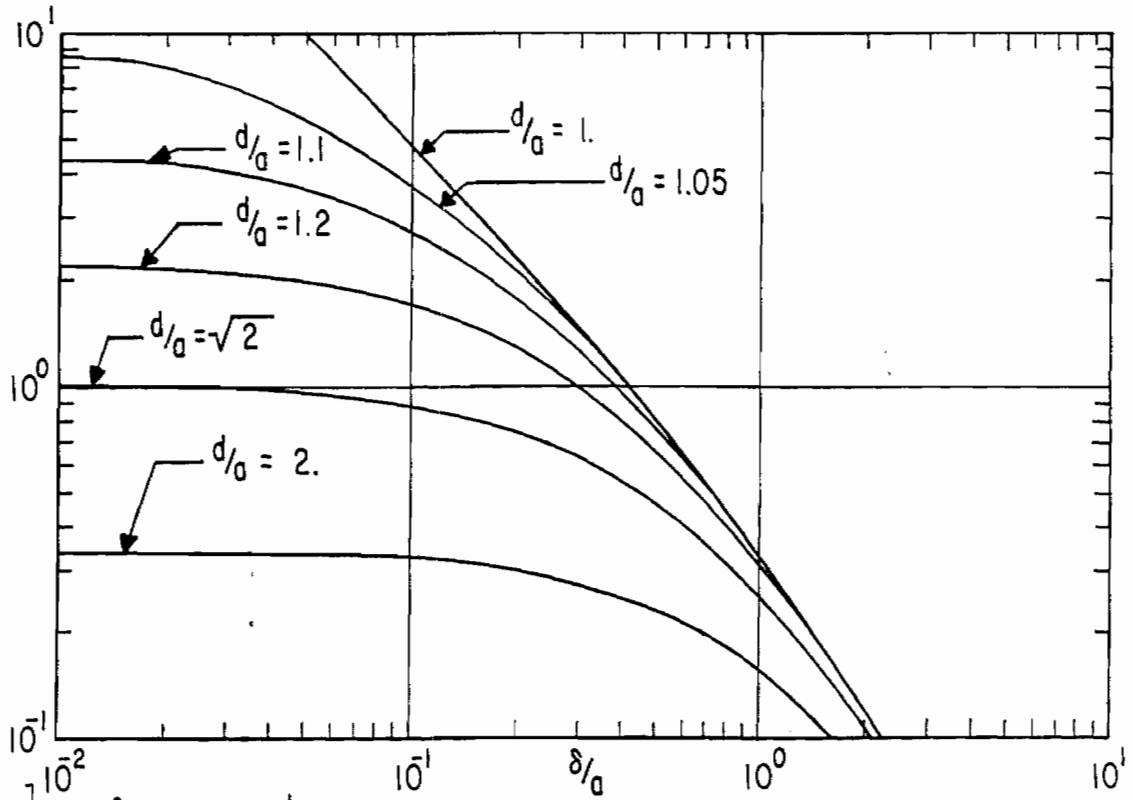

A. $\mathrm{Re}\left[Y_{ext}\right]$ vs. δ/a WITH d/a AS A PARAMETER

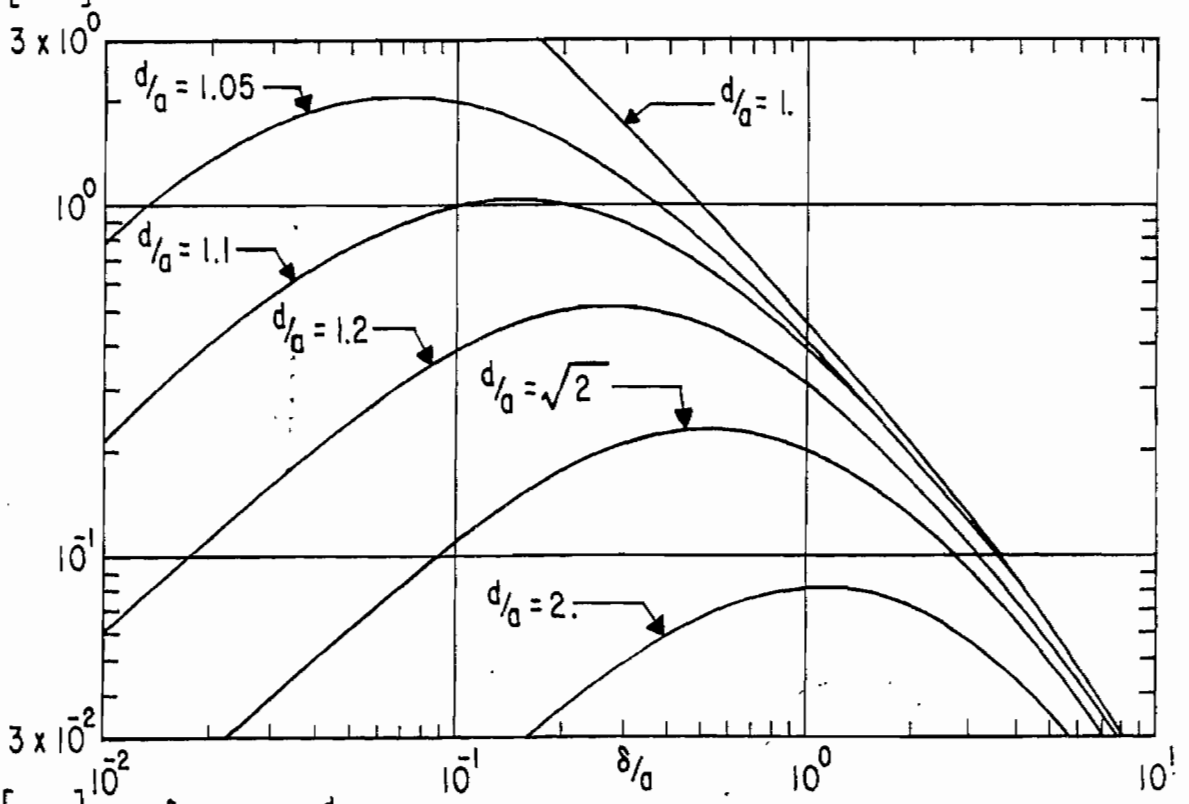

B. $\mathrm{Im}\left[Y_{ext}\right]$ vs. δ/a WITH d/a AS A PARAMETER

FIGURE 44. NORMALIZED EXTERNAL ADMITTANCE OF EXPOSED CYLINDRICAL LOOP, COVERED WITH INSULATING DIELECTRIC, & WITH HIGH EXTERNAL CONDUCTIVITY

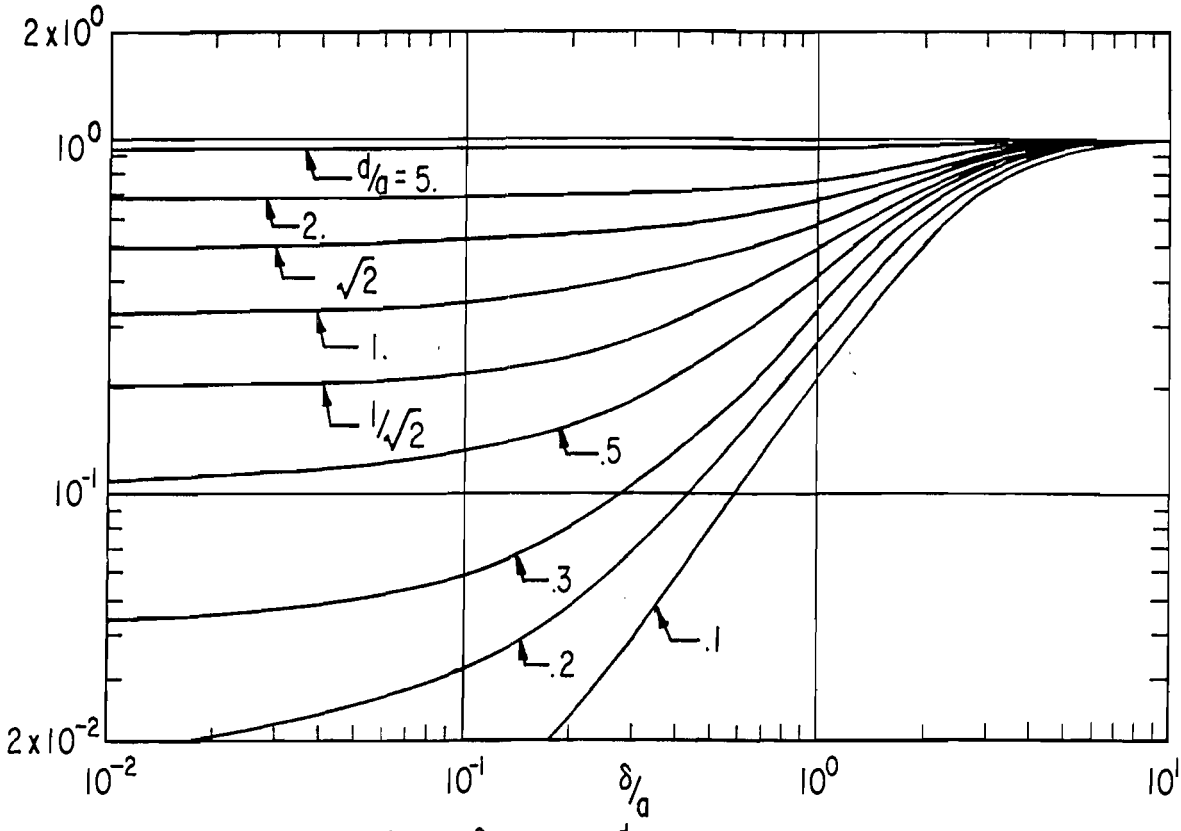

A. MAGNITUDE OF R_y' vs. δ/a WITH d/a AS A PARAMETER

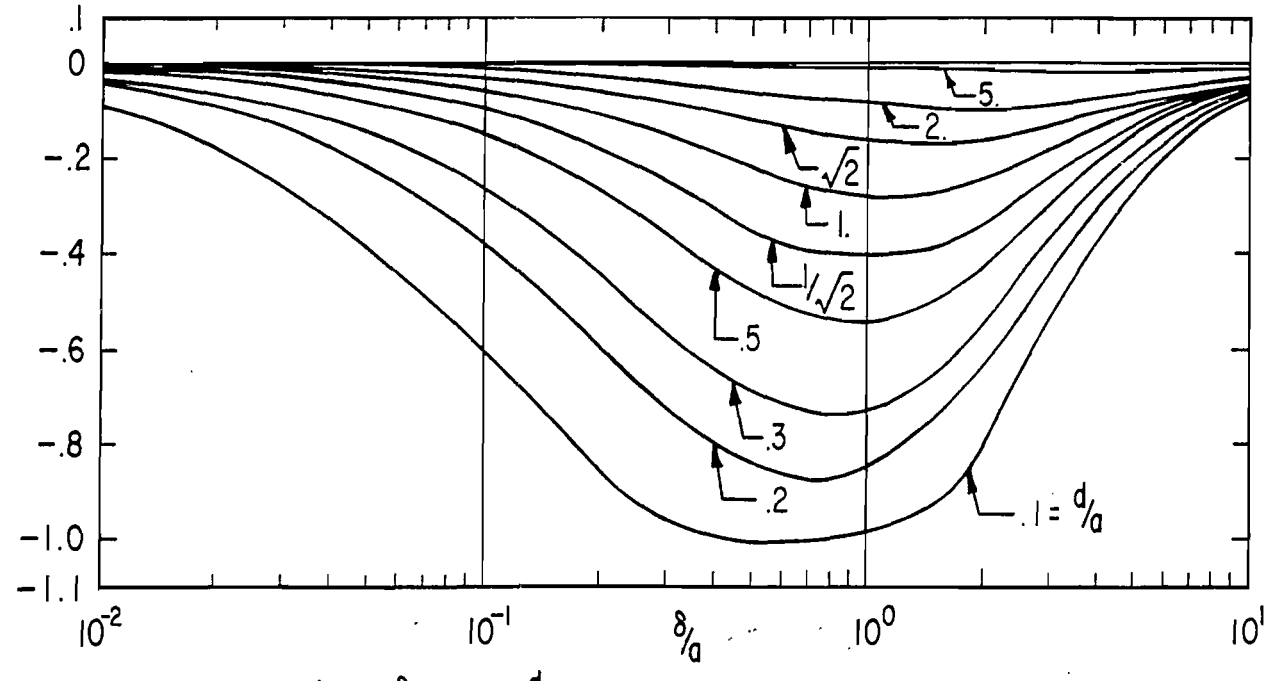

B. PHASE OF R_y' vs. δ/a WITH d/a AS A PARAMETER

FIGURE 45. EFFECT OF ADMITTANCES ON RESPONSE OF CYLINDRICAL LOOP BELOW GROUND PLANE, COVERED WITH INSULATING DIELECTRIC, & WITH HIGH EXTERNAL CONDUCTIVITY: $g_c = 0$

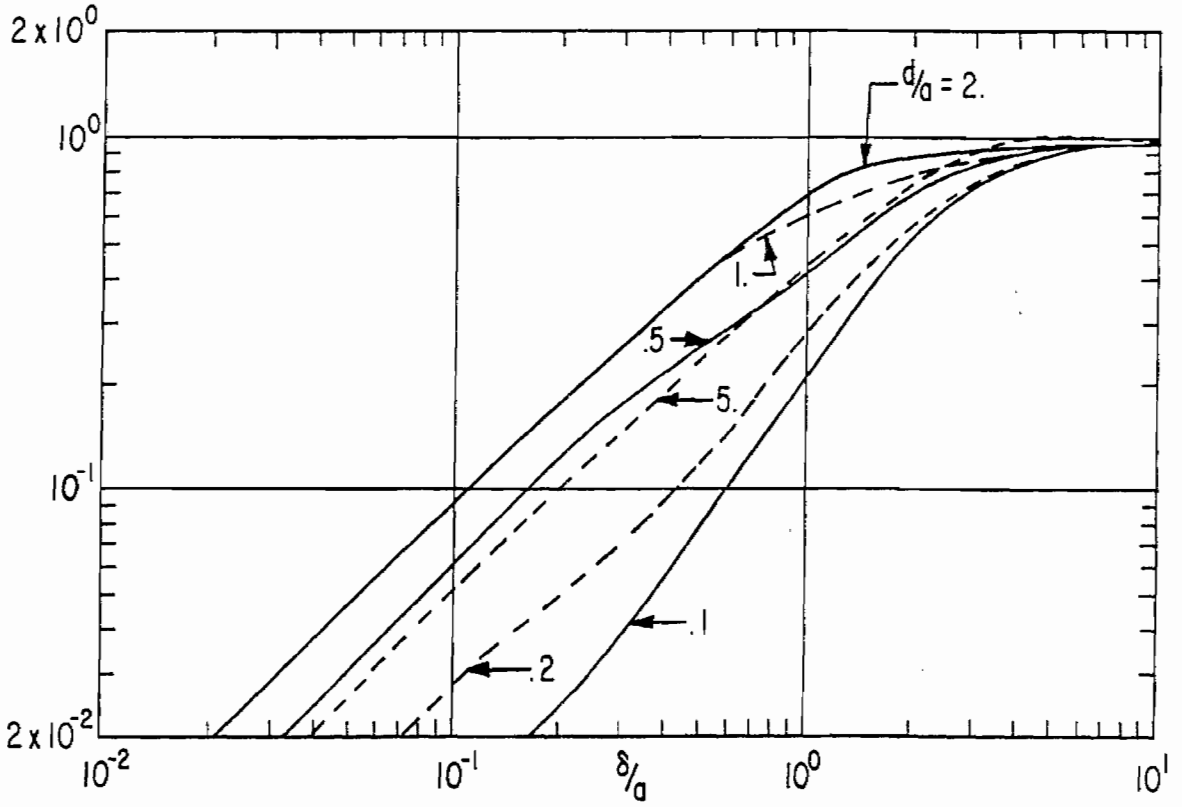

A. MAGNITUDE OF R'_{avg} vs. δ/a WITH d/a AS A PARAMETER

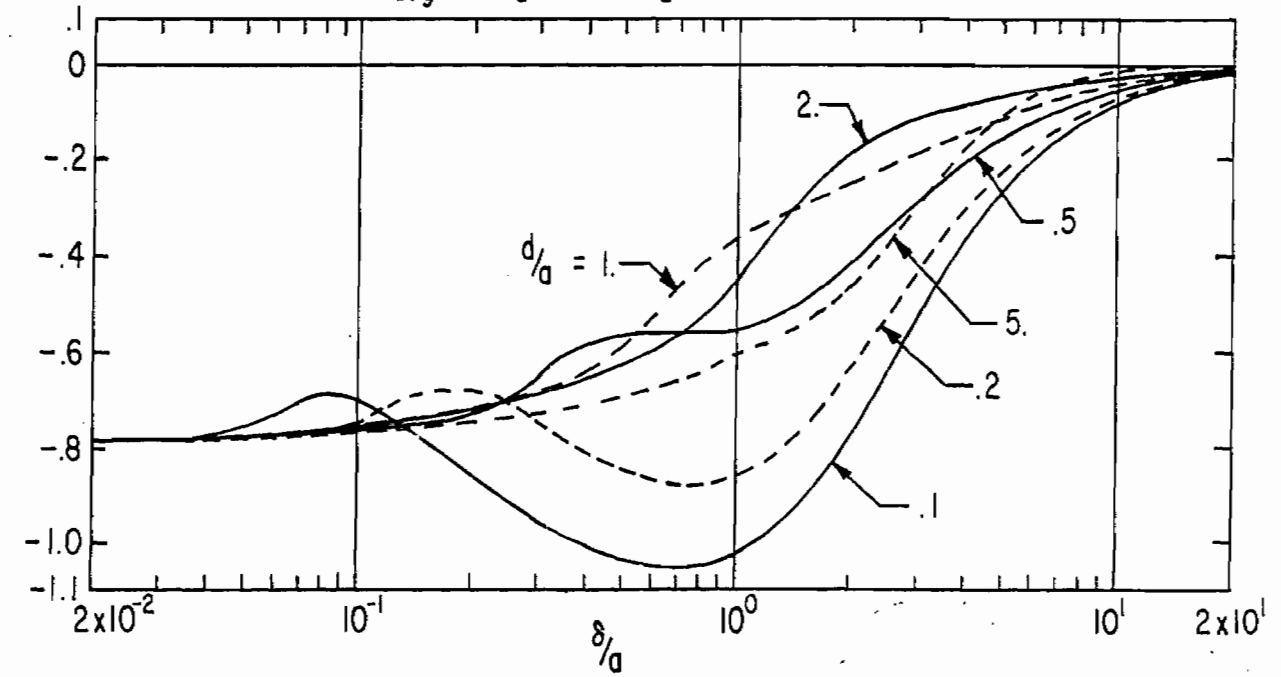

B. PHASE OF R'_{avg} vs. δ/a WITH d/a AS A PARAMETER

FIGURE 46. RESPONSE CHARACTERISTICS OF CYLINDRICAL LOOP BELOW GROUND PLANE, COVERED WITH INSULATING DIELECTRIC, & WITH HIGH EXTERNAL CONDUCTIVITY: $g_c = 0$

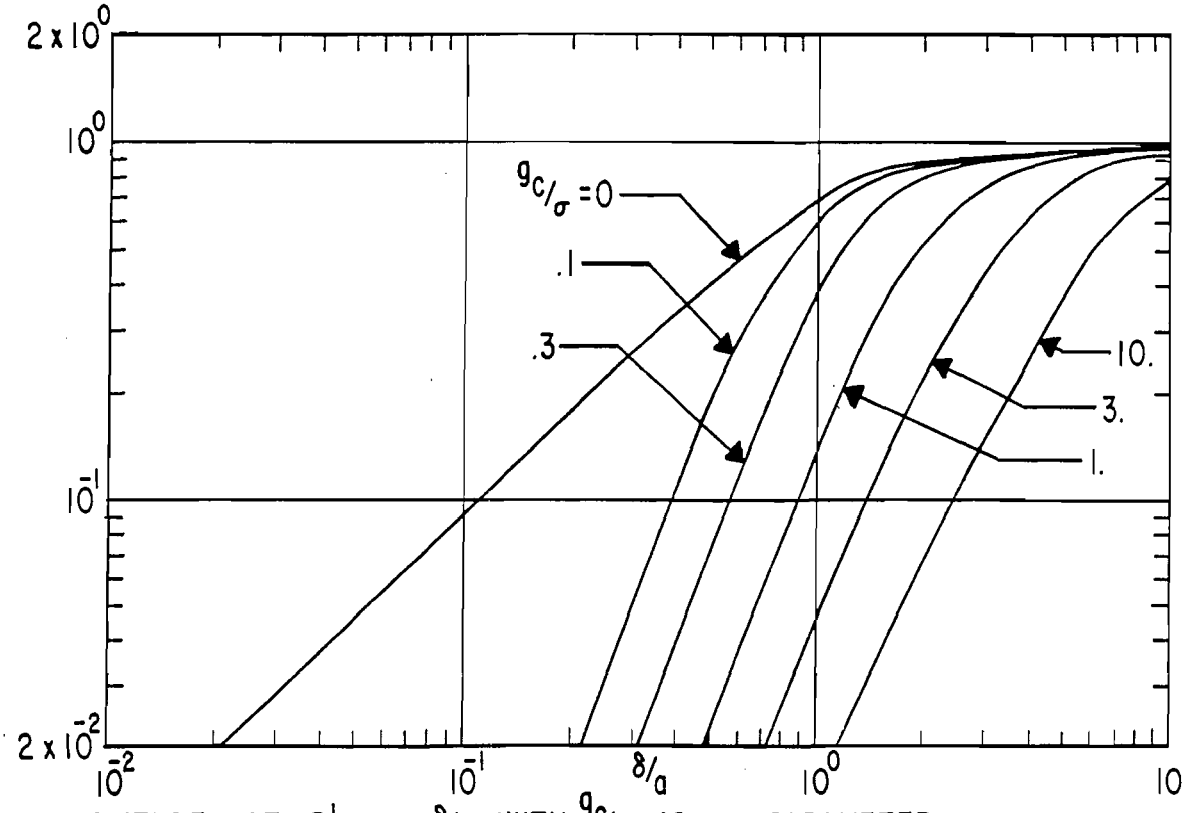

A. MAGNITUDE OF R'_{avg} vs. δ/a WITH g_c/σ AS A PARAMETER

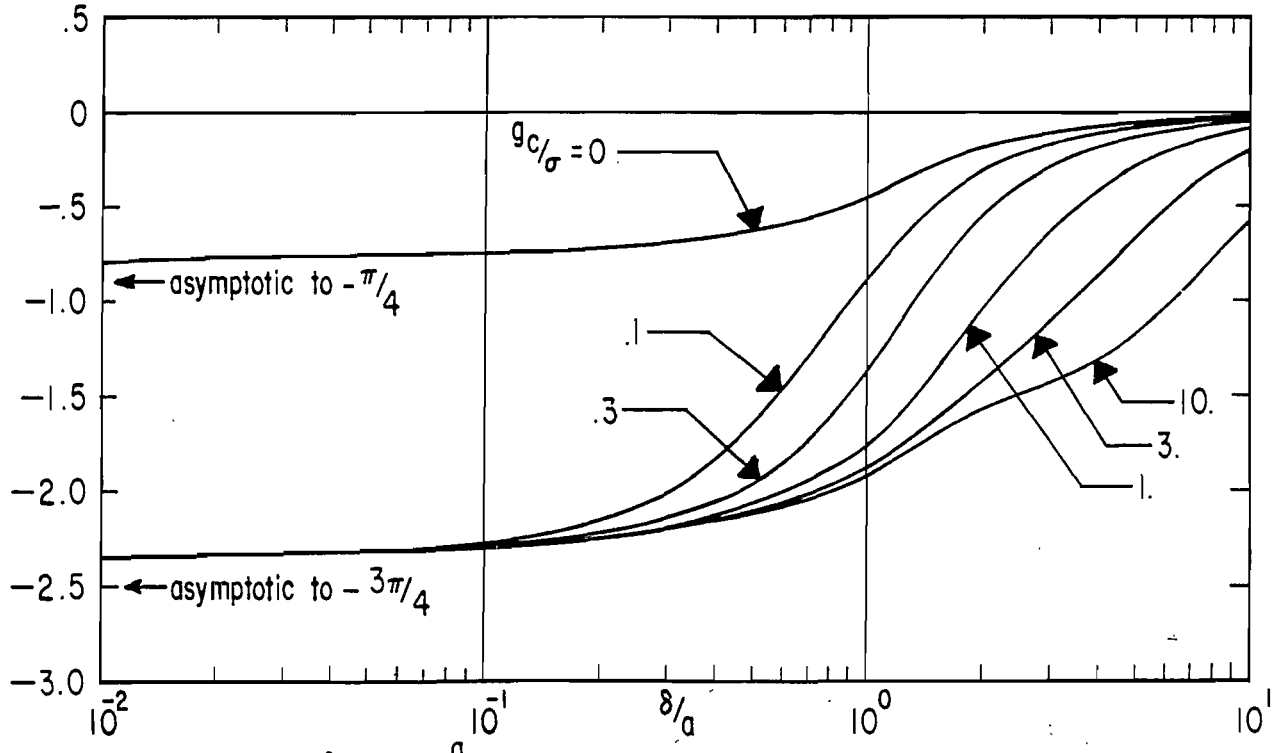

B. PHASE OF R'_{avg} vs. δ/a WITH g_c/σ AS A PARAMETER

FIGURE 47. RESPONSE CHARACTERISTICS OF CYLINDRICAL LOOP BELOW GROUND PLANE, COVERED WITH INSULATING DIELECTRIC, & WITH HIGH EXTERNAL CONDUCTIVITY : $d/a = 2.0$

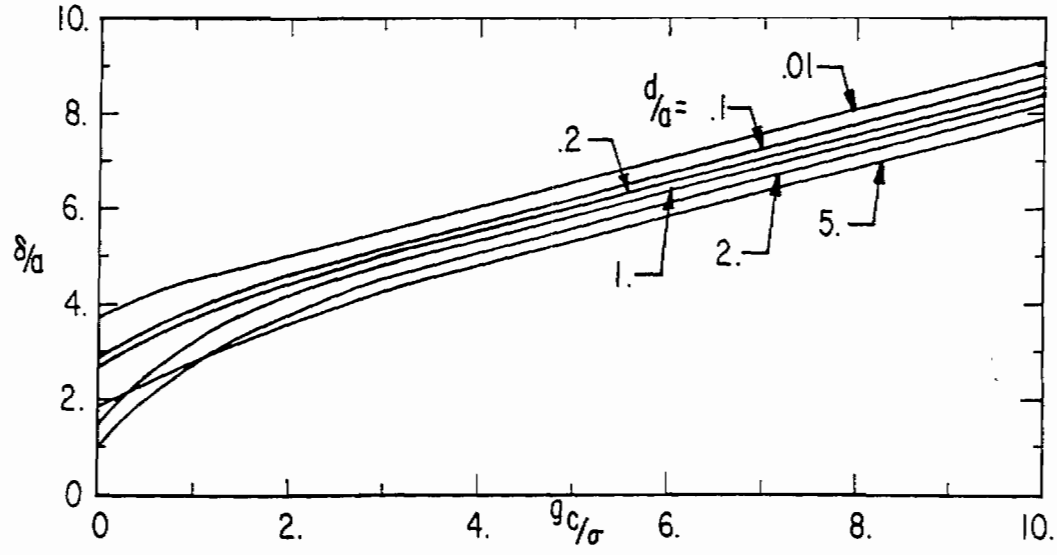

A. δ/a vs. $g_{c/\sigma}$ WITH d/a AS A PARAMETER

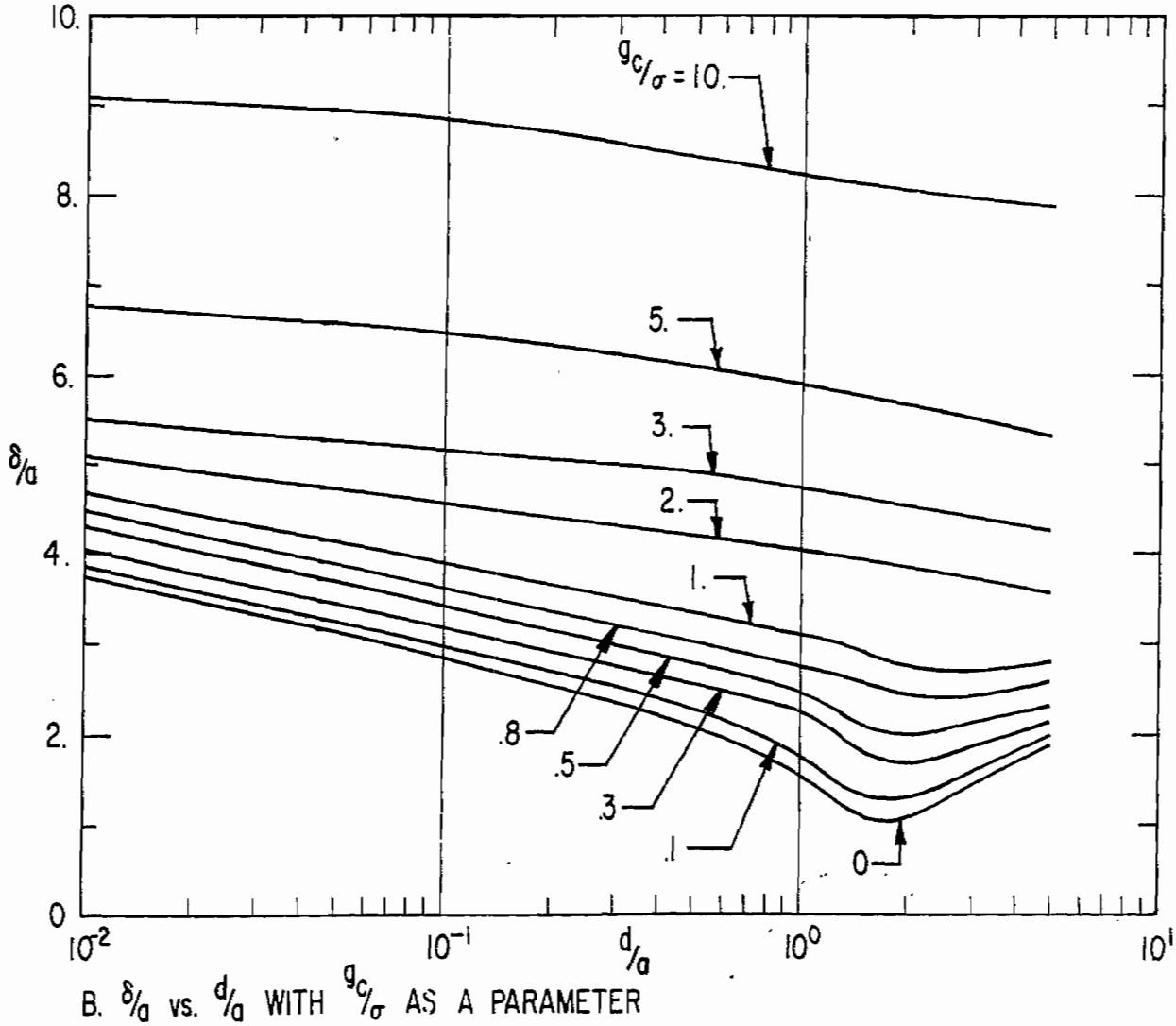

B. δ/a vs. d/a WITH $g_{c/\sigma}$ AS A PARAMETER

FIGURE 48. DEPENDENCE OF FREQUENCY RESPONSE ON CABLE CONDUCTANCE FOR CYLINDRICAL LOOP BELOW GROUND PLANE, COVERED WITH INSULATING DIELECTRIC, & WITH HIGH EXTERNAL CONDUCTIVITY: $|R'_{avg}| = 1/\sqrt{2}$

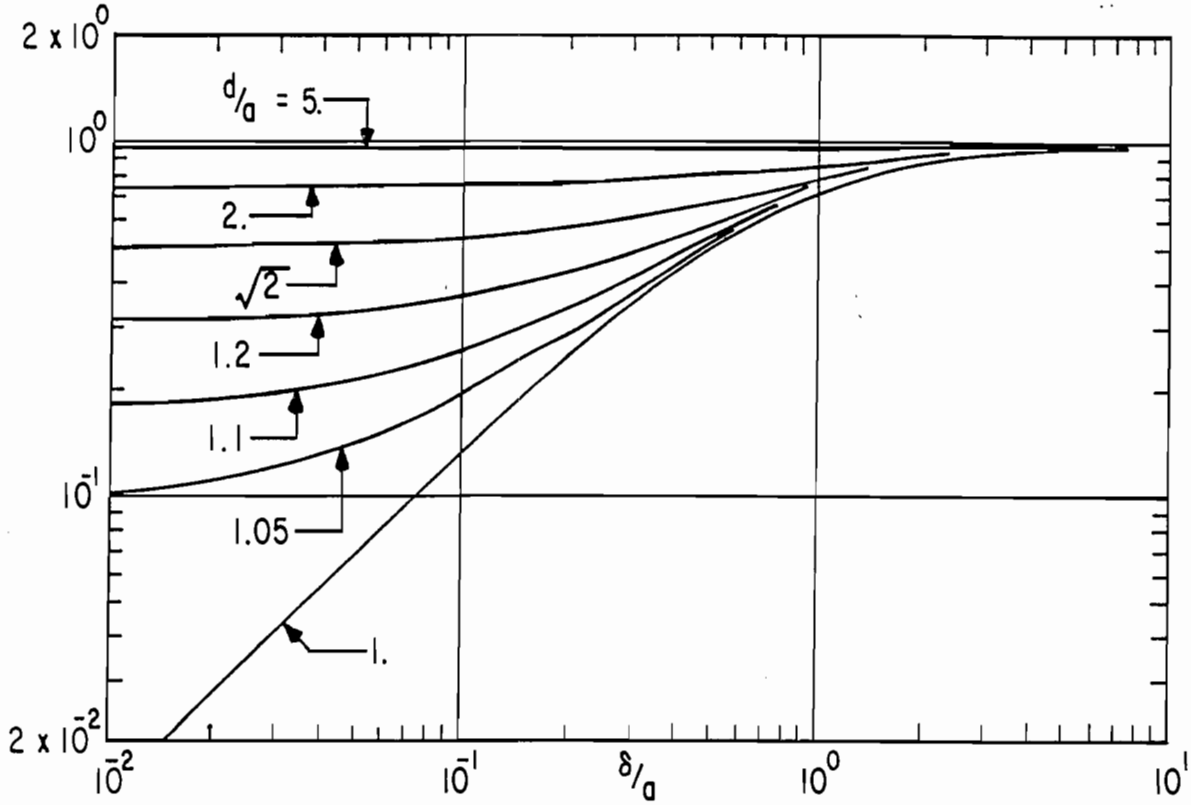

A. MAGNITUDE OF R_y vs. δ/a WITH d/a AS A PARAMETER

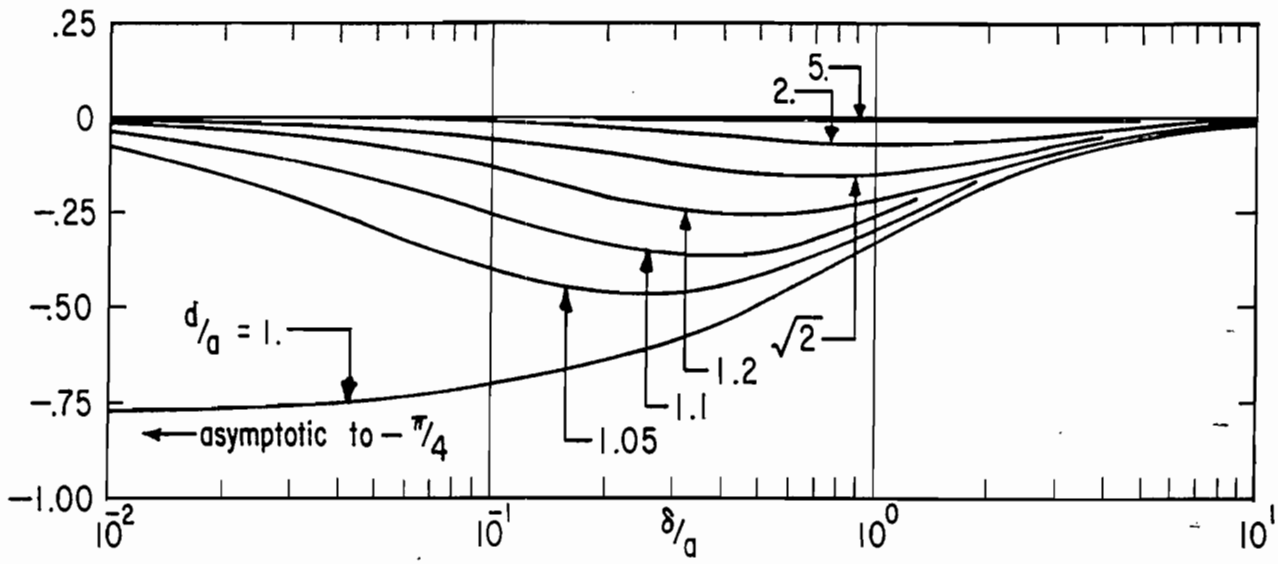

B. PHASE OF R_y vs. δ/a WITH d/a AS A PARAMETER

FIGURE 49. EFFECT OF ADMITTANCES ON RESPONSE OF EXPOSED CYLINDRICAL LOOP, COVERED WITH INSULATING DIELECTRIC, & WITH HIGH EXTERNAL CONDUCTIVITY : $g_c = 0$

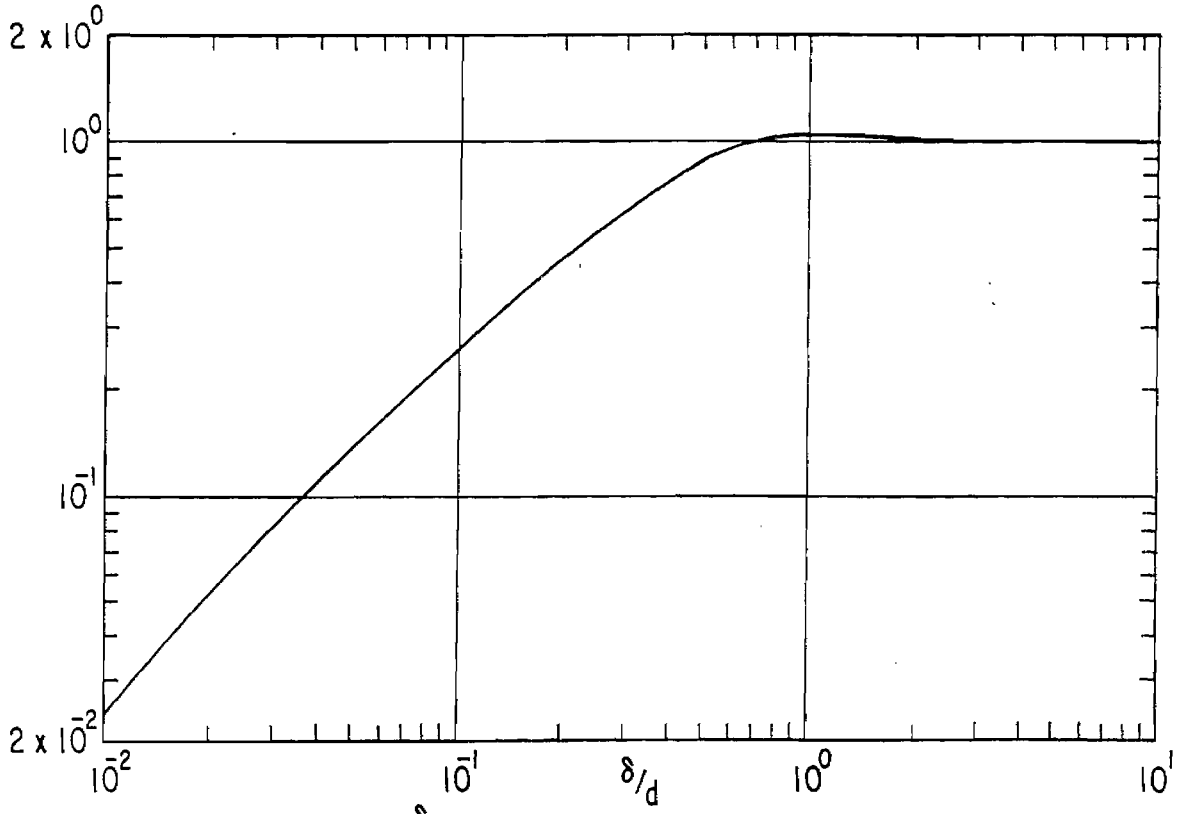

A. MAGNITUDE OF R_{avg} vs. δ/d

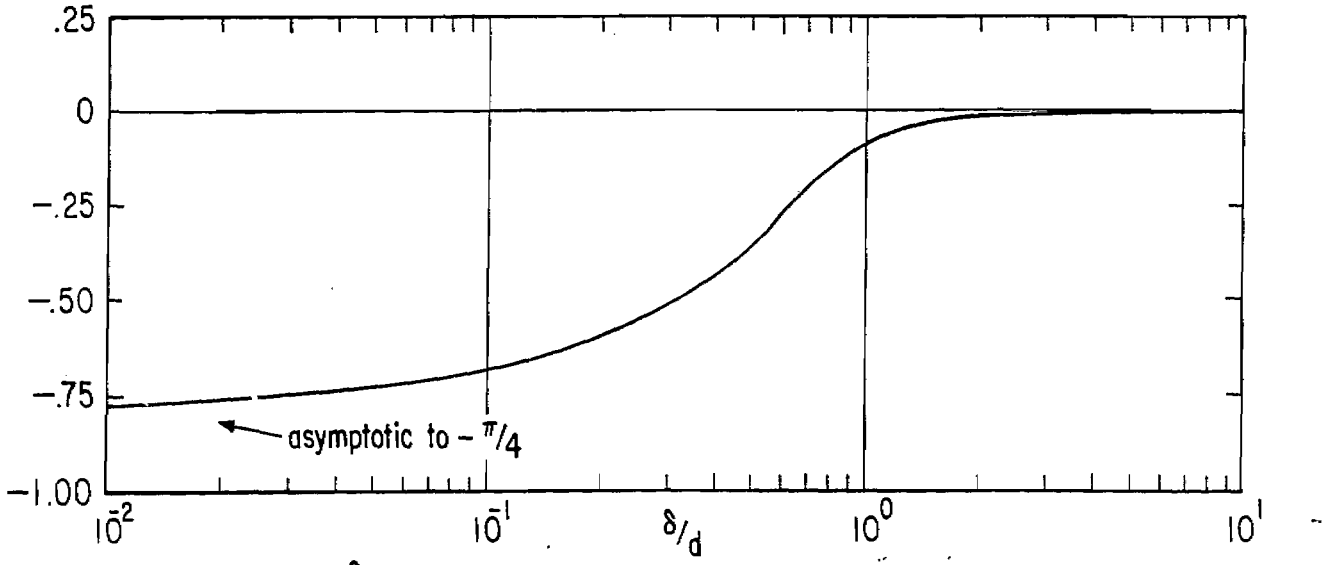

B. PHASE OF R_{avg} vs. δ/d

FIGURE 50. RESPONSE CHARACTERISTICS OF EXPOSED CYLINDRICAL LOOP, COVERED WITH INSULATING DIELECTRIC, AND WITH HIGH EXTERNAL CONDUCTIVITY : $g_c = 0$

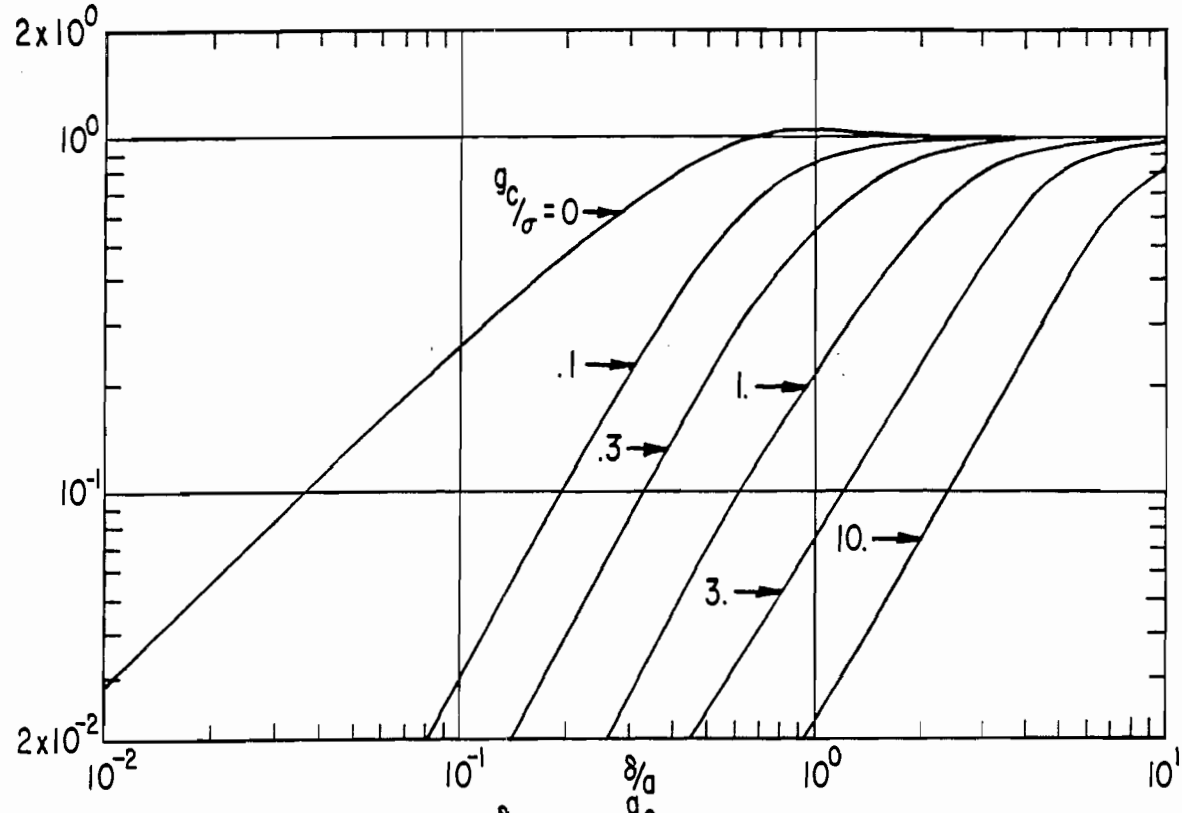

A. MAGNITUDE OF R_{avg} vs. δ/a WITH g_c/σ AS A PARAMETER

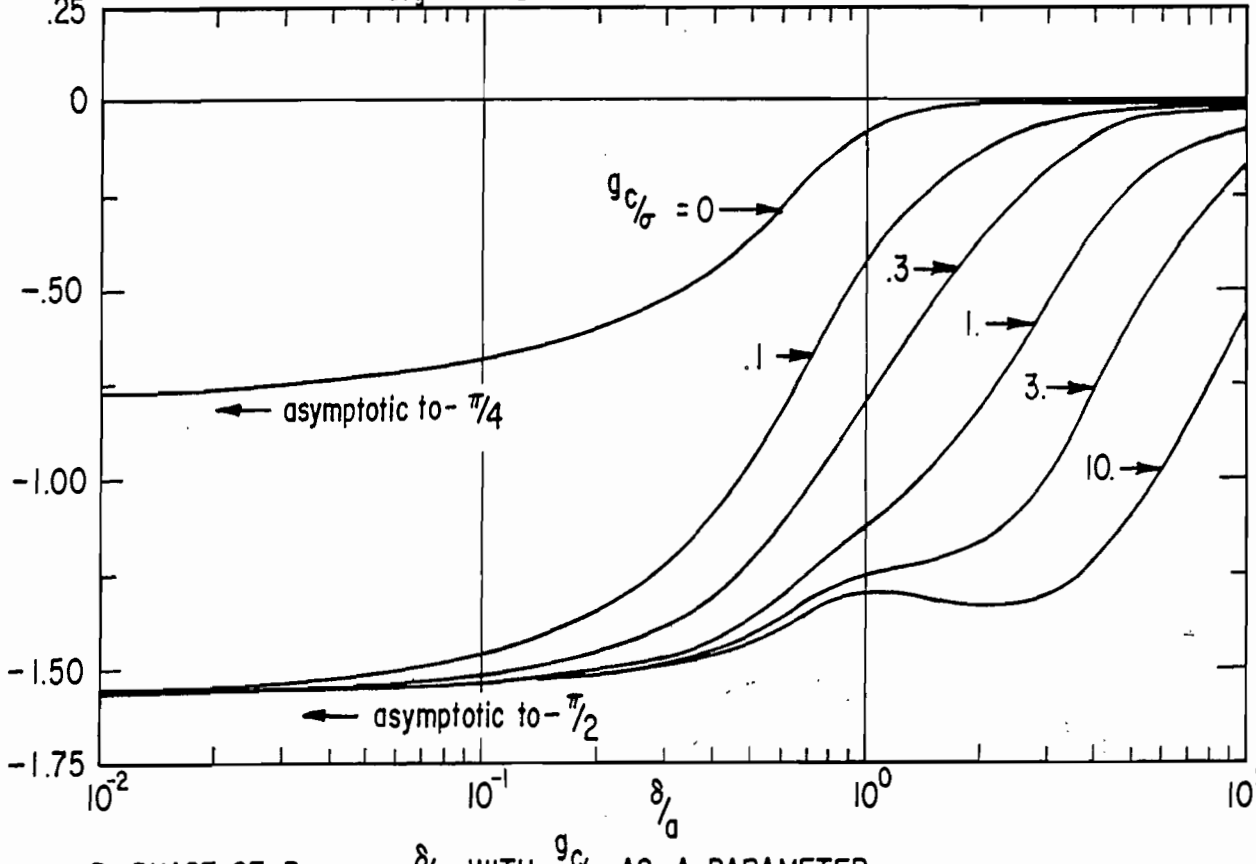

B. PHASE OF R_{avg} vs. δ/a WITH g_c/σ AS A PARAMETER

FIGURE 51. RESPONSE CHARACTERISTICS OF EXPOSED CYLINDRICAL LOOP, COVERED WITH INSULATING DIELECTRIC, & WITH HIGH EXTERNAL CONDUCTIVITY: $d/a = 1.0$

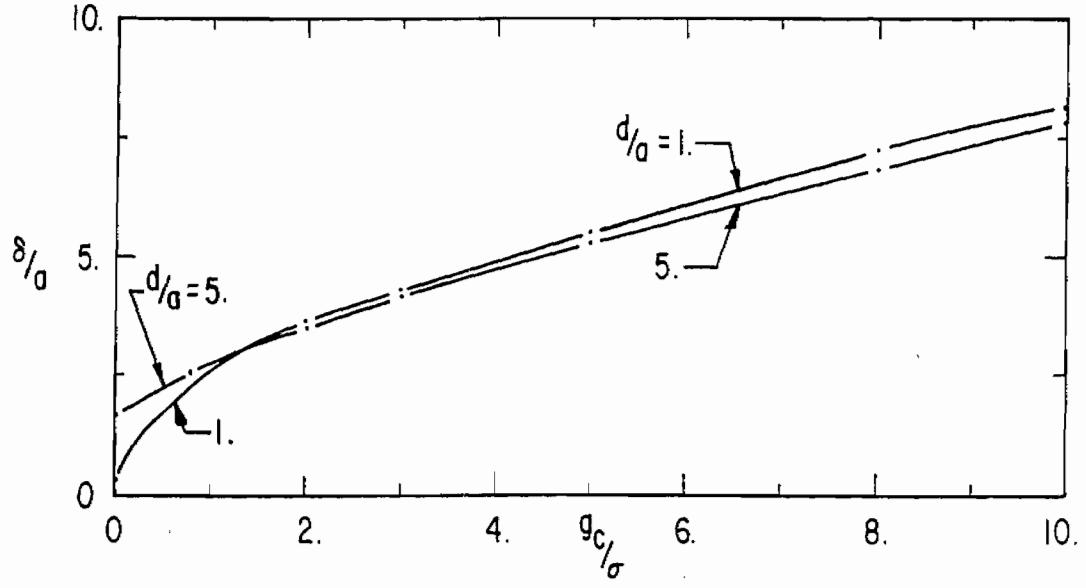

A. δ/a vs. g_c/σ WITH d/a AS A PARAMETER

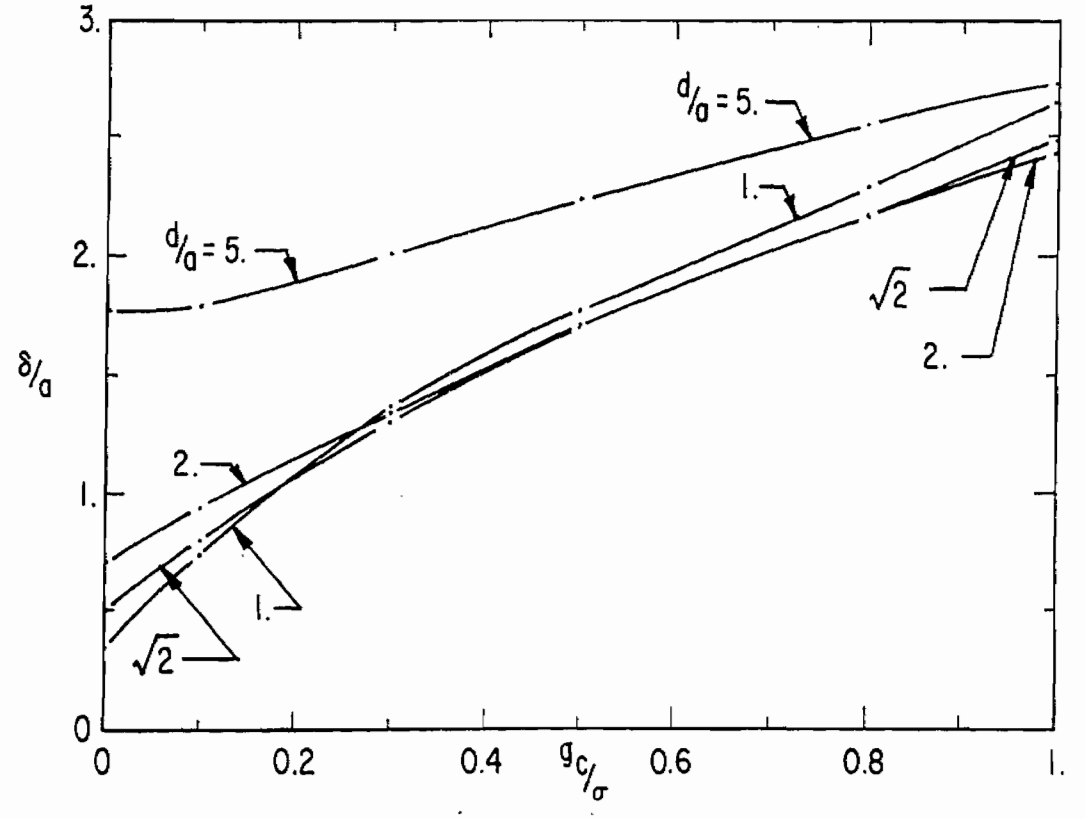

B. (SCALE OF A EXPANDED)

FIGURE 52. DEPENDENCE OF FREQUENCY RESPONSE ON CABLE CONDUCTANCE FOR EXPOSED CYLINDRICAL LOOP, COVERED WITH INSULATING DIELECTRIC, AND WITH HIGH EXTERNAL CONDUCTIVITY: $|R_{avg}| = 1/\sqrt{2}$

Appendix

Numerical Techniques for Computer Calculations

D. E. Brannon
Dikewood Corporation

A2C F. Brewster, Jr.
Air Force Weapons Laboratory

The numerical results plotted in figures 3 through 38 and 40 through 52 were calculated using the CDC-6600 in the Weapons Laboratory at Kirtland Air Force Base. Most of the numerical techniques programmed for these calculations are straightforward and require no explanation. A description of the methods used to generate the first, second, and third kinds of cylindrical Bessel functions, appearing throughout the equations in the test, may be found in a previously published math note.[1]

Upper bounds on truncation error when calculating the values of infinite series representing: (1) the internal admittance of a cylindrical loop, and (2) the external admittance of an exposed cylindrical loop are derived below. A general term of the summation in the equation for the normalized internal admittance (equation (46)) is in the form

$$A_n = \left(\frac{n}{z} - \frac{J_{n+1}(z)}{J_n(z)} \right)^{-1} J_o(n\phi_o)\cos(n\phi_o) \tag{A1}$$

where ϕ_o is the angular gap half width, and $J_n(z)$ the nth order Bessel function of the first kind. To derive an expression for an upper bound to the relative error when forming the sum, a limit must be obtained for

$$\varepsilon = \left| \sum_{n=N}^{\infty} A_n(z,\phi_o) \right| \tag{A2}$$

where N is the order of the term past which truncation of the series is allowed.

It can be shown that, for $n>>|z|$

$$\frac{J_{n+1}(z)}{J_n(z)} \approx z/(2n+1) \tag{A3}$$

(For the admittances, the summations were carried in every instance until $n = 100|z| + 100.$) Then,

$$A_n \approx zJ_o(n\phi_o)\cos(n\phi_o)/n \tag{A4}$$

Also, for $n\phi_o>10$,

$$|J_o(n\phi_o)|<0.8/\sqrt{n\phi_o} \tag{A5}$$

1. Lindberg, R. C., "Bessel, A Subroutine for the Generation of Bessel Functions with Real or Complex Arguments;" Mathematics Note I, The Dikewood Corporation, October 15, 1966.

and a criterion was set such that $N>10\phi_o^{-1}$, thereby causing

$$\left|A_n\right| \leq \left| \frac{0.8\ z\ \cos\ (n\phi_o)}{n\ \sqrt{n\phi_o}} \right| \tag{A6}$$

so that ε, the absolute error, can be expressed as

$$\varepsilon = \left| \sum_{n=N}^{\infty} A_n \right| \leq 0.8 \sum_{n=N}^{\infty} \left| \frac{z\ \cos(n\phi_o)}{n^{3/2}\phi_o^{1/2}} \right| \tag{A7}$$

Also,

$$\varepsilon \leq 0.8|z| \sum_{n=N}^{\infty} \left| \frac{1}{n^{3/2}\phi_o^{1/2}} \right| \leq 0.8|z| \int_{N\phi_o}^{\infty} \frac{1}{(n\phi_o)^{3/2}}\, d(n\phi_o), \tag{A8}$$

so that an upper bound for absolute error may then be expressed as

$$\varepsilon \leq \frac{1.6|z|}{(N\phi_o)^{1/2}} . \tag{A9}$$

The relative error, a more informative error expression, is expressed as

$$\varepsilon_r = \frac{2\varepsilon}{\left|\frac{2}{z}\ Y_\ell\right|} \leq E, \tag{A10}$$

where E is an input value of the allowable relative error (generally desired E = .001). In practice, our relative error was calculated excluding the zero order term of the summation, because it was more convenient.

A general term in the equation for the normalized external admittance of an exposed loop (equation (74)) may be expressed as

$$A_n = \left(\frac{n}{z} - \frac{H_{n+1}^{(2)}(z)}{H_n^{(2)}(z)} \right)^{-1} J_o(n\phi_o)\cos(n\phi_o) \tag{A11}$$

It can further be shown that, for $n>>|z|$ (again, $n \geq 100|z|+100$),

$$\frac{H_{n+1}^{(2)}(z)}{H_n^{(2)}(z)} \approx \frac{2n}{z} , \tag{A12}$$

thereby reducing the general term to

$$A_n \simeq \frac{z}{n} J_o(n\phi_o)\cos(n\phi_o) \tag{A13}$$

and the same error criteria apply to this expression as derived for the calculations of the normalized internal admittance. Here again our relative error calculations were made excluding the zero order term of the summation.

A slightly different approach was used to obtain an upper bound on truncation error for the infinite series in equation (25). A general term for that series has the form

$$A_n(z) = \frac{1}{H_n^{(2)}(z)} \left[\frac{n}{z} - \frac{H_{n+1}^{(2)}(z)}{H_n^{(2)}(z)} \right]^{-1} . \tag{A14}$$

If the summation is performed until $n \gg |z|$ then

$$A_n(z) \simeq \frac{z}{nH_n^{(2)}(z)} \tag{A15}$$

from a preceding argument. The ratio of adjacent terms is then

$$R_n = \frac{A_{n+2}}{A_n} = \frac{n}{n+2} \frac{H_n^{(2)}(z)}{H_{n+2}^{(2)}(z)} \tag{A16}$$

But, it can be shown that

$$\frac{H_n^{(2)}(z)}{H_{n+2}^{(2)}(z)} \simeq \left(\frac{z}{2}\right)^2 \frac{1}{n(n+1)} \tag{A17}$$

and the ratio of successive terms then becomes

$$R_n \simeq \left(\frac{z}{2}\right)^2 \frac{1}{(n+1)(n+2)} \tag{A18}$$

and therefore, for z fixed and $n \to \infty$

$$\lim_{n\to\infty} R_n = 0. \tag{A19}$$

Further, R_n is monotonically decreasing as $n \to \infty$. These conditions then allow an upper bound on this absolute error to be expressed as

$$\varepsilon \leq \frac{|A_{N-2}|^2}{|A_{N-2}| - |A_N|} \qquad \text{(A20)}$$

where N is the index of the last term (even) taken in the summation, and where the summation is performed only over even numbered n. The relative error is then calculated in the normal manner, yielding

$$\varepsilon_r = \left|\frac{2\varepsilon}{T}\right| \leq E. \qquad \text{(A21)}$$

(Again we set E = .001) In practice, our calculation of relative error for short circuit current ratio omitted the zero order term and involved only sums where $n \geq 2$. Because of the very rapid convergence of the T sum, we did not require that $n \geq 100|z| + 100$.

A few general comments about the operating characteristics of the program might be made. Only the high speed of the CDC 6600 made these calculations practical. The technique for forming the Bessels to a limited number of orders appears in Mathematics Note 1. We required 100,000 orders for each plotted point in some cases, so our program was necessarily different from the program in the mathematics note. All calculations satisfy the requirement that either the relative error was less than 10^{-3}, or 100,000 orders had been calculated per point.

An early series convergence in the sums for T (Figures 3,4) generally satisfied the error criterion described above in fewer than 20 orders.

Normalized internal admittances (Figures 6,7) all converged so slowly that 100,000 orders were calculated for each point, at which time $10^{-3} \leq \varepsilon_r \leq 10^{-2}$. There was a direct connection between the magnitude of the arguments of the Bessel functions and the relative error.

Normalized external admittances (Figures 8,9) for the loop below ground plane involved only the first 2 orders of Bessels.

Another slow convergence was encountered in the calculations for normalized external admittances for the exposed loop (Figures 10,11). This time, after calculating 100,000 orders for each point, our relative error was still of the order $10^{-3} \leq \varepsilon_r \leq 2 \times 10^{-2}$.

The rest of the quantities were obtained either from arithmetic combinations with the quantities described above or from substitutions from handbooks. In either case, the accuracy we had already achieved was maintained throughout.